SAND79-0626
Unlimited Release

Predictions of Nuisance Damage and Hazard From Accidental Explosions During Trident Missile Test Flights

Jack W. Reed

Sandia National Laboratories

SF 2900-Q(3-80)

Issued by Sandia Laboratories, operated for the United States Department of Energy by Sandia Corporation.

Printed in the United States of America

Available from
National Technical Information Service
U. S. Department of Commerce
5285 Port Royal Road
Springfield, VA 22161

Price: Printed Copy $6.00; Microfiche $3.00

SAND79-0626
Unlimited Release
Printed March 1980

PREDICTIONS OF NUISANCE DAMAGE AND HAZARD FROM ACCIDENTAL EXPLOSIONS DURING TRIDENT MISSILE TEST FLIGHTS*

Jack W. Reed
Environmental Research Division 4533
Sandia Laboratories
Albuquerque, NM 87185

ABSTRACT

The damage and hazard potential of an accidental explosion of a Trident I C-4 motor near the Cape Canaveral Launch Pad 25 has been assessed. Under some weather conditions, the airblast propagation could break thousands of windows in the Cape Canaveral community; in other weather conditions only a few might be broken. A "weather watch" was developed and operated during Trident tests to hold threatened damage and hazard down to an acceptable minimum level. Test delays, while awaiting suitable weather, averaged near the predicted 2 days per launch test.

*Work described in this report was jointly supported by the U.S. Navy Strategic Systems Project Office (SSPO) and the U.S. Department of Energy (DOE).

ACKNOWLEDGMENT

Encouragement and assistance to this project were provided by many individuals, and they were much appreciated. The initial impetus and support were furnished by Dr. John Kincaid and Capt. C. L. Gooding of the Strategic Systems Project Office (SSPO). Later, continuing SSPO support, right down to reviewing this report, was provided by Cdr. W. G. Clautice and Michael Brodsky.

In Florida, friendly Naval Ordnance Test Unit (NOTU) help was always available from Capt. Styres, D. Leffler, D. Walker, E. F. Gormel, and L. LaMarre. W. L. Hendrickson, of Lockheed, interpreted to his employers all the delays caused by the weather problems here reported. The United States Air Force (USAF) Range Safety officials were most supportive, particularly Col. H. Taffett, Lt. Col. Pilipovich, and L. J. Ullian.

Assistance with the project initiation by the Los Alamos Scientific Laboratory (LASL) was most helpful, with B. G. Craig providing explosives data and assistance on the first report draft and R. J. Bartholomew participating in the Cape Canaveral site and window survey.

USAF weather support for this project was extensive and excellent, with special efforts rendered by Major Czagas, Major Ashman, and Lt. Reinke, in climatic data collection, in forecasting, and in arranging the computer data support.

At Sandia Laboratories Albuquerque (SLA), H. W. Church served as alternate blast predictor, B. C. Holt, G. S. Worthen, and D. Fogel manned the pressure gage network, and R. D. Pace furnished field support needs.

PREFACE

While this report was being prepared, joint SLA-USAF-National Aeronautics and Space Administration (NASA) Project Propa-gator series of explosions were conducted at Kennedy Space Center with a comprehensive array of airblast and meteorological instrumentation (described in Reference 8). The purpose was to refine our understanding of the correlations between weather conditions and blast propagation. Preliminary field checks of results have not shown any great surprises. Final analyses will allow significant improvements in numerical blast predictions, but it is not expected that they would significantly affect the conclusions of this report.

SYMBOLS AND ABBREVIATIONS

Quantity Symbols	
A	Area (m^2)
B	Breadth (short dimension) of a window pane (m)
b	Window breaking overpressure (kPa)
c	Sound speed in air (m/s)
c_o	Sea level standard sound speed in air, 347 m/s (m/s)
D	Direction (degrees clockwise from north)
E	Energy (J)
F	Atmospheric acoustic focus factor (magnification) referenced to spherical wave expansion
$\vec{F}$	Vector wind forecast (degrees, m/s)
f	Central (maximum) stress in a plate (MPa)
H	Window pane thickness (m)
k	Proportionality constant
L	Length (long dimension) of a window pane (m)
P	Probability
p	Ambient air pressure (kPa)
p_o	Sea level standard air pressure, 101.325 kPa (kPa)
Δp	Peak blast overpressure or maximum positive deviation from ambient pressure in the blast wave (kPa)
ΔP_s	Blast overpressure with unrefracted standard propagation (kPa)
$\Delta p/p$	Shock strength
R	Slant range from the explosion center (m)
R_p	Radius to acoustic ray turnover point (m)
r	Aspect ratio, length/breadth
$\mathcal{R}$	Poisson's ratio, 0.25
S	Strength factor for rectangular window panes
T(a,h)	Probability integral, in a circular normal distribution
T_c	Temperature (degrees Celsius) (°C)
T_k	Temperature (Kelvin) (K)
t	Time (s)
u,v	Wind components toward east, north (m/s)
V	Sound velocity (m/s)
V_o	Sound velocity at surface level (m/s)
V_p	Sound velocity at ray turnover level (m/s)
W	Explosion energy yield (J)
W_a	Apparent airblast yield (nuclear kt)
x,y,z	Cartesian coordinates toward east, north, zenith (m)
z_o	Height of "surface" weather observations (m)
z_p	Height of acoustic ray turnover (m)
α	Sound speed lapse rate, dc/dz (s^{-1})
θ	Elevation or incidence angle, measured from the horizontal (°)
θ_p	Emission angle of the limit ray turned over by refraction at level z_p (°)
ξ	Energy flux, dW/dA (J/m^2)
ρ	Correlation coefficient

ϕ	Azimuth angle (degrees clockwise from north)
σ	Standard deviation
σ_g	Geometric standard deviation

Unit Symbols

Metric		English	
g	gram	kt	kiloton
J	joule	lb	pound mass
K	kelvin	psi	pound force per square inch
m	metre		
Pa	pascal		
s	second		

Prefixes

Multiplication Factors	Prefix	Symbol
10^6	mega	M
10^3	kilo	k
10^{-3}	milli	m

Abbreviations and Acronyms

AFWL	Air Force Weapons Laboratory, Kirtland Air Force Base, Albuquerque, NM
AWS	Air Force Air Weather Service
ANSI	American National Standards Institute
CC	Cape Canaveral (town), FL
CCAFS	Cape Canaveral Air Force Station, FL
CERL	Army Corps of Engineers Construction Engineering Research Laboratory, Champaign, IL
DOE	U.S. Department of Energy
EST	Eastern (75th Meridian) Standard Time
ETR	Eastern Test Range, Patrick AFB, FL
GMT	Greenwich (0° Meridian) Mean Time
HE	Chemical high explosives
HOB	Explosion height of burst above ground level
LASL	Los Alamos Scientific Laboratory, Los Alamos, NM
MSL	Mean sea level
NE	Nuclear explosive
NOTU	Naval Ordnance Test Unit, Patrick AFB, FL
NSWC	Navy Surface Weapons Center, Silver Spring, MD
Raob	Radiosonde (rawinsonde) upper air observation
SAMTEC	Space and Missile Test and Evaluation Command (USAF)
SSPO	Navy Strategic Systems Project Office, Washington, DC
STP	Standard sea level pressure and temperature (101.325 kPa, 288 K)
STS	Space Transportation System ("Shuttle")
TNT	Trinitrotoluene (HE)
VAB	Vertical Assembly Building, Kennedy Space Center, FL
WTR	Western Test Range, Vandenberg Air Force Base, CA

CONTENTS

ILLUSTRATIONS

TABLES

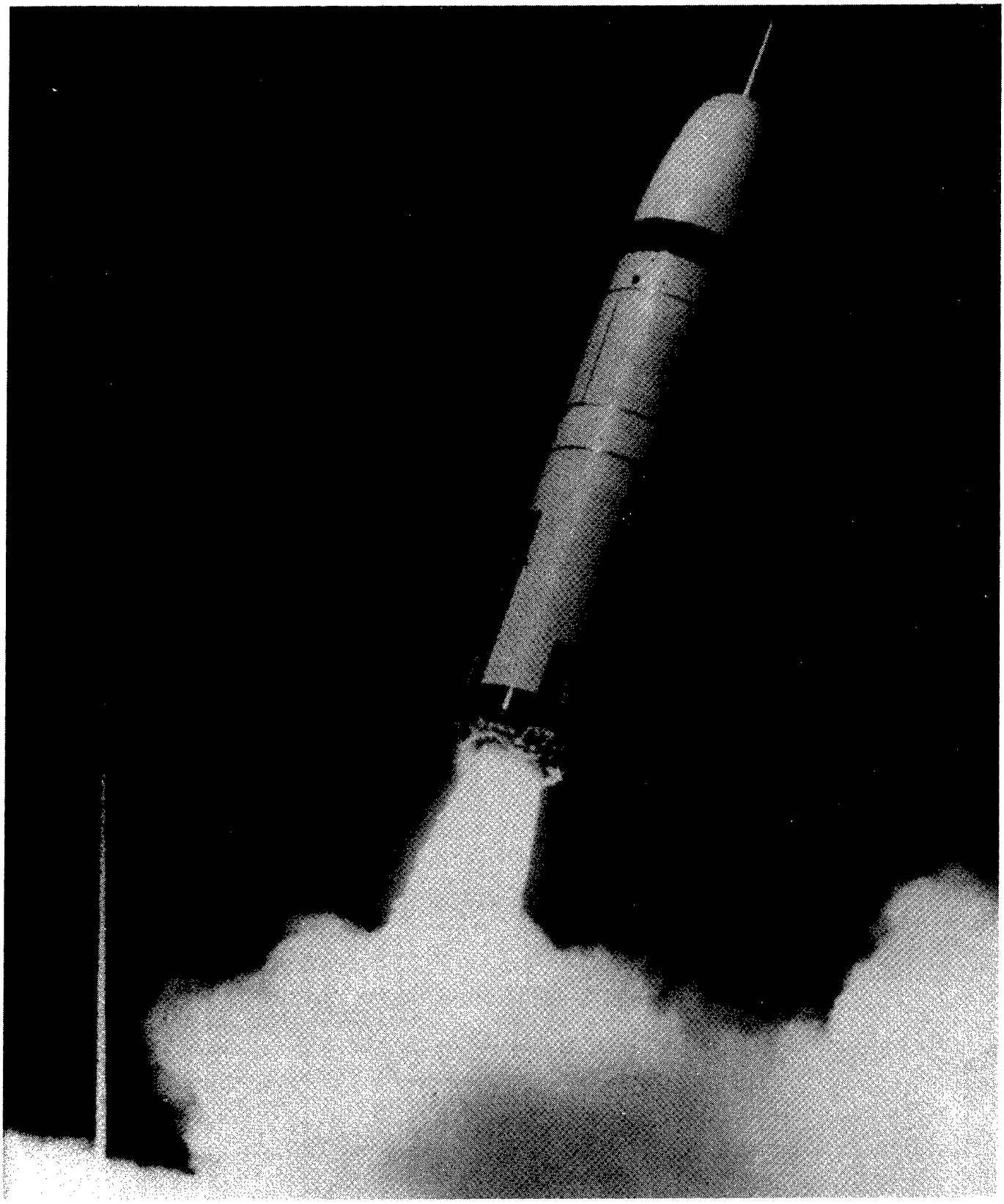

Trident I Launch at Cape Canaveral

FRONTISPIECE

PREDICTIONS OF NUISANCE DAMAGE AND HAZARD FROM ACCIDENTAL EXPLOSIONS DURING TRIDENT MISSILE TEST FLIGHTS

INTRODUCTION

The Trident Explosion Problem

C-4 motor failures in static tests begun in 1974, prior to use of the C-4 in the Trident I missile (see frontispiece), have resulted in explosions. Fuels were the new high-performance VRA-7 and VOP XLDB (cross-linked, double-based), which are Class VII explosives. In contrast, lower performance, large solid missiles use Class II "explosive" fuels that destruct by conflagration rather than by detonation.

A Trident launch facility, built at Pad 25, Cape Canaveral Air Force Station (CCAFS), before C-4 motor explosions occurred and before the overpressure hazard potential was identified, is only 3 km from the city limits of Cape Canaveral (CC) and 5 km from the center of town (Figure 1). About 20 test flights from this location were planned for 1977-78 before Trident was scheduled for sea trials. An accidental explosion near the launch points during these tests could significantly damage the nearby community unless adequate precautions were taken.

Among the precautions taken were design of the missile motor and modification of the command destruct system to reduce the likelihood of an explosion under accidental or commanded flight termination. Although subsequent tests showed that these design changes were effective, it was not possible to assure absolutely that an explosion could not occur.

The U.S. Navy SSPO requested DOE assistance in addressing this explosion problem and its implications for Trident launch tests. Sandia Laboratories help on long range airblast propagation aspects was obtained, first through Los Alamos Scientific Laboratory (LASL), which conducted the explosives assessments, and later as a separately funded Sandia project under SSPO Purchase Order No. N0003076MD76024, dated 24 August 1976.

Background

Assessment of the impact of an explosion airblast wave on neighboring communities is conveniently made in the order of occurrence, that is, with descriptions of source, propagation, and effects.[1] First, the explosion magnitude had to be determined for some credible Trident accidents. Standard explosion airblast wave and propagation characteristics could then be defined for these events.

Second, atmospheric effects, which can modify standard airblast propagation,[2] must be considered to show the range of impacts that could result on neighboring communities, depending upon weather variables. And third, the effects on these communities, such as damage to window glass[3] and the possibility of hazards to individuals,[4] needed evaluation over the range of possible explosions and propagation conditions. The estimated severity of possible effects determines the type and level of control strategy that is necessary to minimize damage and hazard or, at least, to restrict these insults to acceptable levels. In a blast prediction exercise, no attempt is made to define the "acceptable" level of insult. Management must determine what controls are acceptable and cost-effective under specific local political, economic, and environmental conditions.

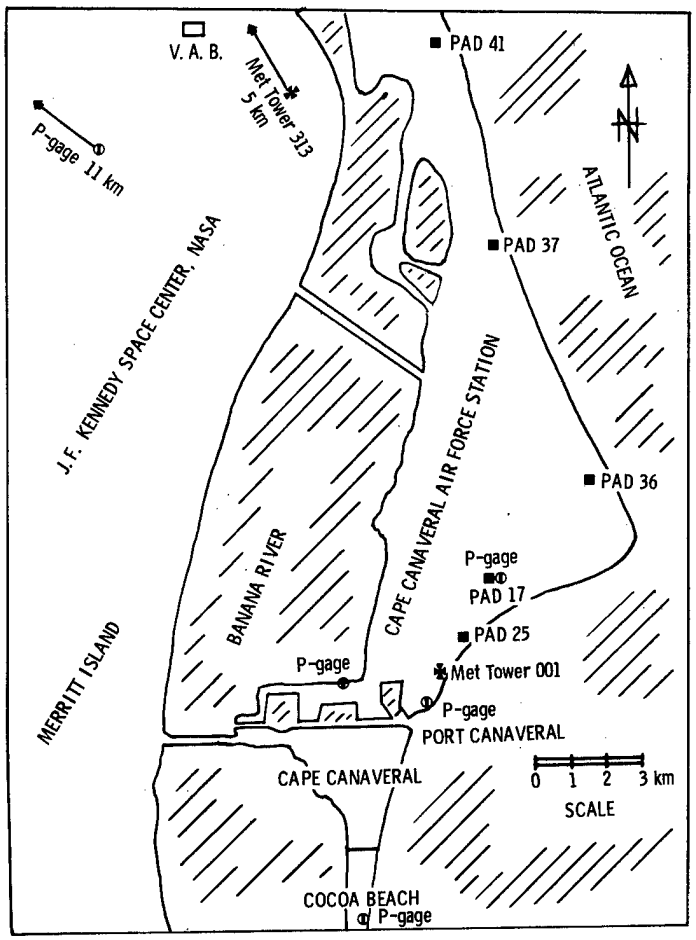

Figure 1. Map of Cape Canaveral, Florida, and Trident-Related Facilities

Project History

Preliminary discussions between SSPO, LASL, and Sandia representatives, in November 1975, established that the Trident explosion potential needed to be quantified to determine the potential threat of damage and hazard to the launch test-site neighborhood. A detailed assessment was ordered, to evaluate (1) the magnitude of damage and hazard that could result from a launch accident, (2) the damage levels associated with airblast propagation enhancement or attenuation, (3) the climatological probability of occurrence of important weather conditions, and (4) methods for limiting the damage potential to acceptable levels.

A review of weather records was made by the Eastern Test Range (ETR) Staff Weather Office and the Air Weather Service (AWS) station at CCAFS. Chemical explosion yield estimates were made by LASL. An on-site survey of CC buildings and windows was made by Sandia and LASL. The possibility of building structure damage was assessed by LASL. Results were assembled, propagation potentials were calculated, and preliminary probabilities were estimated in a draft Sandia report to SSPO, dated 27 February 1976. The conclusion was reached that minimized atmospheric airblast propagation was necessary to limit window damages to a few dozen panes in case of an accidental explosion during a Trident launch test. Under various combinations of weather conditions, however, airblast overpressures could break hundreds or even thousands of window panes which could cause injury from breaking or flying glass. Weather conditions for minimal propagation were found to occur sometime during about half of the days, and 2 or 3 days of delay could be expected for each test while awaiting such weather.

As a result of these conclusions, the SSPO considered moving the Trident launch complex north to a more remote pad, farther from CC. It was finally decided, however, to go ahead with test launches from the existing facility at Pad 25, while (1) accepting weather restrictions to limit damages in case of an accidental explosion and (2) using a low-flow trajectory to get the missile downrange from the launch site as quickly as possible.

A "weather-watch" procedure was developed by the CCAFS Weather Station incorporating balloon raobs of upper air conditions, meteorological tower measurements of the atmospheric boundary layer to a 150-metre height, real-time computer evaluation of atmospheric sound velocity (acoustic refraction) structure, and a video screen display of results. Sandia was tasked to provide blast prediction advisory service and to operate a network of blast pressure gages to document the blast waves in event of an accident. A set of launch weather criteria was adopted, requiring a moderately strong sound velocity-height gradient for the 210° azimuth (CC direction) and allowing no strong or focused propagation toward other communities in the SW-NW quadrant.

After eight Trident test launches without incident, Sandia participation was terminated for reasons of economy. CCAFS weather and ETR range safety organizations had developed adequate appreciation, understanding, and experience to make prelaunch evaluations without Sandia assistance. Confidence in Trident had

improved to the point where gaged records of accidental explosions were not deemed necessary.

During Trident operations, several efforts were undertaken to improve the credibility of blast predictions. In 1973, the Army Construction Engineering Research Laboratory (CERL) collected a large set of sound level meter data on propagations from 2.3 kg (5 lb) high explosive (HE).[5] These data were reviewed in hope of better defining the response of atmospheric propagation to boundary layer wind and temperature conditions. It turned out, however, that U.S. Army Corps of Engineers Construction Engineering Research Laboratory weather observations were inadequate for any clear resolution of a response function.

Also, Navy Surface Weapons Center (NSWC) was conducting Trident-related, 454 kg (1 000 lb) HE tests in 1977, at Dahlgren Naval Air Station, Virginia.[6] Blast gages and meteorological measurements were added for these events, with some encouraging results. On the other hand, their data showed one strong anomalous propagation that may be attributed to wind effects on height of burst (HOB) phenomena. A disturbing conclusion was reached from these two sets of small HE experiments. The wide and unexplained scatter in their results made the sound velocity gradient criteria, already adopted for Trident launches, appear rather optimistic.

Principles and procedures developed for Trident I tests are being used to evaluate test plans for future large missile systems. The next generation Trident II with a D-5 motor is being considered,[7] along with the USAF-MX and the STS-Space Shuttle. A test site should be selected where weather restrictions on acoustic propagation will not be prohibitive. A series of HE tests of propagation under carefully observed weather conditions is planned to resolve several questions and reduce the uncertainty associated with blast predictions.[8]

EVALUATION OF DAMAGE AND HAZARD POTENTIAL

Explosion Source Definition

Equivalent Yield Determination

The explosion yield potential for an intact detonation of a Trident I vehicle with a C-4 motor, was determined by Craig[9] to be the equivalent of 36 Mg (80 000 lb) HE (TNT) as a "best" estimate, with an upper limit of 45 Mg (100 000 lb) HE. For scaling from standard nuclear explosion phenomena,[10] two factors must be considered. First, at intermediate to long ranges, wherever pressures are below about 30 kPa (4 psi), 907 Mg (1 kt) HE gives about the same blast wave characteristics[10] as 1 814 Mg (2 kt) nuclear explosive (NE).* Also, a near-surface burst generates a hemispheric shock wave while a free-air burst emits a spherical wave,[1] so that the same overpressure may be observed at the same distance from a 907-Mg (1-kt) surface burst or a 1 814-Mg (2-kt) free-air burst. Thus, the conservative upper limit 45-Mg HE yield near the launch pad would have the same blast characteristics as 181-Mg (0.2-kt) NE free-air burst.

Standard Scaled Propagation

The standard overpressure-distance curve for a 907-Mg (1-kt) NE free-air burst at sea-level pressure altitude,[1] may be drawn for 181.4-Mg (0.2-kt) NE yield by using the simultaneous equations for explosion scaling,[10] which are

$$\frac{\Delta p}{\Delta p_o} = \frac{p}{p_o} \tag{1}$$

$$\frac{R}{R_o} = \left(\frac{W p_o}{W_o p}\right)^{1/3} \tag{2}$$

$$\frac{t}{t_o} = \left(\frac{W p_o}{W_o p}\right)^{1/3} \left(\frac{c_o}{c}\right) \tag{3}$$

for overpressure, radius, and time. Symbols are subscripted o for the reference explosion and are without subscripts for the predicted explosion. The scaled incident overpressure curve for 45.4 Mg (50 t) HE is shown in Figure 2, along with a short dotted section of the 36.3 Mg (40 t) "best" estimate curve.

Preliminary calculations for this project used an early hydrodynamic explosion wave model, called IBM Problem M,[11] and a power-law extension for $\Delta p < 2.55$ kPa

*The standard 907-Mg (1-kt) nuclear explosion releases 4.2 TJ total energy.

that followed $\Delta p \sim R^{-1.2}$ (see Reference 12). The recent Air Force Weapons Laboratory (AFWL) calculation[13] closely follows IBM Problem M for strong shocks, but decays like $\Delta p \sim R^{-1.1}$ in the far field of interest to Trident. Since Reference 1 is in the process of being reviewed for adoption by the American National Standards Institute (ANSI), $R^{-1.1}$ decay was used for this report. Within the limits of measurement accuracy and repeatability, there may be no significant difference between these two explosion models.

Atmospheric Effects on Propagated Overpressures

Range of Possible Overpressures

In the far field of atmospheric propagation, incident overpressures are usually doubled by ground reflection. Recording pressure gages observe values shown by the curve in Figure 2 that is labelled "gage (reflected)."

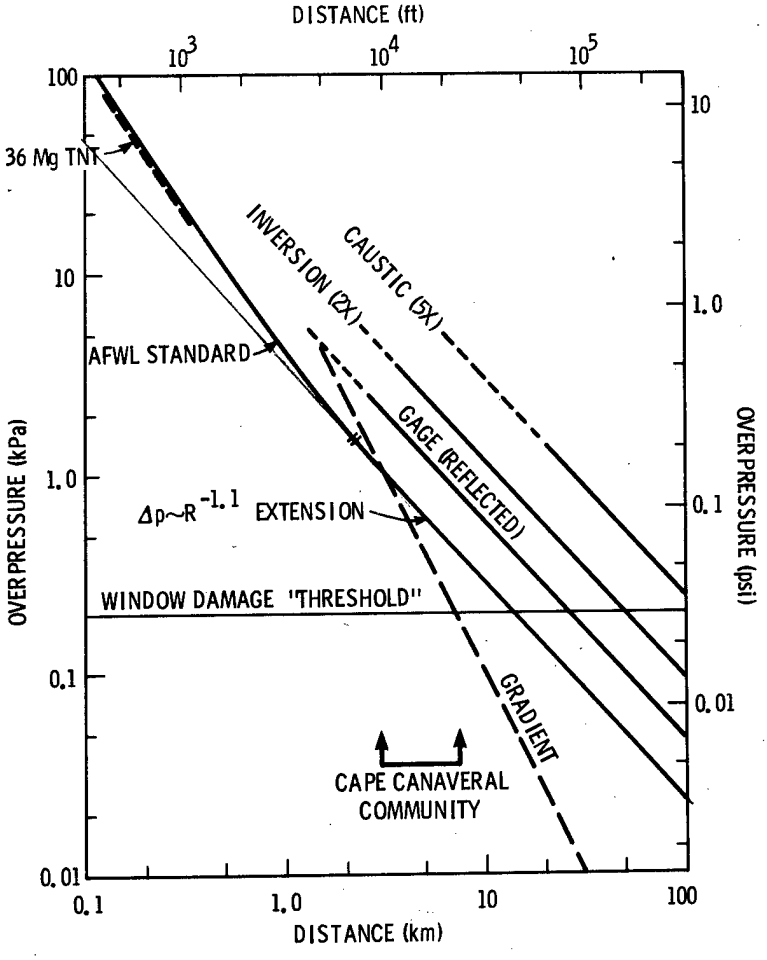

Figure 2. Airblast Predictions for 45.4 Mg HE Equivalent Surface Burst

Atmospheric refraction can duct, or even focus, blast waves. The curve labelled "inversion" is for boundary layer ducting under a surface temperature inversion or in downwind directions. Complex refraction may generate "caustic" curve conditions from focusing by high-speed winds at heights well above ground level.[2] The inversion curve shows 2X blast amplitude magnification; the caustic focus factor is 5X. Both magnifications are rough upper bounds of our experience,[14] although there are ample indications that they may, on occasion, be exceeded. More typically, average inversion magnification is near 1.5X.[14] Caustic magnification averages near 2X over a distance range of ±30% from a calculated ray-path caustic.[15]

Conversely, when there is a strong vertical temperature gradient, propagation in upwind directions will be greatly reduced as the blast wave is refracted away from the ground, gages, and structures.[16] In result, the "gradient" curve represents a typical overpressure-distance condition that can often be found by selecting the weather.[17 18]

The "window threshold" at 200-Pa-gaged overpressure is based upon observations of atmospheric nuclear tests[14 19-21] made in Las Vegas, Nevada, and St. George, Utah. Sonic boom investigations, as well as accidental explosion incidents, have proven that this threshold line should be painted with a very broad brush.[3 22 23] Nevertheless, under even the best of weather and propagation conditions, the town of Cape Canaveral falls entirely within range of this window damage threshold condition. Therefore, a weather watch appeared needed to identify propagation conditions and hold damages down to a minimum nuisance level in the event of an accidental explosion during Trident tests.

These broad categories which have been described for enhanced or attenuated propagations did not appear to be very satisfactory for real-time decision making in a Trident test countdown. Some continuous functional relationship was needed between atmospheric conditions and expected airblast enhancement. Such a relationship had never been previously determined because it was never seriously required for the conduct of large explosion tests.

Trident's problem falls in the class of "intermediate" range propagation. Expected overpressures at CC are below the "close-in" range of concern with militarily interesting airblasts that have been extensively explored.[10] In addition, large explosion tests have been located at "long" range from any community, so that only infrequent strong atmospheric enhancements of propagation have caused nuisance damages or interfered with testing. In previous tests, the yield-scaled distance from Pad 25 to CC fell either within a test reservation, overwater, or on a sparsely populated desert. To understand and appreciate the Trident problem and the prediction uncertainties that are involved, atmospheric acoustic refraction must be considered.

Atmospheric Refraction

Temperature Effects -- Sound speed in air is proportional to the square root of the (absolute) air temperature. Over the range of temperatures found in the troposphere (below ~10 km altitude), sound speed may be estimated from

$$c = 20.55 T_K^{\frac{1}{2}} \text{ (m/s)}$$

$$= 1088 \sqrt{1 + \frac{T_C}{273}} \simeq 1088 + 2T_C \text{ (ft/s)} \quad (4)$$

In temperate latitudes, Standard Atmosphere[24] temperature decreases with height at -6.5 K/km (-2°C/1 000 ft). On sunny days with convection currents, or with at least moderate wind speeds to cause mechanical mixing, a -10 K/km (-3°C/1 000 ft) adiabatic lapse rate[25] is established. Sound speed decreases ~6 m/s per kilometer of altitude (-0.006 s^{-1}) in an adiabatic atmosphere.

To illustrate the refraction effect of a sound speed gradient, assume a vertical line sound source extended above the ground as shown in Figure 3a. Cylindrical acoustic emissions would travel slower from the top than from the bottom of this line.

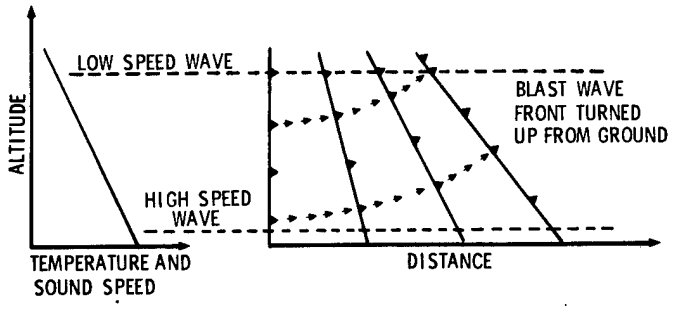

A. TEMPERATURE DECREASING WITH ALTITUDE (GRADIENT)

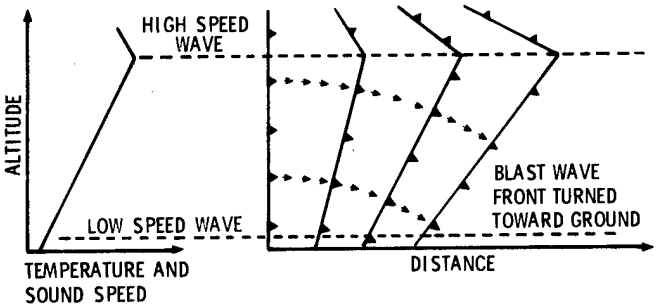

B. TEMPERATURE INCREASING WITH ALTITUDE (INVERSION)

Figure 3. Blast Wave Distortion Caused by Atmospheric Conditions

The front of a sound wave would be increasingly inclined from the vertical as it propagates. An associated sound ray, perpendicular to this front, would thus be gradually turned away from ground along a circular path (for a linear gradient).[2] Some acoustic energy would be scattered or diffracted into the "silent" zone below the lowest ray path.

Wind Effects -- Conversely, if the wind increased from a surface calm to 12 m/s at 1 000 metres altitude in adiabatic thermal conditions, downwind propagation at the top would be 6 m/s faster than at ground level, and sound rays would be bent toward the surface as shown in Figure 3b. In general terms, whenever directed sound velocity (sound speed plus directed wind component) at any altitude exceeds the surface value for that direction, some of the sound emitted by a ground-level sound radiator will be trapped in a sound duct along the ground.[2] Thus restricted from spherical wave expansion, a point source explosion wave would maintain its intensity to increased distance.

Ground friction slows the wind flow to zero immediately on the surface. With a moderate surface wind, and neutral thermodynamic stability (adiabatic lapse rate), the wind speed over open flat terrain typically increases in proportion to the one-seventh power of height above this surface.[26] Thus, sound speed plus wind gives sound velocity as a function of height above the "surface" observation level[27] (with o subscripted values), following

$$V(z) = c\ (z) + u(z) \tag{5}$$

$$= c_o - \alpha z + u_o (z/z_o)^{1/7}$$

The top of a downwind duct would be where

$$\frac{dV}{dz} = 0 = -\alpha + 1/7\ u_o (z_o z^6)^{-1/7} \tag{6}$$

Reference to standard anemometer height z_o = 10 m,[27] and with an adiabatic lapse rate, the duct depth in metres is

$$z = 27.5\ (u_o)^{7/6} \tag{7}$$

Thus, even with light wind speeds, there would be some downwind blast ducting. Observations of transportation noises[28] have shown qualitative verification of this downwind sound enhancement.

Inversion Propagation -- Intuition indicates that propagation enhancement by a sound velocity inversion (increase with height) should depend upon both the depth and strength (velocity difference) of the inversion. A simplified model was developed for inversion ducting which limits a surface burst explosion wave to cylindrical expansion (rather than hemispherical) as shown in Figure 4. It was assumed that beyond the radius R_p, where the highest ducted ray is refracted to horizontal

travel (turnover), the ducted wave front is confined to cylindrical rather than spherical expansion. This radius is defined by[2]

$$R_p = z_p \sqrt{\frac{V_p + V_o}{V_p - V_o}} \tag{8}$$

This limiting ray was emitted from the point source with an elevation angle defined by

$$\cos \theta_p = V_o/V_p \tag{9}$$

In unrefracted spherical expansion to R_p, the energy emitted over $0 \leq \theta \leq \theta_p$ would be distributed uniformly over a frontal surface area

$$A = 2\pi R_p^2 \sin \theta_p \tag{10}$$

so the energy propagated through this spherical surface is

$$E = k\Delta p_s^2 \cdot 2\pi R_p^2 \sin \theta_p \tag{11}$$

where the subscript s designates the standard spherical explosion overpressure at distance R_p.

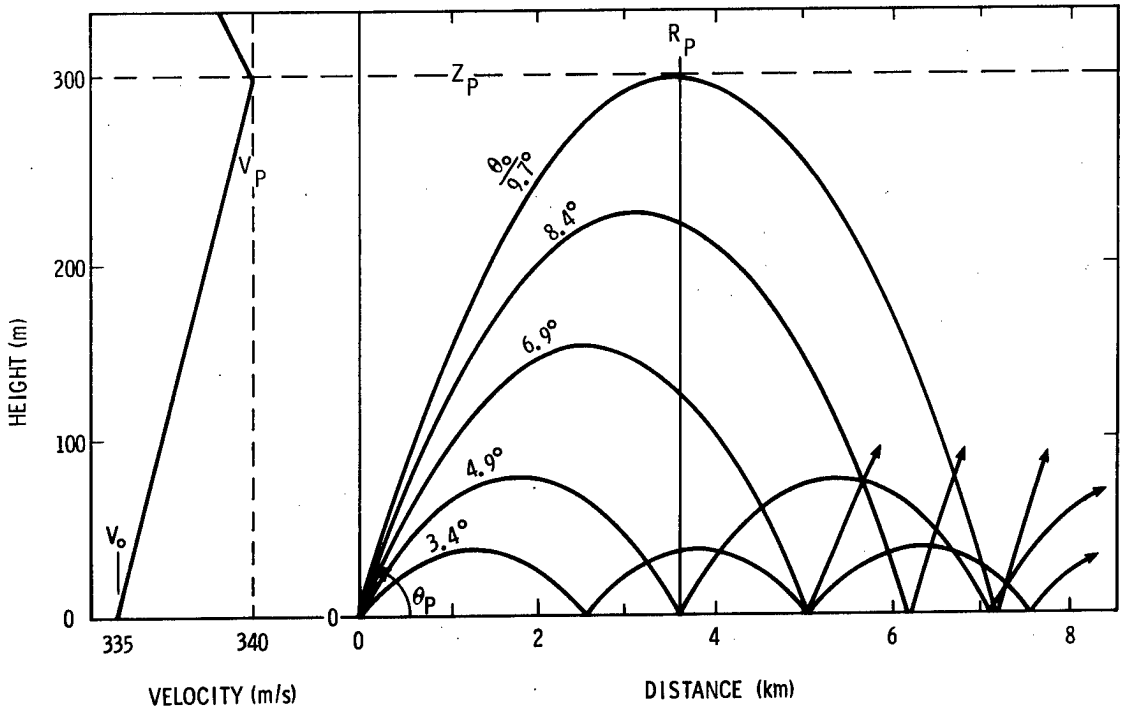

Figure 4. Inversion Propagation Model and Acoustic Ray Paths

Confined to a cylinder, this same energy would be given by

$$E = k\Delta p_c^2 \cdot 2\pi R_p z_p \tag{12}$$

where Δp_c is the cylindrical wave overpressure. The ratio

$$(\Delta p_c/\Delta p_s)^2 = z_p^{-1} R_p \sin \theta_p \tag{13}$$

results in

$$\Delta p_c/\Delta p_s = (R_p/z_p)^{1/2}\left[1 - (V_o/V_p)^2\right]^{1/4} \tag{14}$$

combined with Eq. (8), z_p is cancelled out, leaving an independence of layer thickness. The remainder reduces to

$$\Delta p_c/\Delta p_s = \left(1 + \frac{V_o}{V_p}\right)^{1/2} \simeq 2^{1/2} \tag{15}$$

since V_p is usually less than a few percent larger than V_o. Thus, from acoustic ray considerations, any inversion would cause approximately constant enhancement of propagation.

The trouble with such a simple model is that airblast frontal energy is not uniformly spread at R_p, as the example in Figure 4 clearly shows. Divergence of ray tubes is greater for the higher emission angles. In this example, 35% as much energy is ducted below the 3.4° ray as below the 9.7° ray but in a layer that is only one-eighth as deep. In addition, the 9.7° ray is calculated to arrive at $2R_p$ at 21.294 seconds, the 4.9° ray reaches that distance at 21.372 seconds, and the 0° ray arrives at 21.397 seconds. There would be 103 ms separation between these multipath arrivals. With a 907-Mg (1-kt) NE source and a 375-ms overpressure phase duration, the dispersion would not be significant because arrivals would appear roughly in phase. With a 45-kg HE, a 17-ms overpressure phase duration, and 67-ms total (positive and negative) wave duration, however, arrivals would be spread over an interval of nearly two wave periods. Further complicating an analytic solution is the fact that the later arrivals are reflected by the ground, and the reflection factor, though near unity for most incidence angles, depends upon incidence angle and approaches zero for 0° incidence. To the author's knowledge, there have been no adequate formulations for angle-dependent reflection factors, even with common ground types, for the relatively long wavelengths of explosion waves. A very substantial experimental program appears necessary to "solve" the inversion propagation problem in terms of inversion strength and depth, explosion yield, and ground surface acoustic reflective properties.

Gradient Propagation -- All acoustic rays from a surface source with a gradient atmosphere would be refracted upward and away from ground level targets or gages (see Figure 3a). Thus ray acoustics would predict no propagated disturbance, although diffraction and scattering mechanisms do cause measurable propagation into the "silent" or shadow zone. If there is any gradient ($dV/dz < 0$) there would be no overpressure propagation ($\Delta p/\Delta p_s = 0$). If there is a uniform atmosphere ($dV/dz = 0$) there would be radial spherical wave expansion and standard explosion wave propagation ($\Delta p/\Delta p_s = 1$). If the cylindrical expansion model is assumed for inversion ($dV/dz > 0$) propagation, constant amplification occurs ($\Delta p/\Delta p_s = 2^{1/2}$). This discontinuous result is probably rounded off by real conditions, so there should be a correlation (not necessarily linear) between boundary layer sound velocity difference and propagation attenuation or magnification. This correlation has not been adequately investigated.

To minimize blast propagation in a direction of specific concern (such as 210° azimuth from Launch Pad 25 to CC), the sound velocity should have a strong vertical gradient, and there should be no surface wind component toward that direction. During Trident test planning, it was assumed that $-0.005\ s^{-1}$ represented a "good" strong gradient for the lower 1 200 metres of atmosphere of concern to CC-directed propagation. Also, to allow for short term wind variations, a 0.6 m/s (2 ft/s) surface wind component away from CC was assumed necessary to assure adequate propagation attenuation under typically variable wind conditions.

Considerable concern was expressed that these criteria were unnecessarily restrictive, based as they were upon limited measurements under rather dissimilar conditions of weather, yield, and distance.[14 16 18] To refine our understanding, a preliminary reconsideration was given to a data set obtained by CERL.[5] Results, shown in Figure 5, indicate that a gradient stronger than $-0.005\ s^{-1}$ may be needed to assure acceptably weak propagations. There were a number of problems with the CERL experimental data,[29] in determining source strength, in establishing whether the sound level meters received incident or reflected peak amplitudes, and in estimating the atmospheric sound velocity structures. Further analyses are planned in hope of salvaging some better correlation function from this mass of CERL data (about 20 000 pressure measurements from 735 shots of 2.3 kg HE).

The NSWC test program[6] also provided a few data points from three explosions for evaluating amplification versus boundary layer sound velocity gradient. Results, shown in Figure 6, indicate an anomaly in that the strongest observed propagation occurred in the upwind direction from one event. That 454 kg HE was fired at 3 metres HOB, while the other two tests were fired at 1.5 metres HOB. This may indicate that upwind HOB effects are strengthened for some HOBs. Further exploration of this phenomena is planned.[8]

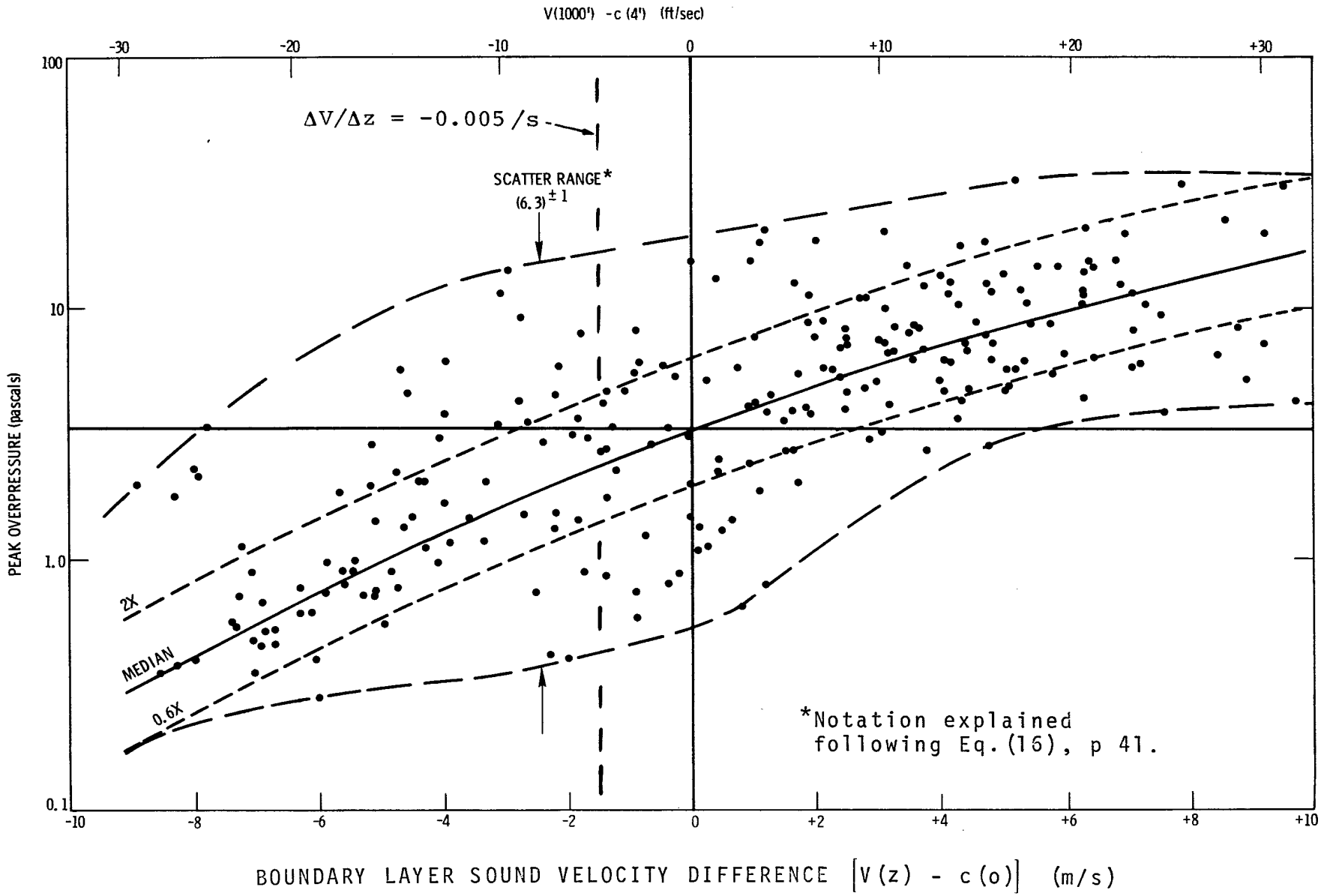

Figure 5. Summary of CERL Measurements at 2 mi (3.2 km) from 5 lb (2.3 kg) HE

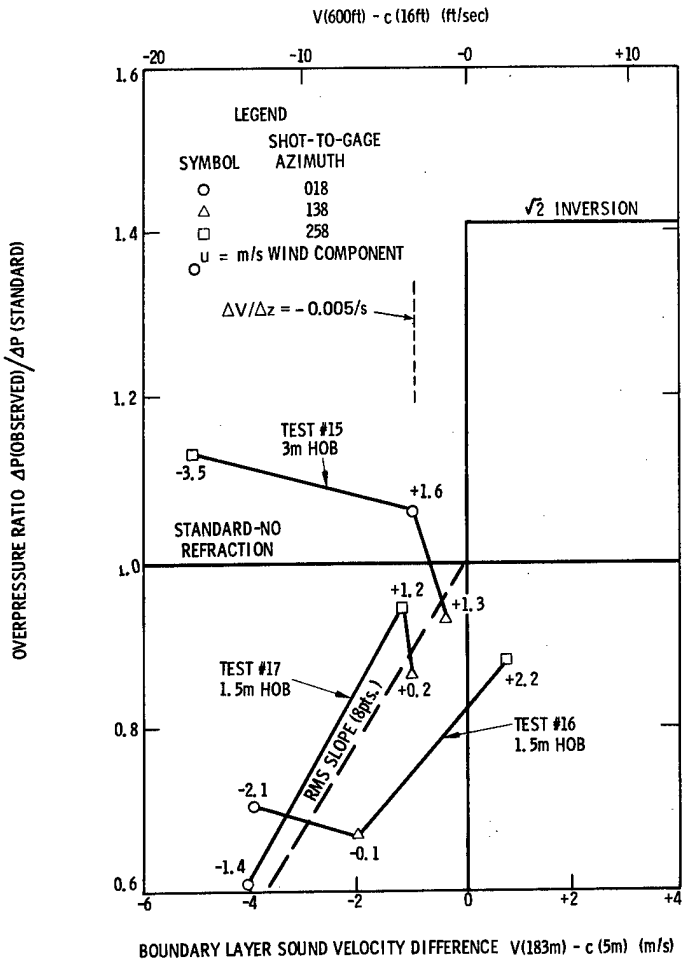

Figure 6. Summary of NSWC Measurements of Three 1 000 lb (454 kg) HE

Airblast Climatology

Propagation Condition Occurrences

Having assumed the weather conditions necessary to limit propagation toward CC, the expectation for "good" weather was assessed. Problems with the bulk and availability of data combined with changing specific demands for results as Trident test schedules changed resulted in a mixed collection of output from Sandia and ETR. The first assessment was made by Sandia from July to August 1975 raob reports. Next, an evaluation was made from October to December, 1974 and 1975, meteorological tower data. Finally, an hourly, daily, and monthly analysis of 1976 was made at ETR.

Radiosonde Data, Summer 1975 -- This analysis consisted of calculating the sound velocity difference versus height above ground, relative to sound velocity at the surface, in the 210° azimuth direction toward CC. Some typical sound velocity difference structures from raob data are shown in Figure 7 for a strong gradient,

for strong ducting, for moderate ducting, and for "marginal" conditions. Curves for each sounding made during July and August 1975 are shown in Figure 8. These curves were taken mostly from regular early morning balloon soundings, although there were some supplemental soundings made during the day. Conditions for each balloon run are graded in Table 1. In summary, shown by Table 2, 57% of the dates in July had a good gradient and no downwind component of wind, but only 33% of the August dates met these criteria. Conditions frequently run in long spells, both good and bad. As an extreme example, there were no good conditions observed after 20 August. If this condition were encountered by a scheduled test, it would require at least 11 days of delay.

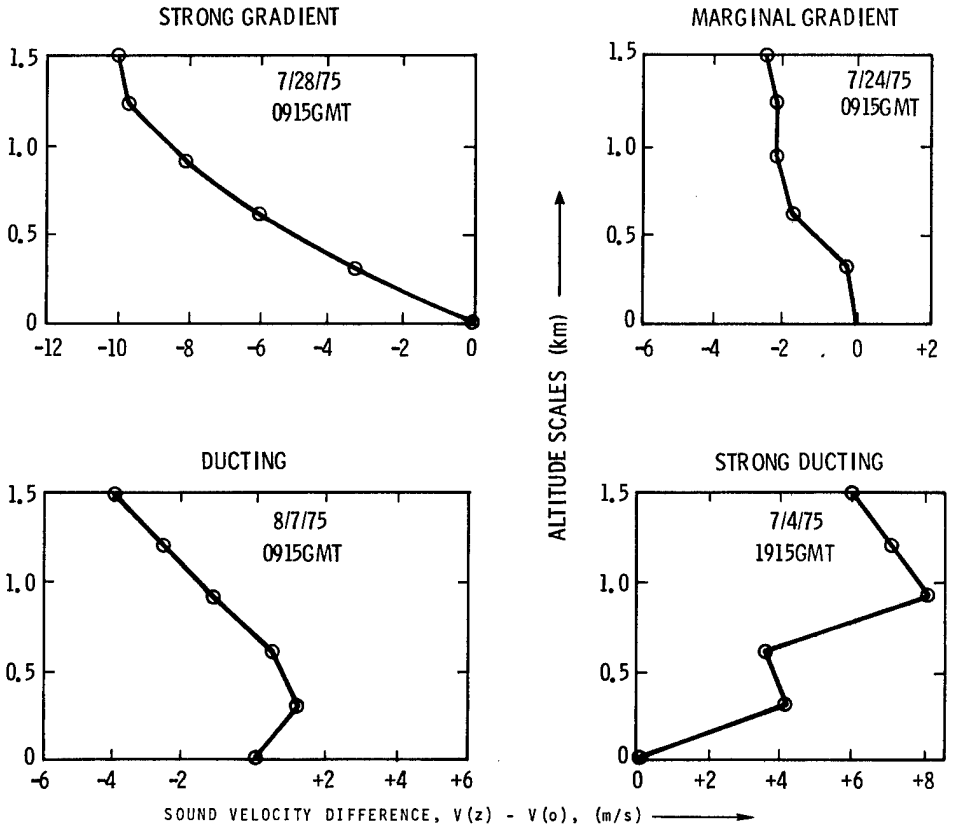

Figure 7. Selected Examples of Sound Velocity-Height Structures with Resultant Acoustic Propagation Conditions

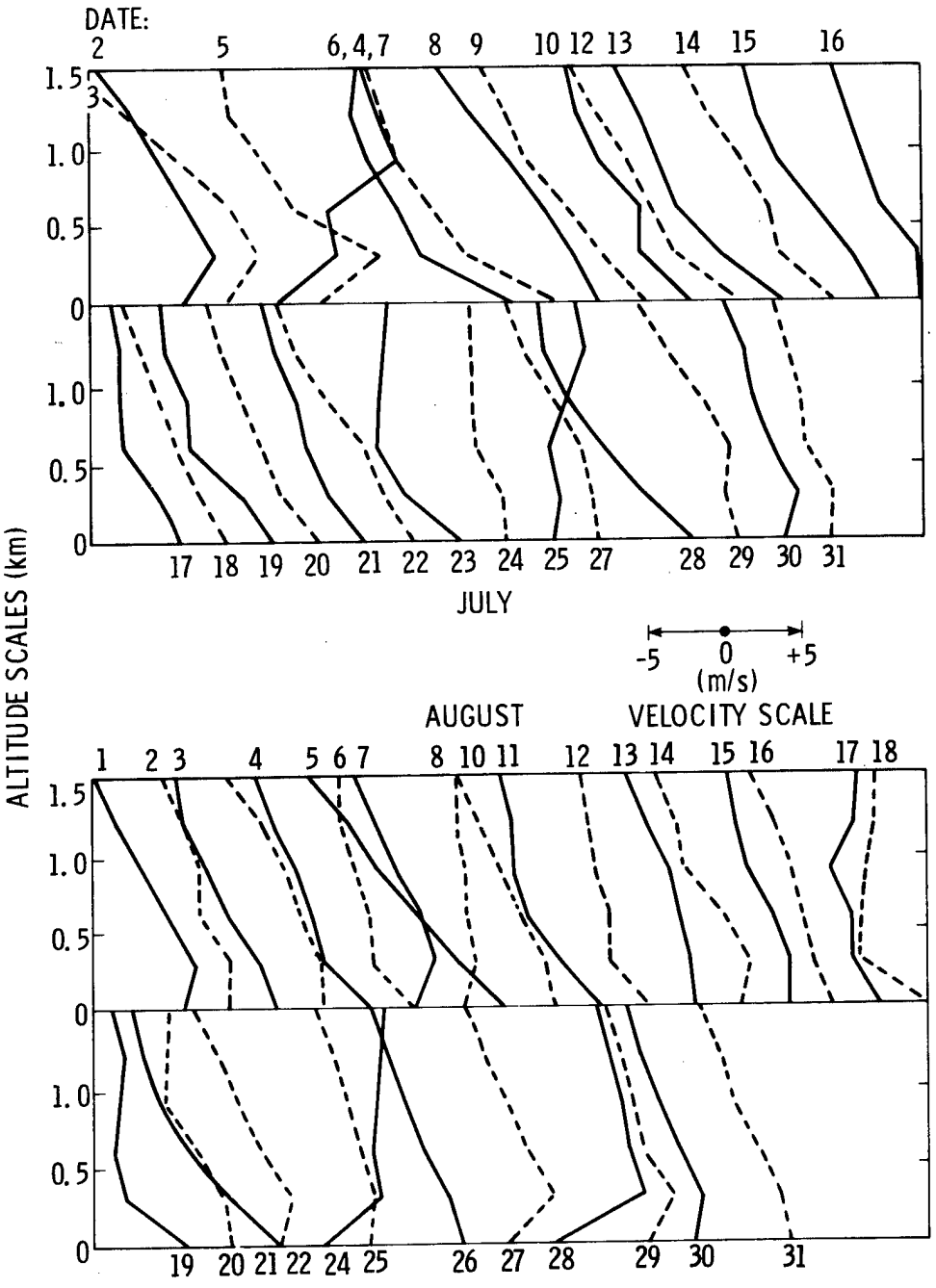

Figure 8. Sound Velocity versus Altitude, Cape Canaveral Rawinsondes

Table 1

Airblast Propagation Conditions, July and August 1975, Azimuth 210°

Cape Canaveral, Florida

July Date	Time (GMT)	Ducting	Downwind	Marginal	Good Gradient	August Date	Time (GMT)	Ducting	Downwind	Marginal	Good Gradient
2	1030	X				1	0915	X			
3	1118	X				1	1220		X		
4	1015	X				2	0940	X			
5	1015	X				3	0915				X
6	1015				X	4	0915			X	
7	1015				X	5	1607				X
8	0930				X	6	0915				X
9	0930				X	6	2019			X	
10	0930				X	7	0915	X			
12	0915				X	7	1230				X
13	0915				X	8	0915	X			
14	0915				X	9	0915		X		
14	1350				X	10	0915			X	
15	0700				X	11	0659				X
15	1350		X			11	0900				X
15	2000		X			11	1559				X
16	0915		X			11	2100				X
17	0915				X	12	0915				X
18	0915		X			12	1240				X
19	0915		X			13	0915			X	
20	0915				X	14	0915	X			
21	0930				X	15	0915	X			
22	0915				X	15	1349		X		
23	0915				X	16	0915				X
24	0915			X		17	0915			X	
24	1350		X			18	0915				X
24	1715		X			19	0915				X
25	0915	X				19	1130				X
27	0915			X		20	0922			X	
28	0915				X	20	1222				X
28	1250				X	21	1309		X		
29	0915			X		22	0930	X			
30	0915	X				24	0915	X			
30	1330				X	25	0700	X			
31	0915	X				25	0915	X			
						26	0142	X			
						26	0252		X		
						26	0915	X			
						27	0818	X			
						28	0915	X			
						29	1730		X		
						29	1945		X		
						30	0915	X			
						31	0915			X	

Table 2

Summary of Acoustic Propagation Occurrence Statistics from Rawinsonde Observations, 210° Azimuth

	July 1975		August 1975	
	Days	%	Days	%
Days with raobs*	28	100	30	100
Days with good gradients	16	57	10	33
Days with marginal conditions	3	11	7	23
Days with downwind propagations	5	18	6	20
Days with ducting propagations	7	25	13	43

*Sums do not give 100% for "Days with raobs" because the several soundings on a given day might contain several categories of conditions.

Tower Data, Fall 1974-75 -- Meteorological tower data were recorded throughout the day, so October-December analyses for good test days were made from both 1200 GMT (0700 EST) and 1800 GMT (1300 EST) observations. Near midday and near the diurnal maximum of surface temperature, conditions were expected to be better than at early morning 1000 GMT raob ascension time or near sunrise at 1200 GMT Results, summarized in Table 3, show the percentage of days in each of three categories. Two years of climatological data were insufficient to establish statistical confidence levels in these figures.

Table 3

Summary of Propagation Conditions from Meteorological Tower Observations, 210° Azimuth, 1974-75

Occurrences (%)

	1200 GMT			1800 GMT		
Month	Very Good	Marginal	Total	Very Good	Marginal	Total
October	4.1	8.2	12.3	5.1	3.9	9.0
November	16.7	6.7	23.4	15.5	17.2	32.7
December	24.6	14.0	38.6	24.6	17.5	42.1

A strong gradient ($dV/dz \leq -0.005\ s^{-1}$) was categorized as a very good condition. Weaker gradients ($-0.005 < \frac{dV}{dz} \leq 0\ s^{-1}$) were categorized as marginal conditions. There probably were earlier or later hours on those dates when very good conditions occurred. It appeared that fall was not a very good season for launch tests, and that winter conditions were nearly as good as summer (Table 2). Although favorably high surface temperatures were observed in summer, in winter, there were a number of favorable prefrontal southwest winds observed.

Tower Data, 1976 -- An evaluation of 11 months of 1976 tower weather conditions was made by ETR[30] with results summarized in Tables 4 and 5. Although only from 4% to 38% of hourly observations showed GO conditions, depending upon the month, there was at least one hourly observation of satisfactory weather and propagation conditions on 48% of the days. The worst operational conditions occurred in November and January, and the best appeared in July. The percentages for 1976 do not agree well with those of 1974 and 1975 (Tables 2 and 3), but differences were probably caused by year-to-year variations in general circulation. Again, statistical confidence levels should not be attempted from so short a data set.

Table 4

Occurrence of Hourly Propagation Conditions,
210° Azimuth, 1976

	Occurrences (%)	
Month	GO	NO GO
January	7.1	92.9
February	25.2	74.8
March	25.8	74.2
April	14.6	85.4
May	25.5	74.5
June	16.2	83.8
July	37.7	62.3
August	4.9	95.1
September	6.1	93.9
October	8.2	91.8
November	4.4	95.6

Table 5

Summary of Days with at Least 1 Hour of GO
Propagation Conditions, 210° Azimuth, 1976

	Occurrences (%)	
Month	GO	NO GO
January	21.4	78.6
February	60.7	39.3
March	64.5	35.5
April	42.9	57.1
May	67.7	32.3
June	40.0	60.0
July	90.0	10.0
August	38.7	71.3
September	50.0	50.0
October	29.0	71.0
November	23.3	76.7
11-Month Average	48.2	51.8

It thus appeared from various analyses that there is a significant probability of requiring a weather delay at any time of year, but there are no prohibitive odds against GO conditions during any specific month. This contrasts with problems which have surfaced at other explosion test sites where only a few "good enough" days occur per year. It appeared that 1 to 3 days delay should be expected for each scheduled Trident test flight.

Cape Canaveral Sea Breeze -- A detailed investigation of meteorological tower data showed that a relatively strong summer sea breeze[31] tended to enhance propagation conditions toward CC during the warmest time of day. The diurnal sea breeze oscillation is shown by a schematic ellipse in Figure 9. The average sea breeze vector should be added to the general circulation wind vector (obtained from the isobar pattern on a synoptic weather map) to estimate the total observed wind vector for a specified time. Average sea breeze vectors for each hour and month are shown in Figures 10 and 11 and for cool and warm half-years, respectively. Twenty-four hourly points are connected for 3.6-metre and for 151-metre heights, but only 6-hourly points are shown at 16-metre, 49-metre, and 62-metre heights. Detailed numerical results are tabulated in Appendix A.

Most of these diagrams show that the sea breeze component toward CC is at or near its diurnal maximum during midday or early afternoon. Diurnal curves of CC-directed surface winds are shown in Figures 12a through 12c, for three heights. Note that the vertical scale of Figure 12c is one-fourth the scale of lower height figures to accommodate a large amplitude in July. Conditions were worsened by winds during the day at the same time as surface heating tended to weaken propagation conditions. Thus, no general conclusion could be reached as to the best hour for scheduling launches, except that in early morning, with minimum surface temperature conditions, enhanced propagations were usually observed. Short term predictions, for consideration during a launch countdown, depend upon combined and daily-varying influences of boundary layer temperature structure, diurnal temperature oscillation (which is dependent upon cloudiness), general wind circulation, and sea breeze oscillation.

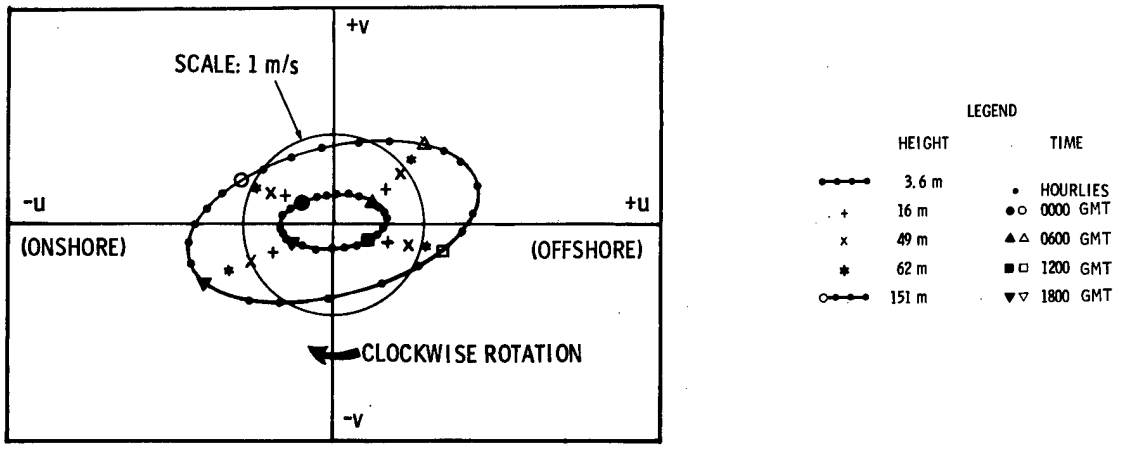

Figure 9. Schematic Sea-Breeze Vector Oscillation Diagram

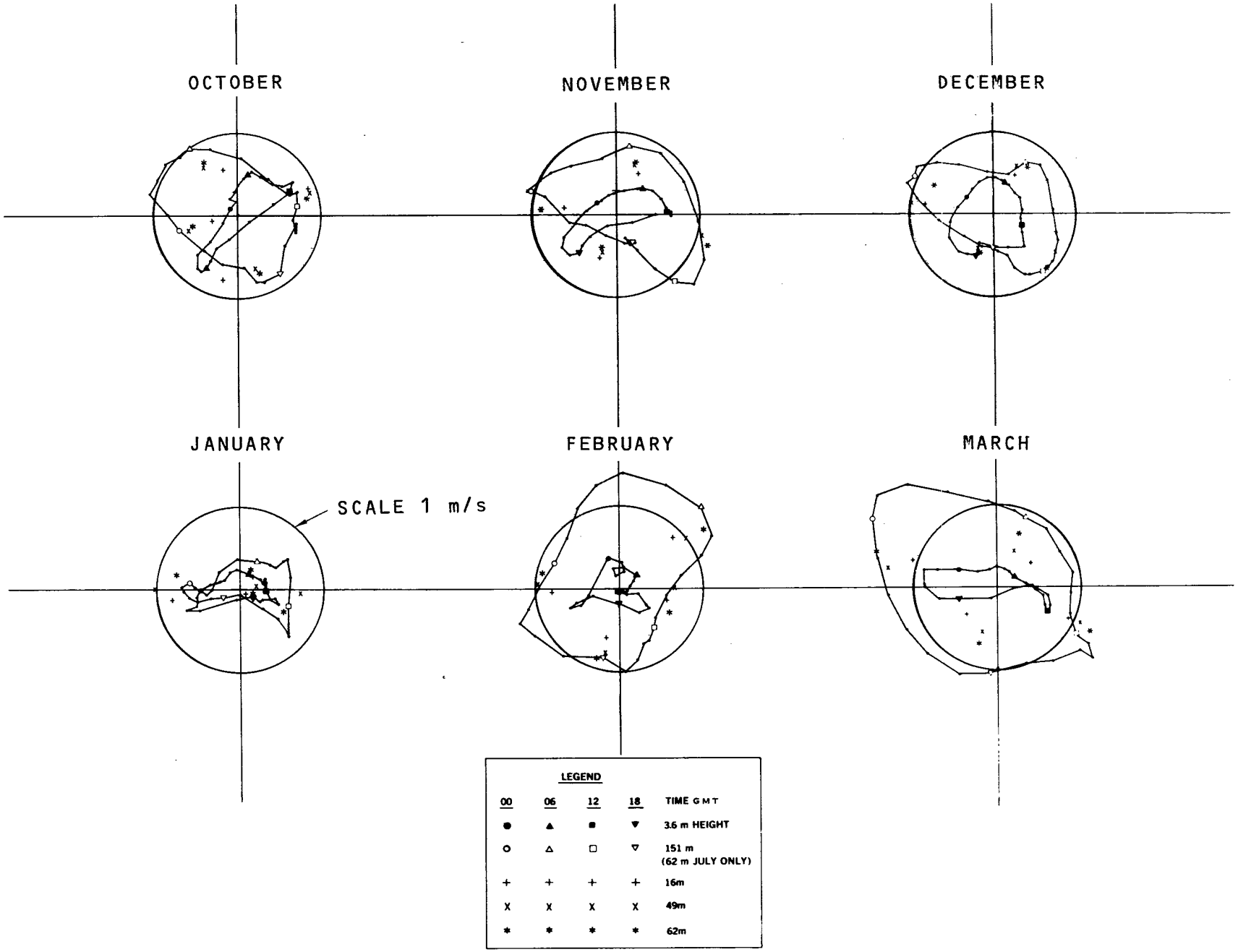

Figure 10. Cape Canaveral Diurnal Sea-Breeze Oscillations at Five Heights, October through March

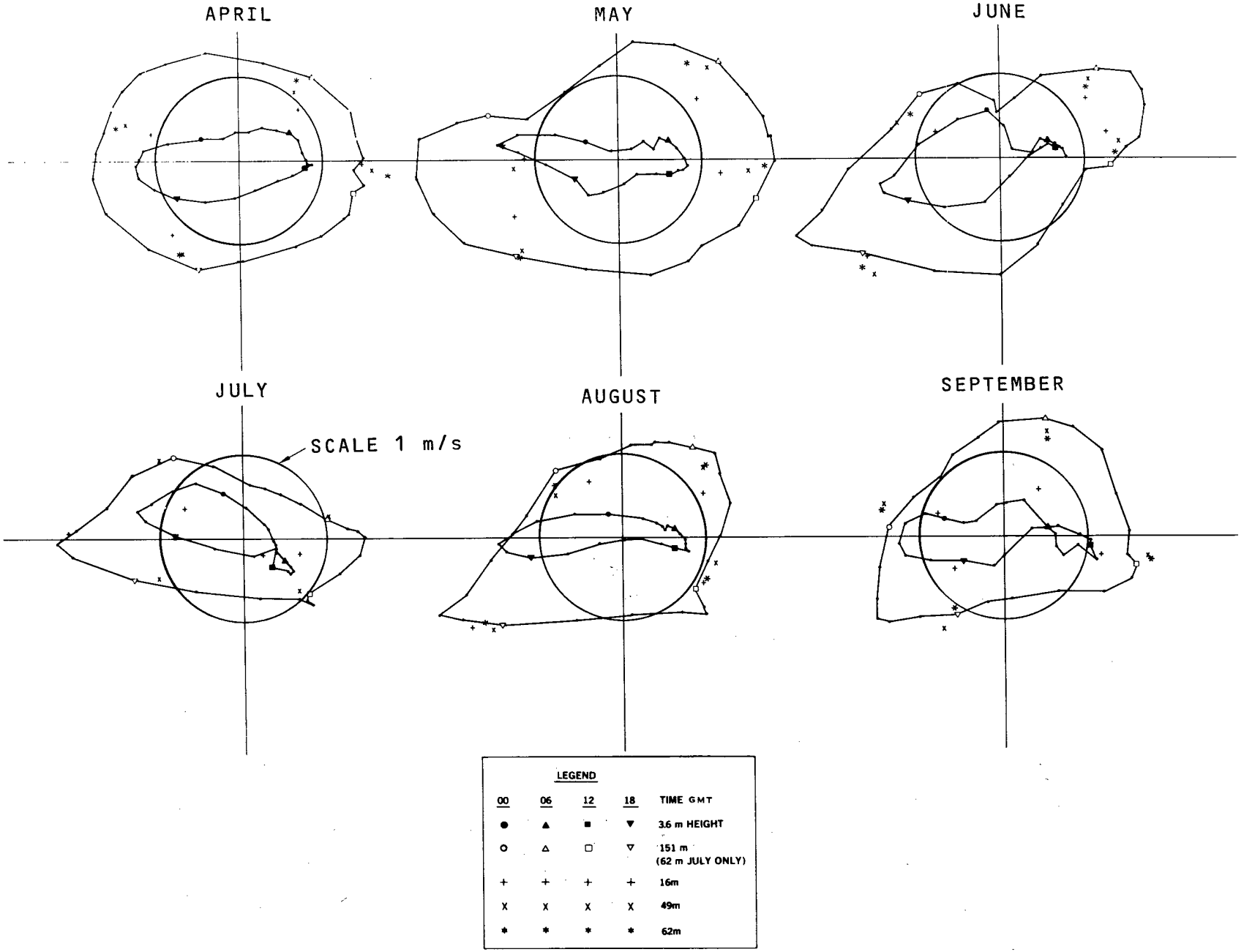

Figure 11. Cape Canaveral Diurnal Sea-Breeze Oscillations at Five Heights, April through September

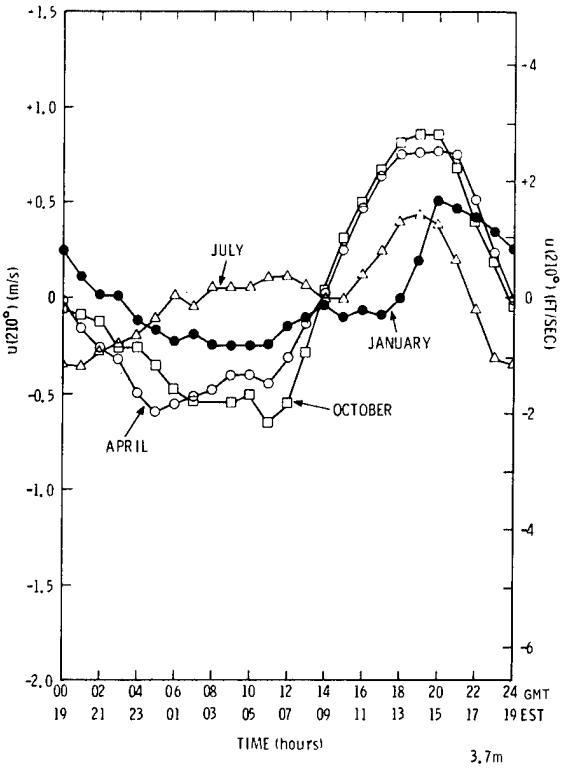

a.

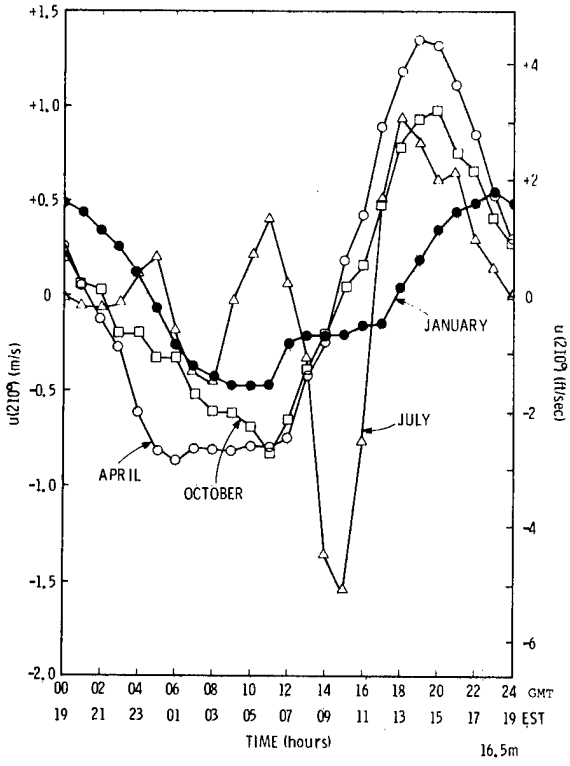

b.

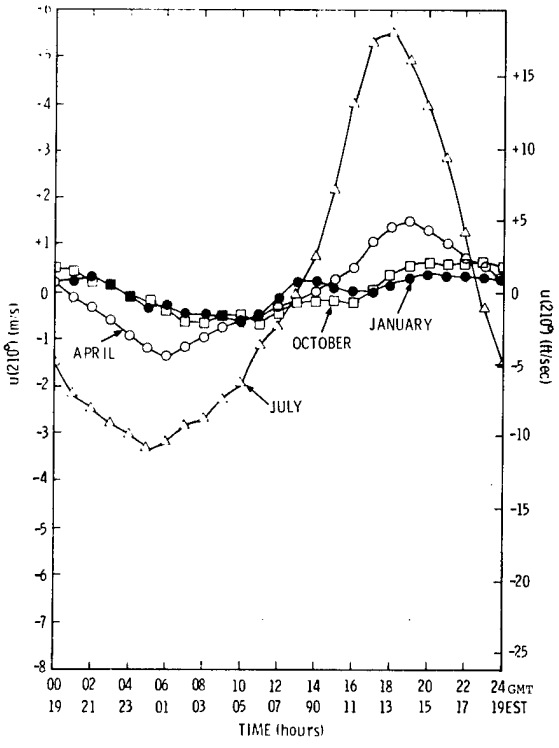

c.

Figure 12. CC-Directed Sea Breeze Components

Diurnal Temperature and Wind Effects on Propagation -- Most raobs were released at CCAFS near 0900 GMT (0400 EST) and in relatively cool surface temperatures. In early afternoon, when surface temperatures reach their normal diurnal maximum, there would be a reduced chance of sound ducting expected in any direction. That would be true unless a diurnal sea breeze wind shift enhanced ducting in critical directions more than surface heating diminished ducting.

An "AWS Climatic Brief" showed that there was about 5.5 K (10°F) difference between average daily maximum and minimum temperatures. An assumed typical diurnal temperature curve is shown in Figure 13. This indicates that surface temperatures were likely to drop 0.5 K (1°F) below the 0400 EST sounding value to a minimum at 0600 EST, and then rise to a peak at 1400 EST of 5 K (9°F) above the value at raob time.

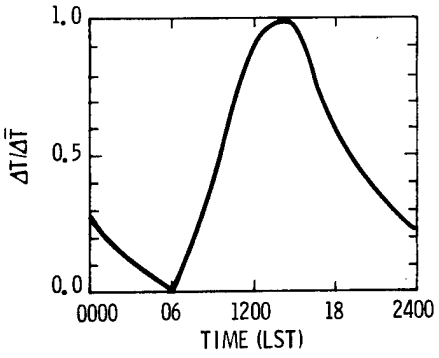

Figure 13. Typical Diurnal Temperature Curve

Sea breeze winds were combined with the assumed 5.5 K diurnal temperature wave to generate diurnal curves for the change of sound velocity, at surface level, toward 210° (CC) in Figure 14 and toward 310° (Titusville) in Figure 15. These figures show that, relative to a typical 0400 EST raob, sound velocity toward both 210° and 310° would rise about 4.5 m/s by early afternoon in June and about 3.5 m/s in January. There would thus be considerable reduction in blast propagation potential from upper air conditions as a typical morning progressed, since upper air conditions vary little with time of day.

To summarize diurnal weather effects on propagation, it appears that during most of the year only about 1 to 2 m/s average circulation component away from CC is necessary to prevent the afternoon sea breeze from causing a CC-directed wind component. In summer, however, when the sea breeze intensity is at its peak, more than 5 m/s average circulation away from CC is needed at 150 metres to avoid midday winds that could enhance propagation. When acoustic ducting is indicated toward either 210° or 310° from an early morning raob, about 4 m/s improvement can usually be expected during the day from combined surface heating and sea breeze effects.

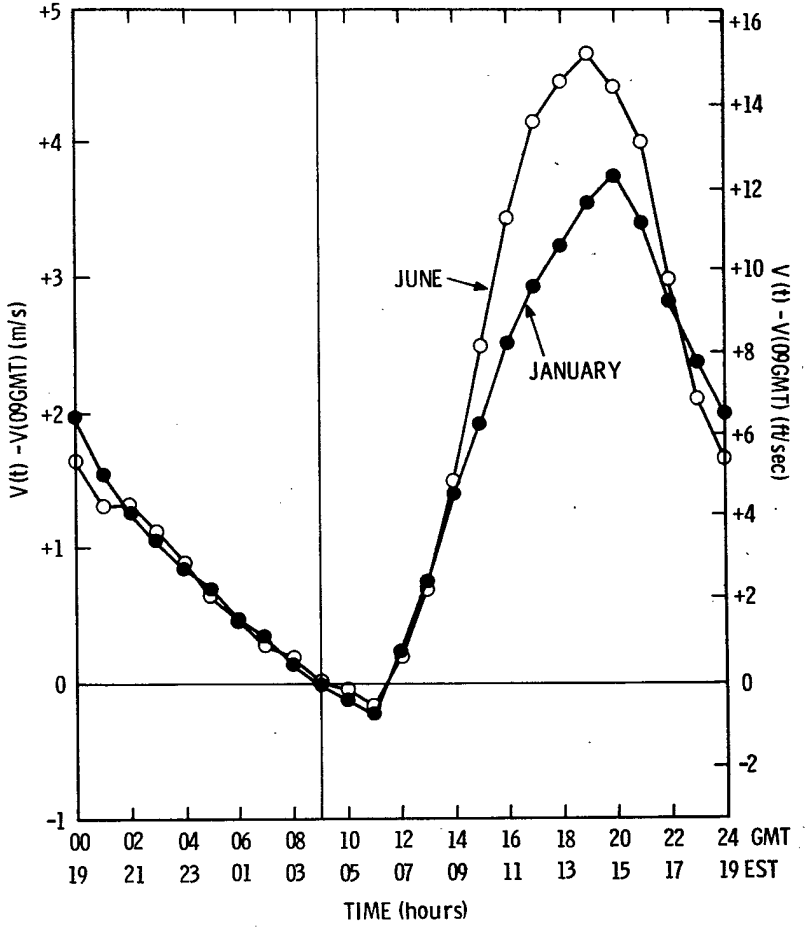

Figure 14. Diurnal Variation of Surface Sound Velocity, 210° Azimuth

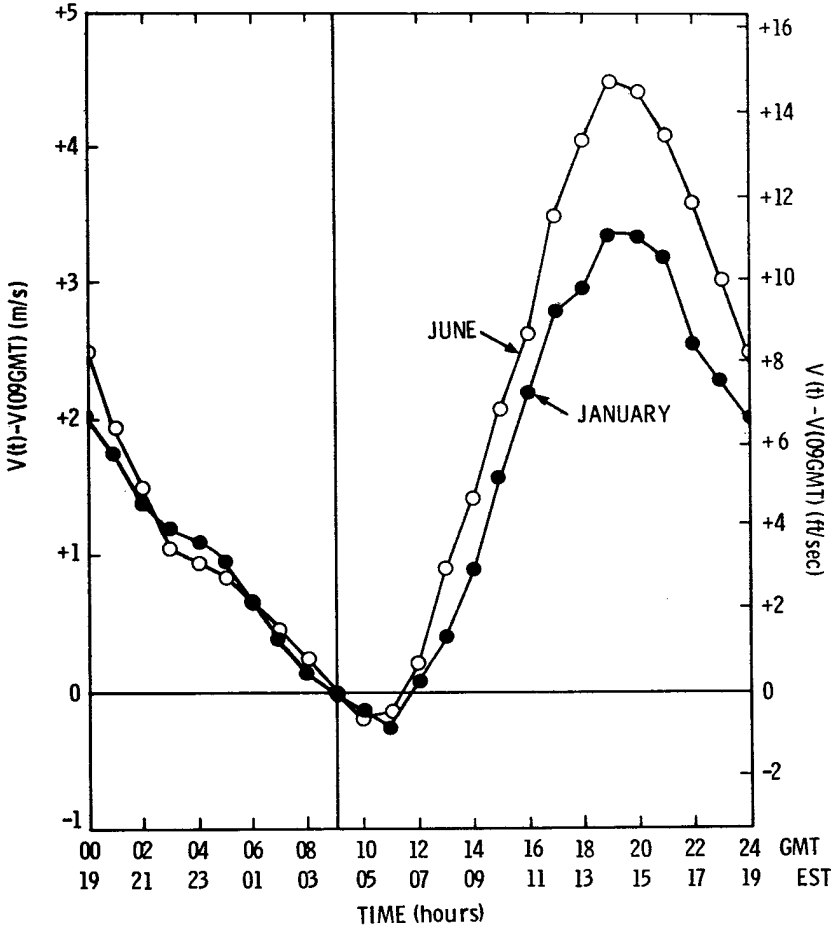

Figure 15. Diurnal Variation of Surface Sound Velocity, 310° Azimuth

Damage Assessment

General Procedure

As previously discussed, gradient propagation toward CC was required to avoid considerably exceeding the window damage threshold overpressure, given the assumption of a Trident I C-4 accidental explosion. Climatological evaluation showed that weather delay should be expected while waiting for suitable gradient conditions. The cost of such delay, involving hundreds, even thousands, of workers, could be significant. This cost had to be justified against the expectation of cost and hazard of an accidental explosion during a launch test with enhanced airblast propagation.

Damage to a community from an overpressure airblast wave is most easily quantified in terms of broken window panes.[3] Glass panes are simple structures, they are widely distributed, and they are often the first and most obvious things that are damaged by an airblast wave. There are, however, complications involved in relating imposed wave overpressure to glass breakage. The methodology has not yet been perfected, and large error in prediction is possible. Nevertheless, state-of-the-art methods have been used in hope of at least making order-of-magnitude estimates of the consequences of a Trident explosion.

The procedure followed was to first establish breakage probability functions of overpressure for typical CC windows. Next, a census of windows in CC was made. Then, for each of various atmospheric propagation assumptions and related overpressure-distance curves, the amount of expected damage was calculated. Finally, the potential injury hazard was established as a function of the amount of broken glass and the causative overpressure (missile velocity).

Glass Breakage Models

A lognormal probability model[32] for glass breakage versus airblast overpressure was developed[22] from damage evaluations of test structures at high overpressures[33] and the Medina Incident[3] at low overpressures. This relationship may be expressed as

$$b = 7.5 \times (2.5)^{\pm 1} \text{ (kPa)} \tag{16}$$

which means that 50% of the exposed panes will break with 7.5 kPa incident overpressure, and 15.87% (1σ) will break with $7.5/2.5 = 3$ kPa. A colloquial but equivalent statement of Eq. (16) is that an average pane would be broken by 7.5 kPa incident overpressure, within a factor of 2.5.

The lognormal statistical format[32] is used because of the large scatter in glass-breaking response. For example, in Eq. (16) the scatter would be $\pm 33\%$ in normal statistical format. This implies that 13 panes in 10 000 would break with no load, from the probability of exceeding a 3σ deviation.[34] Thus, a one-tailed distribution is necessary to describe extremely small probabilities of damage. Of

the popular one-tailed distribution functions, the lognormal has been used because it satisfactorily fits glass test results, and it is convenient to calculate and graph.

Close to an explosion, where the blast wave sphere (or hemisphere) moves radially from the source, a blast gage mounted side-on to wave passage (i.e., flush to the ground) would record this free-air incident overpressure. At longer ranges, atmospheric refraction usually causes the wave to strike ground at some incident angle so that ground reflection doubles the overpressure recorded by a ground-level pressure gage. Since far field window damage[3] was correlated against estimated incident overpressure in deriving Eq. (16), this same conclusion would hold for doubled gaged pressures. Thus, in the far field, a gaged 15 kPa would be required to break 50% of the exposed window panes.

Furthermore, this simplified equation pertains to the total pane population without regard to pane area, thickness, orientation, etc. For a specified pane distribution, such as was obtained by the survey of CC, separate probability curves are needed for each pane-size category.

Laboratory glass test data, reported by Ansevin,[35] showed that the mean tension breaking stress for common window glass was 102 MPa (14 816 psi), with a geometric standard deviation of $\sigma_g = 1.42$. Plate glass breaking stress was 66 MPa (9 600 psi), with $\sigma_g = 1.48$. The Marcus formula,[36] as stated by Bowles and Sugarman,[37] for maximum stress in uniformly loaded rectangular plates (neglecting membrane stress) is

$$f = \frac{3\Delta p}{4H^2}\left[\left(1 - \frac{5B^2L^2}{6(B^4 + L^4)}\right)\left(\frac{B^4L^2}{B^4 + L^4}\right)\left(1 + R\frac{B^2}{L^2}\right)\right] \qquad (17)$$

in terms of the uniform applied overpressure, pane dimensions, and Poisson's ratio. Symbols for length (long dimension) and breadth (short dimension) have been transposed from the expression in Eq. (1) in Bowles and Sugarman,[37] following the argument of Appendix B. For square plates, Eq. (17) reduces to

$$f = 0.2734\ \Delta p\ A/H^2 \qquad (18)$$

In alternate form, and with allowance for variation in glass strength, the breaking load for square panes is

$$b = (3.658\ fH^2/A)\ x\ \sigma_g^{\pm 1} \qquad (19)$$

For rectangular panes, breaking loads are increased by a strength factor, shown in Figure 16, as a function of pane dimension aspect ratio. The strength factor relationship, from evaluation of Eq. (17), is shown by curve "A." Other references provide lower values for this strength factor, shown by curve "B" by PPG,[38] and curve "C" from a tabulation[39] reproduced from nuclear weapons effects data.[40] These alternate shape factors do not satisfy intuitive concepts for the mechanics that are involved.

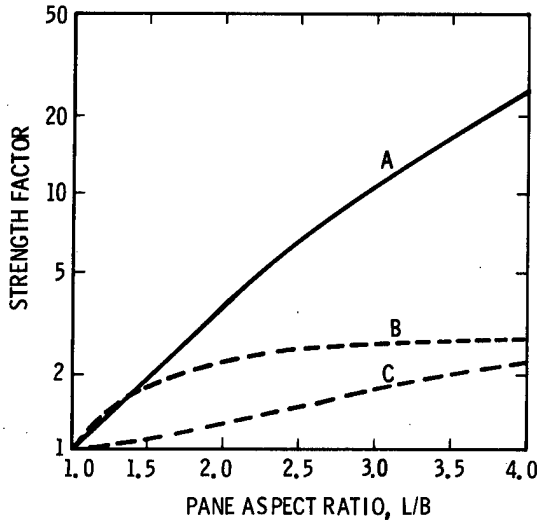

CURVE	REFERENCE
A:	MARCUS (36)
B:	PPG (38)
C:	SRI (40)

Figure 16. Glass Plate Strength Factor for Rectangular Plates

Laboratory results[35] have been graphed in Figure 17 for $f = 102 \times (1.422)^{\pm 1}$ MPa, $A = 0.093\ m^2$, $H = 2.54$ mm, for one common window glass, Pittsburgh Plate Glass (PPG) Annealed Herculite II, where the average $\bar{b} = 25.88$ kPa. The great discrepancy with the curve of Eq. (16) indicates that other factors must also be involved in explaining empirical response observations.

First, there is considerable variance in gage overpressure caused by atmospheric propagation through turbulence as well as wavy stratifications of both wind and temperature. Experiments have shown that duplicate explosions, fired only minutes apart, give overpressures that have a scatter factor of about $1.63^{\pm 1}$.[41] These results were obtained at very long range, near 220 km. There are, however, indications from sonic boom and transportation noise studies that this variance is generated in relatively short propagation distances in the atmospheric boundary layer. Thus, for lack of a better figure, this same variance, for explosion wave propagation out from and back into or entirely within the boundary layer, has been statistically combined with glass variance to give a net scatter factor (σ_g) of $(1.83)^{\pm 1}$ and $(1.87)^{\pm 1}$ for common and plate glasses, respectively.

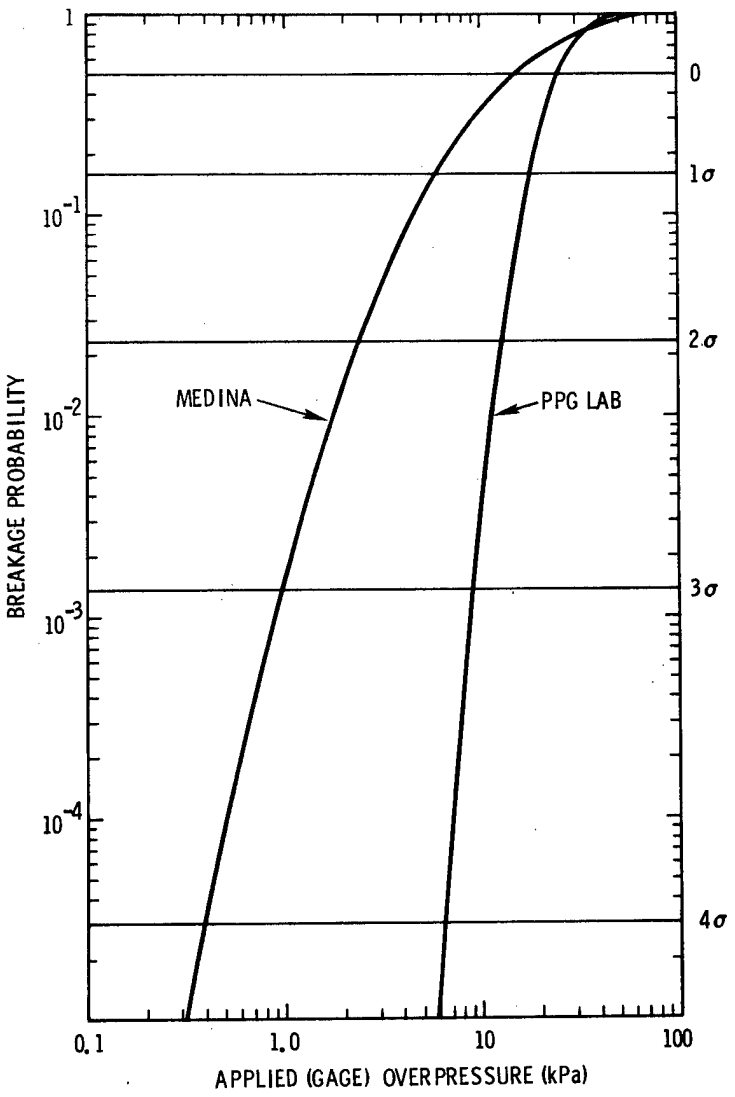

Figure 17. Lognormal Probabilities of Glass Breakage versus Applied Pressure

Orientation of a glass pane with respect to a blast wave is also important. Sonic boom studies showed that a pane facing in the direction of an incoming wave (incidence angle $\theta = 90°$) caused another reflective doubling of overpressure (above gage overpressure).[42] Side-on panes ($\theta = 0°$) were loaded by gage overpresssure, while rear-facing panes ($\theta = -90°$) only received half of the gage overpressure. For other orientations, these results may be assumed to infer a $2^{\sin \theta}$ multiplier, shown in Figure 18. Randomized orientation of building faces and windows was assumed and combined with a low-pressure response approximation to Eq. (16) that breakage probability is proportional to the 2.87-power of overpressure. This allowed estimation of 1.32 for the average "effective" ratio of pane overpressure to gage overpressure.

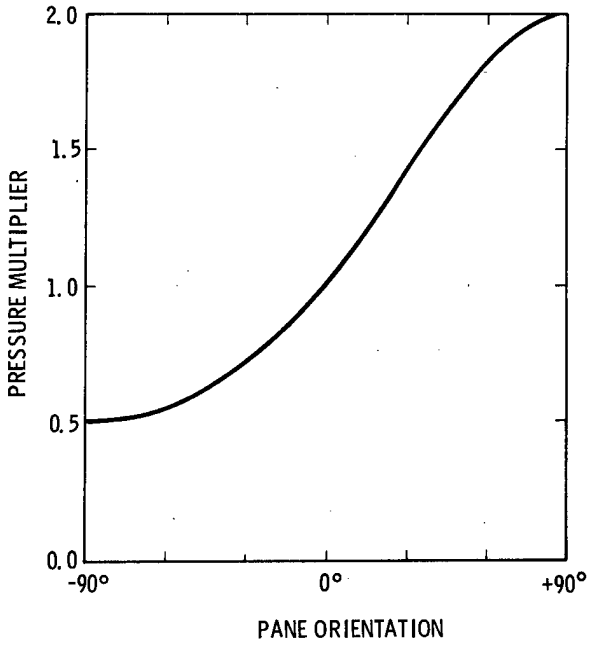

Figure 18. Pressure Reflection Factor versus Pane Orientation to Airblast Wave

Combination of glass average strength and variance, propagation variance, and orientation effects into Eq. (19) yields

$$\text{Common window glass:} \quad b_c = 282.87 \frac{SH^2}{A} \times (1.83)^{\pm 1} \text{ (MPa)} \tag{20a}$$

$$\text{Plate glass:} \quad b_p = 183.26 \frac{SH^2}{A} \times (1.87)^{\pm 1} \text{ (MPa)} \tag{20b}$$

These relationships were used to calculate damage probability functions for some typical window panes as shown in Table 6 and Figure 19. The selection of pane dimensions will be discussed in the following section.

Several questions have been raised about these damage relationships,[7] but it is felt that they are adequate for order-of-magnitude predictions. Some glass-test data led Hershey and Higgins[43] to conclude that breaking overpressure was proportional to $H^{1.54}$, contrary to plate theory results, but this appears to have resulted from other uncontrolled variables in their source data. A similar result can be obtained by blind correlation of PPG test data,[35] but it was caused by anomalous poor performance of the thickest 19-mm (0.75-inch) test specimens. An unexplained weakness in thick Russian glass has also been found by Kazakov et al.[44] Another analysis leads to areal dependence of $A^{-1.1}$, but this is believed to be a statistical aberration in the limited sample of test specimens. Experiments have also shown that static tests yield conservative (low) strengths as compared to results from rapid compressions in sonic booms and moderate yield airblast loads.[45]

This high-frequency dynamic response characteristic of window glass is not well understood. Dynamic amplification, from interaction between the natural frequency of large windows and an airblast wave, may be by more than a factor of 2.[46 47] In specific instances, a Helmholtz resonance may develop in an airblast-impacted structure by appropriate combination of window, room, and door configurations.

Membrane stresses may also need consideration when large pane deflections are assumed necessary for plate failure. There is conflicting evidence about age and weather effects on glass strength. Tests at Texas Tech[48] showed that indoor glass surfaces were about 40% weaker than the outdoor, weathered, and occasionally sand-blasted (by dust storms) surfaces. Russian data[44] indicated, however, that rain and washing considerably reduce panel strength, and this water effect should most seriously affect outdoor surfaces.

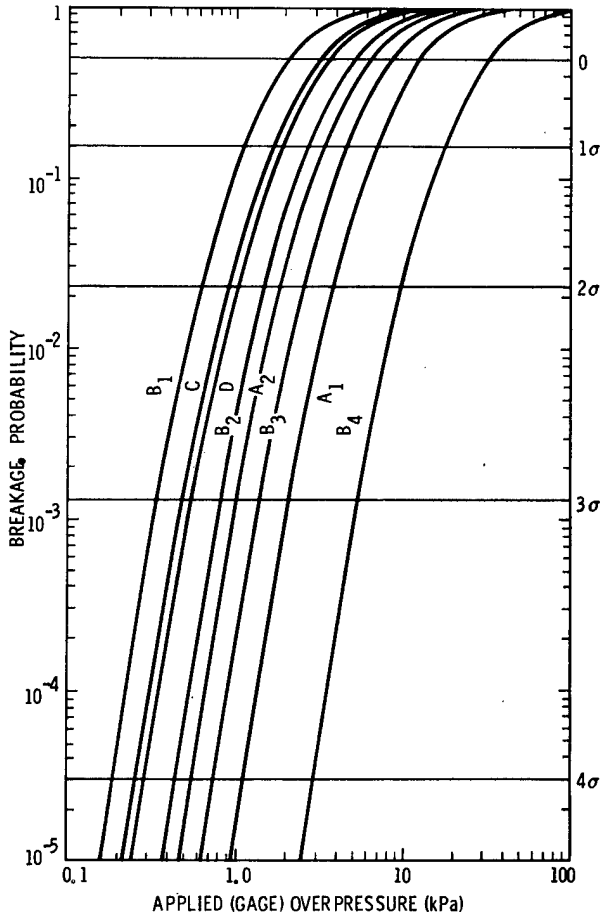

Figure 19. Breakage Probabilities for Selected Glass Pane Categories

Table 6

Window Pane Census Categories and Characteristics
(SS: Single Strength Common Glass; DS: Double Strength Common Glass; P: Polished Plate Glass)

Category	Glass Type	Pane Dimensions (m)	Pane Dimensions (in)	Pane Area (m^2)	Pane Area (ft^2)	Pane Thickness (mm)	Pane Thickness (in)	Mean Breaking Strength (kPa)	Mean Breaking Strength (psi)	Scatter Factor
San Antonio, Texas, Model										
A_1	SS	0.30 x 0.30	12 x 12	0.09	1	2.0	0.08	12.57	1.82	1.83
B_1	SS	0.75 x 0.75	29 x 29	0.56	6	2.0	0.08	2.10	0.30	1.83
C	P	1.52 x 1.52	60 x 60	2.32	25	6.4	0.25	3.18	0.46	1.87
D	P	2.16 x 2.16	85 x 85	4.65	50	9.5	0.375	3.58	0.52	1.87
Cape Canaveral, Florida, Model										
A_2	SS	0.43 x 0.43	17 x 17	0.19	2	2.0	0.08	6.29	0.91	1.83
B_2	SS	0.48 x 0.48	19 x 19	0.23	2.5	2.0	0.08	5.03	0.73	1.83
Some Other Panes*										
B_3	SS	0.30 x 0.76	12 x 30	0.23	2.5	2.0	0.08	8.57	1.24	1.83
B_4	SS	0.30 x 0.76	12 x 30	0.23	2.5	2.0	0.08	32.49	4.71	1.83
1	SS	0.23 x 0.61	9 x 24	0.14	1.5	2.0	0.08	66.21	9.60	1.83
2	DS	0.75 x 0.75	29 x 29	0.56	6	2.8	0.11	4.33	0.63	1.83
3	SS	0.91 x 0.91	36 x 36	0.84	9	2.0	0.08	1.40	0.20	1.83
4	SS	1.02 x 1.27	40 x 50	1.29	13.9	2.2	0.085	1.45	0.21	1.83
5	DS	1.52 x 2.03	60 x 80	3.10	33.3	2.9	0.115	1.20	0.17	1.83
6	D	1.93 x 1.93	76 x 76	3.72	40	6.4	0.25	1.99	0.29	1.87

*Other categories selected for the following reasons:

- B_2 Medium awning windows typical of CC, shape strength factor 1.45.
- B_3 Medium awning windows typical of CC, shape strength factor 5.5.
- 1 Small awning panes typical of CC.
- 2 Double strength B-pane for comparison.
- 3 Maximum size for Texas B-panes.
- 4 Maximum size single strength pane marketed by PPG. 40.
- 5 Maximum size double strength pane marketed by PPG. 40.
- 6 Maximum size for Texas C-panes.

In any discussion of window damage, the question of installation always arises. Stress raisers, such as mounting clips or glazer's points, would be expected to contribute to breakage probability in some way. Also, prestressing by structural settling or other building racking could influence damage susceptibility. Sonic boom damage reviews[46] showed that most glass breaks originated on panel edges and were associated with stress raisers. Laboratory tests[35] also showed many failures associated with edge conditions. Yet a number of tests of large panels[48] showed that all failures began at flaws which were more or less in the central region of maximum stress as predicted by plate theory. Under uniform pressure loading there is relatively little stress on the simply supported edges of a typical window pane.

The general confusion about glass performance led Seaman[47] to conclude that "because the data do not correlate well with the theoretical...curves...it does not appear that stresses at failure can be predicted now" and "the ultimate strength data of glass specimens cannot be used directly to predict failure of glass panes." In the face of so many conflicting and detailed arguments, a pragmatic approach yields the conclusion that, since the simple combination of glass strength variance, propagation variance, and orientation effects reasonably well explains the San Antonio experience,[3] there is not much unexplained variance to be attributed to detailed structural or dynamical characteristics. For low overpressures, this is justified by comparing the curves in Figure 19 with the Medina curve of Figure 16.

Cape Canaveral Window Pane Survey

A census of window panes was conducted in the community of Cape Canaveral. This gave the distribution shown in Figure 20. Four pane area categories were used (see Table 4) as in previous surveys of San Antonio, Texas,[3] and Central America.[49 50] Large buildings were given individual detailed inspection, but in residential areas only those city blocks were sampled where specific counts are shown on the map. A pane count estimate was made for other blocks. An aerial photomap allowed building counts and identifications. The numbers of individual residences, one-story apartment houses, and two-story apartment houses were listed by block. An average distribution by pane-size categories was obtained from the surveyed samples and assigned to each structure. Table 7 shows both census summaries and estimated total pane populations for CC. The analysis area only extended south to McKinley Avenue (aerial photo limit), but relatively little damage was predicted for areas south of this line. Pane count estimates for groups of blocks were then summed to give the totals shown in Figure 21.

In older residential structures, roughly one-fourth of their windows were glazed with jalousies. These small panes of relatively thick glass are quite blast-resistant according to calculation as well as observation at Johnston Island during high-altitude nuclear explosion tests over that Pacific Ocean test site. Jalousies were, therefore, ignored in this damage evaluation.

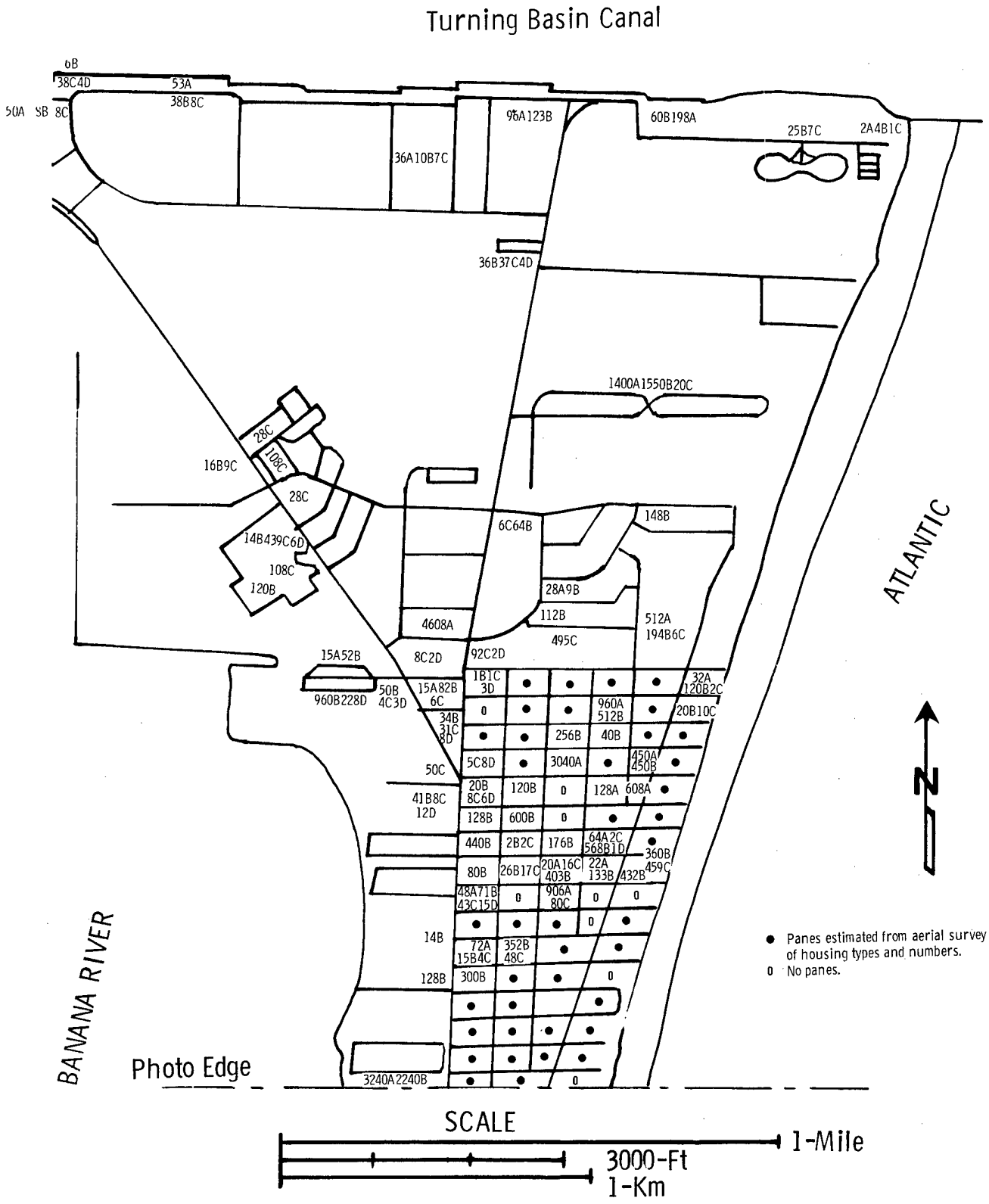

Figure 20. Window Pane Survey Results

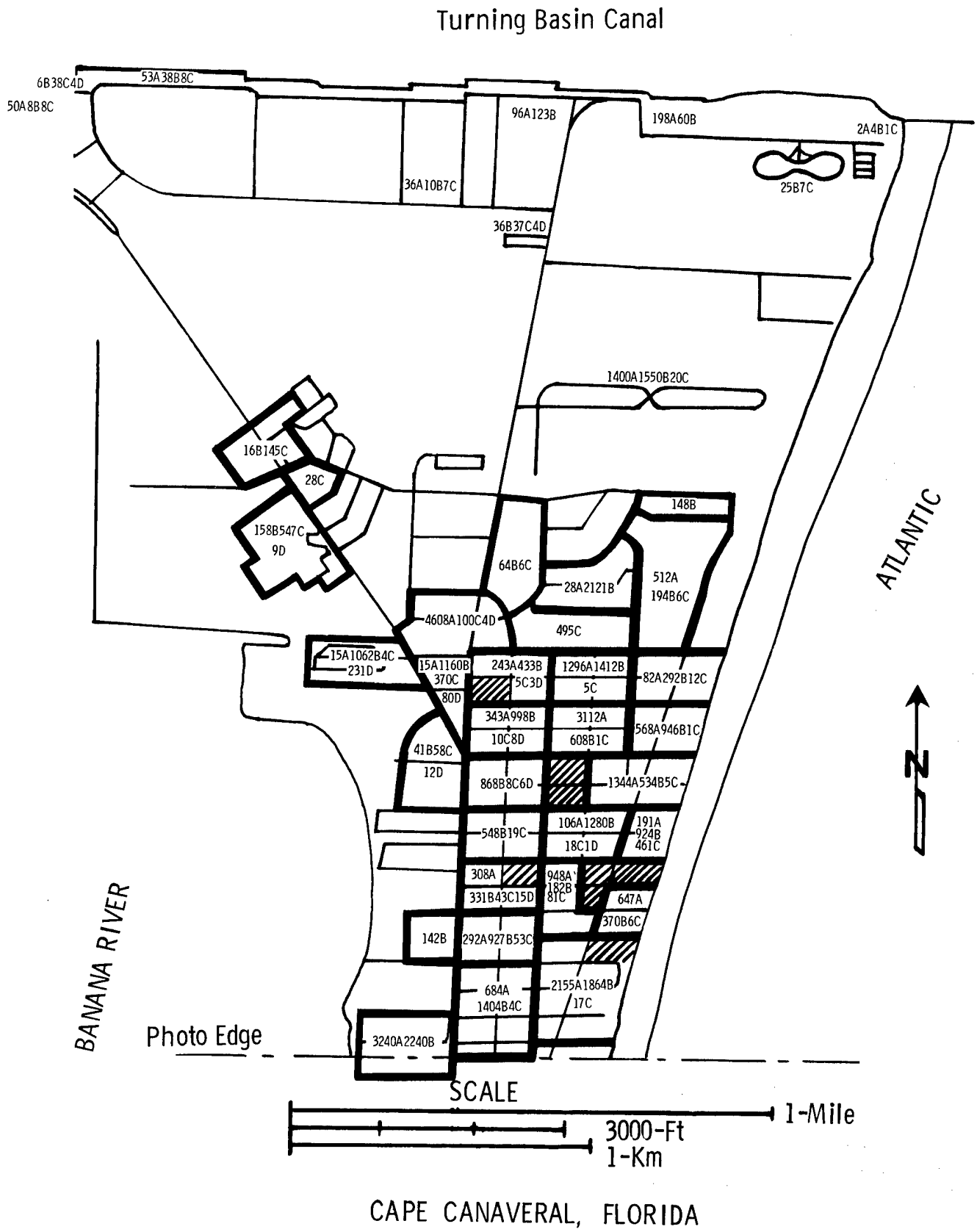

Figure 21. Window Pane Census Estimates Used in Damage Predictions

Table 7

Window Pane Populations and Characteristics

Category	Number Counted	Extrapolated Total Number	Gage Overpressure, 50% damage	Geometric Standard Deviation Factor, σ_G
A_2	16 603	22 572	6.3	1.83
B_2	11 787	19 740	32.5	1.83
C	2 234	2 286	3.2	1.87
D	307	307	3.6	1.87
Total	30 931	44 905		

The four surveyed pane categories were described in Table 6. Several differences from San Antonio glazing practice were noted in Florida. Texas A-panes were often about 0.28 by 0.36 metre (11 by 14 inches), installed in multipane casements, as is common in the Southwest. These casement panes made up nearly 60% of the San Antonio pane population and about 11% of the average 19 panes per capita.[3] Also, damage claims for these small panes considerably exceeded expectations based on damage to larger panes. This may have been caused by casement response rather than single plate response. This casement glazing is almost totally absent in Cape Canaveral.

Instead, small CC panes were usually about 0.23 by 0.61 metre (9 by 24 inches), mounted in individual horizontally-hinged frames, called awning windows, that open upward. From three to six of these panels are used in a window opening. As a consequence, a compromise was made, and CC model A-panes have been assumed as 0.18 m^2 (2 ft^2) square panels, A_2, rather than 0.093 m^2 (1 ft^2). The actual 0.23 by 0.61 metre (9 by 24 inch) unit is much more load resistant than the larger assumed unit. Damage probability for such small panes is very low, however, so this difference in strength was neglected.

Evaluation of B-panes is more critical. There is a great number of these in CC that are also long, narrow, horizontally-hinged awning units. The typical San Antonio B-pane of 0.57 m^2 (6 ft^2) area is more vulnerable to airblast. Thus, the Canaveral B-pane was redefined to a 0.30 by 0.76 metre (12 by 30 inch) pane, B_2, more blast-resistant, yet more typical of the location. A conservative compromise was again adopted, however, in that a 1.45 strength factor[39] was used rather than the 5.5 factor predicted by Eq. (17).

Large C- and D-panes, used as residential picture windows, glass doors, or store fronts, appear to have about the same statistical characteristics in CC as in San Antonio as well as in the whole country. It was assumed that their thickness was 6.4 mm (1/4 inch) and 9.5 mm (3/8 inch), respectively, as in Texas. This assumption may be in error if hurricane design wind standards[26] are enforced by Florida building inspectors. Furthermore, D-panes apparently are not 50% thicker

than C-panes because they have shown a higher probability of failure.[3] Their mean breaking strength should be lower than for C-panes, rather than higher as calculated for Table 6, unless dynamic amplification factors play a dominant role.

Airblast Damage Assessments

Overpressures from Figure 2 have been shown in Figure 22 as isobars crossing CC for gradient, standard, and inversion propagation. Window pane counts from Figure 21 and predicted overpressures were used with the probability of damage from Figure 19 to give an expectation for broken panes. Approximate locations for expected damages from a surface burst and inversion propagation are shown in Figure 23. Summaries from these estimates in Table 8 are given for gradient, standard, and inversion propagation conditions.

In summary, an accidental detonation at near-optimum HOB above Launch Pad 25 would probably break 21 windows in CC if attenuating propagation conditions were present. Yet, if inversion weather and propagation occurred, about 7.5% of all the windows in CC would be broken! With focused propagation, nearly 40% of the panes could be broken in limited areas. This possibility made it necessary to have a "weather watch," based upon rawinsonde balloon and meteorological tower observations, to warn of such a potential.

Table 8

Summary of Expected Damage in Cape Canaveral

		0-m Explosion Height (Surface)			140-m Explosion Height (Optimum)		
		Propagation			Propagation		
Pane Category	Pane Pop.	Gradient	Standard	Inversion	Gradient	Standard	Inversion
		Expected Number of Broken Window Panes					
A_2	22 572	0	34	381	3	125	1 010
B_2	19 740	1	82	738	11	268	1 772
C	2 286	0	45	271	7	120	531
D	307	0	3	27	0	11	57
Total	44 905	1	164	1 417	21	524	3 370

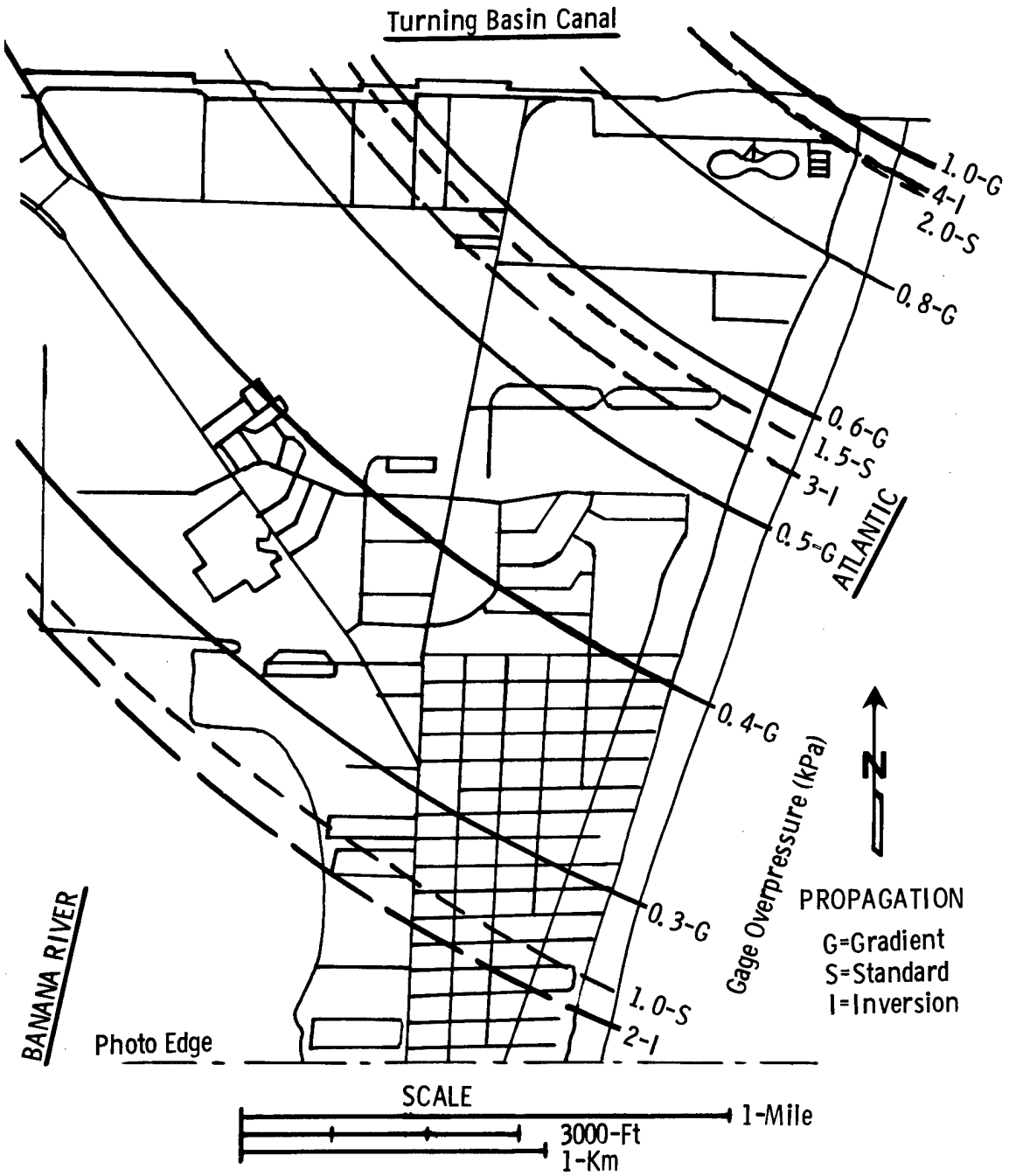

Figure 22. Predicted Airblast Overpressure Isobars

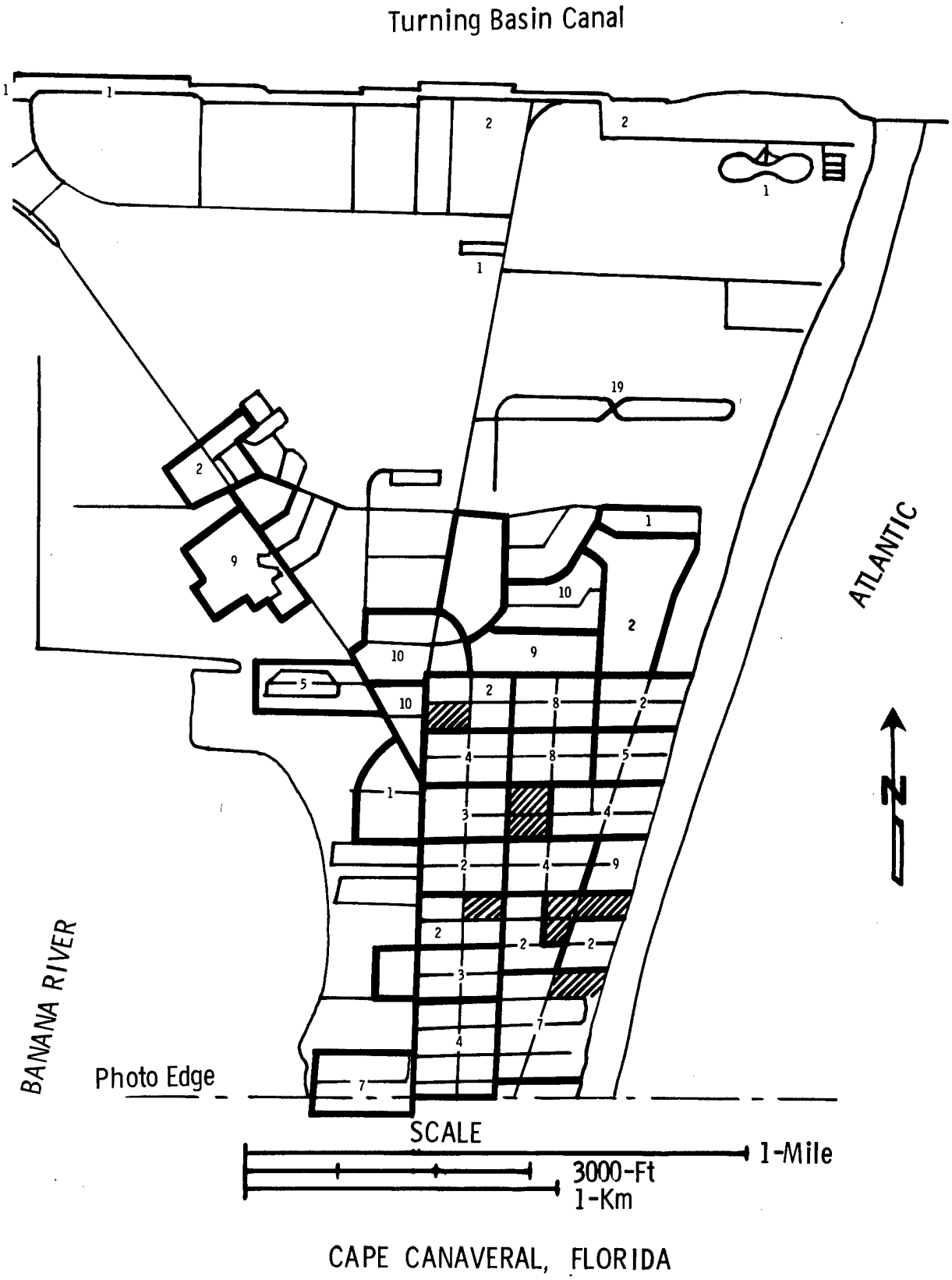

Figure 23. Estimated Numbers and Locations of Broken Window Panes in Cape Canaveral from a Surface Burst with Inversion Propagation Conditions

Other Communities

Window surveys of several communities beyond the distance range of CC were made later during SAMTEC evaluations.[51] Calculations of expected damage in these communities are summarized in Table 9. The large numbers of panes that could be damaged in Cocoa Beach and Merritt Island under inversion propagation conditions would be exceeded in CC, at shorter range and similar azimuths.

Table 9

Summary of Expected Damage to Nearby Communities

	0-m Explosion Height (Surface)			140-m Explosion Height (Optimum)		
	Propagation			Propagation		
City	Gradient	Standard	Inversion	Gradient	Standard	Inversion
Cocoa Beach Panes: 114 869	0	28	456	0	124	1 458
Merritt Island Panes: 323 524	0	24	510	0	124	1 826
Rockledge Panes: 51 625	0	0	17	0	3	71
Coca Panes: 101 740	0	1	31	0	6	132
Coca-Port St. John Panes: 99 923	0	0	19	0	3	90
Port St. John Panes: 16 103	0	0	3	0	0	13
Titusville Panes: 140 596	0	0	4	0	0	23

A small-scale map in Figure 24 shows the ranges of 200-Pa-gaged overpressures, the window-breaking threshold isobars, under various propagation conditions. Population census data for surrounding communities[52] were used with simplified propagation approximations to give damage expectations from enhanced propagation to long ranges. Results in Table 10 show that intense focusing could break a large number of panes in Orlando or Daytona Beach. There is small probability of such focusing on these large cities without more severe, concomitant effects on towns at closer range. Under gradient or standard conditions, there would be no window damage in these distant cities. One difficulty is that, when good conditions are directed toward CC, opposite conditions often prevail in the opposite (Titusville) direction.

Structural Damage

Accident experience[3] and explosion tests[33] have shown that there may be damage other than broken windows. At low overpressures, it is usually cosmetic (cracked plaster, broken ceiling-light fixtures, fallen bric-a-brac, etc.), and resultant claims may be estimated to be about 40% of window damage claims.[3] With overpressures above about 3 kPa, however, other damages probably exceed the cost of total window replacement. Near 7 kPa, there may be some building structural elements broken.

The airblast response of high-rise buildings, such as the nine-story Canaveral Tower condominium, was estimated by LASL[53] through analogy to ground motion effects from underground nuclear explosions. With caveats caused by lack of appropriate experience, their stated results showed that minimized propagation would do little damage, but an enhanced airblast wave could induce significant building motion and cause some structural damage. LASL proposed a structural response study and measurement project to be carried on during Trident tests. With the weather restriction that was adopted to limit window damage, it was felt that no significant structural response would occur.

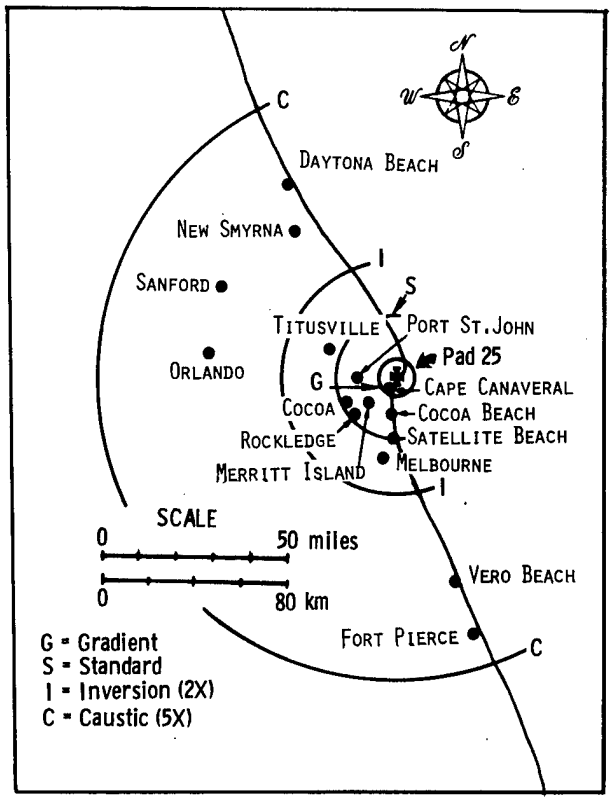

Figure 24. Window Damage "Threshold" Isobars under Various Propagation Conditions

Table 10

Window Damages Calculated for Distant Cities

Surface Burst*			City	140-m HOB*		
I(2X)	F(5X)	F(8X)		I(2X)	F(5X)	F(8X)
3	147	712	Satellite Beach	15	486	1 966
1	82	422	Indian Harbor Beach	8	284	1 217
2	142	792	Eau Gallie	13	522	2 420
7	419	2 263	Melbourne	39	1 503	6 781
0	12	73	Indialantic	1	47	237
0	10	66	West Melbourne	0	42	220
0	15	100	Palm Bay	1	63	346
0	0	8	Vero Beach	0	4	37
0	0	6	Fort Pierce	0	3	30
0	0	0	Stuart	0	0	1
0	1	8	Edgewater	0	5	34
0	2	19	New Smyrna Beach	0	11	83
0	0	4	So. Daytona Beach	0	2	20
0	0	3	Port Orange	0	1	14
0	2	28	Daytona Beach	0	16	131
0	0	3	Holly Hill	0	1	16
0	0	4	Ormand Beach	0	2	23
0	0	5	Deland	0	3	27
0	2	21	Sanford	0	12	94
0	0	3	Longwood	0	2	16
0	1	10	Casselberry	0	6	44
0	0	5	Altamont Springs	0	2	22
0	1	9	Maitland	0	5	40
0	3	27	Winter Park	0	16	121
0	10	100	Orlando	0	58	447
0	0	2	Winter Garden	0	1	9
0	0	1	Ocoee	0	1	8
0	0	6	Kissimee	0	3	29
0	0	8	St. Cloud	0	5	36

*I (2X) = inversion propagation, 2X overpressure magnification
F (5X) = focused propagation, 5X overpressure magnification
F (8X) = focused propagation, 8X overpressure magnification

Injury Hazards

There have been few documented injuries from broken glass caused by accidental airblasts. The Medina explosion, with 3 644 broken windows claimed,[3] caused only one off-base injury (according to unverifiable sources), and that one was not associated with broken glass. On the other hand, a sonic boom at the U.S. Air Force Academy was reported to have broken about 300 windows; 15 people were cut and 1 was hospitalized for injuries from flying glass.[54] Speculative extrapolation from academy figures to the Medina accident leads to an expectation of hundreds of injuries, many serious, and the possibility of a fatality. Injury depends, however, on the size and speed of the glass fragments and the location of people. Conditions were probably worse in the sonic boom case.

SSPO contracted the Lovelace Foundation to elucidate the injury potential of a Trident accident.[55] The conclusion was reached that, under adverse weather conditions, the potential for significant injuries exists. This conclusion was based upon injury estimates from glass fragment numbers, sizes, and speeds expected from 2- to 4-kPa airblast overpressures impinging on the Cape Canaveral population.

With gradient-attenuated propagations, however, there should be no injury from flying glass.[56] The hazard from broken glass falling around multistory buildings or from large storefront displays could not be assessed.

Assessment Conclusions

In the event that a Trident I C-4 motor should explode near Pad 25, a damaging and hazardous airblast wave could strike CC under weather conditions that caused enhanced overpressure propagation. Only a few dozen window panes would be broken, however, if an explosion occurred under weather conditions for minimal airblast propagation. This small number of panes would not be broken with sufficient force to cause a glass-missile hazard. Maximum blast attenuation occurs with a strong decrease in sound velocity with height that refracts the blast wave away from ground level. Weather records indicated that suitable weather conditions could be expected on about half the days in a year. Good conditions were more frequent (65%) in summer months than in winter months (25%). Test delays of 1 to 3 days awaiting good weather could be expected.

TRIDENT TEST OPERATIONS

The Weather Watch

Propagation Criteria

Long-range propagation of explosion waves should be strongly attenuated by a gradient of sound velocity with height above ground. Microbarograph measurements of airblasts at 15- to 50-km distances from the series of large nuclear tests at Christmas Island in 1962[16] indicated that overpressure decayed in approximately inverse proportion to the square of the distance. Deviations occasionally exceeded a factor of 10. Review of data from Nevada nuclear tests[14] and large HE tests[17 18 57] showed that good gradient propagation was usually obtained with a sound velocity gradient of at least $-0.005\ s^{-1}$. There has been no serious attempt to correlate propagation intensity with effective gradient. Also, most measurements have been made at much larger yield-scaled distances than are the primary concern of Trident.

Nevertheless, to satisfy range safety and weather officials, a limit on the sound velocity gradient was needed for "acceptable" test conditions. As a result, criteria delineated in Figure 25 were adopted. A gradient of at least $-0.005\ s^{-1}$ to 1.2 km (4 000 ft) altitude was adopted as the requirement for the CC direction. Also, no surface wind component toward CC was to be acceptable. Standard propagation ($dV/dz = 0$) was adopted as the limit for propagation toward Merritt Island. Furthermore, a 0.6 m/s (2 ft/s) "safety factor" was adopted for surface wind and all sound velocities to allow for likely short-term wind fluctuations.

Toward Titusville, a surface inversion was judged acceptable in that some propagation enhancement to that greater range should not cause more damage than minimal propagations would cause at shorter ranges to Merritt Island and CC. Focused waves directed north to Daytona Beach or south to Vero Beach could be accepted along with the small associated probability of a few broken window panes.

The format of Figure 25 was adopted as a background for plotting directed sound velocity curves from weather observations. When a plotted curve extended to the right of the appropriate criteria curve, the launch could not be fired.

Meteorological Data System

Radiosondes -- Weather balloon observations are normally released twice daily, giving 0000 GMT and 1200 GMT reports from around the world. At CCAFS, however, regular daily ascensions are made about 0900 to 1000 GMT, to better serve local users. Additional ascensions are made at CCAFS when there is a project demand. With a single set of ground station recording equipment, it is possible to make "short" (to about 10 km altitude) ascensions hourly. Atmospheric conditions

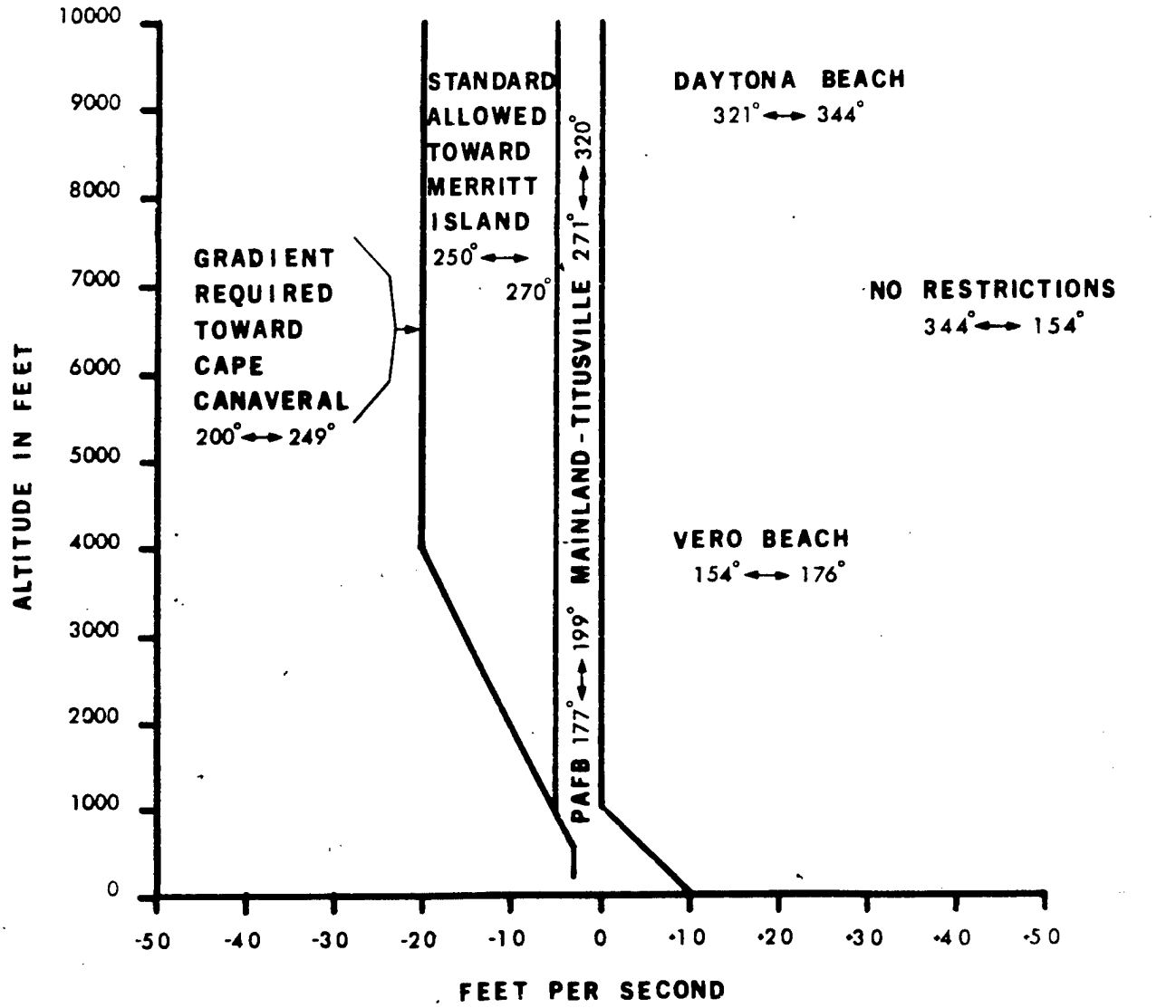

NO VELOCITY COMPONENT IS ALLOWED TO THE RIGHT OF THESE LINES FOR THE CONDITIONS STATED

NO WIND COMPONENT IN LOWER 200 FEET IN DIRECTION OF CAPE CANAVERAL. (200°– 240°)

EFFECTIVE: 23 FEB 77

Figure 25. Ducting Criteria for Launch Complex 25

above the boundary layer change relatively slowly and the inaccuracies of observation usually obscure changes that occur on shorter than 1-hour time scales.

In support of Trident testing, special radiosonde observations could be scheduled to best serve countdown decision-making. If additional data were required, a measurement request could be met with about 1-hour lag.

Meteorological Towers -- There are 13 16.5-metre towers and 1 150-metre meteorological tower in the CCAFS/Kennedy Space Center complex. The tall tower, No. 313, is 24 km north-northwest of Pad 25, but it may be assumed that conditions above approximately 30 metres height are uniform over the horizontal field. Tower No. 001 (16.5 metres) is located about halfway to Jetty Point and 1 km from Pad 25. Its data should be representative of conditions along the propagation path to CC. Wind, temperature, and humidity sensors are operated at various levels on these two towers as shown in Table 11.

Table 11

Meteorological Tower Sensor Installations
(A-Tower 001 and B-Tower 313)

Height (m)	Height (ft)	Sensor: Wind Direction & Speed	Sensor: Temperature	Sensor: Humidity
1.8	6	-	A	A
3.7	12	AB	B	B
16.5	54	AB	AB	A
49.4	162	B	B	-
62.2	204	B	B	B
89.0	292	B	-	-
119.8	393	B	-	-
150.9	495	B	B	B

Tower data readouts are by teletype printer, and include reports from the complete tower network. An example is reproduced in Table 12. Readout is limited to a 5-minute interval between observations.

Computer Evaluations -- The computer, data display, and command system that evolved at CCAFS were very well suited for evaluating Trident launch conditions. Raw radiosonde signals consist of sequences of voltages for temperature, humidity, and calibration with pressure-calibrated switching. These are used in the gas law and hydrostatic equations to calculate the height at which temperature, pressure, and humidity values occur. The radio transmission is also tracked by a direction finder antenna that yields elevation and azimuth angles needed to locate balloon horizontal coordinates (at computed heights). Horizontal balloon coordinate changes with time are assumed to equal the wind. Raob signals are computer-translated to allow evaluation for directed sound velocity for selected azimuths, at 300-metre (1 000-ft) height increments and as short as 1-hour time increments.

Table 12

Example of Meteorological Tower Teletype Report

```
WIND SYSTEM DATA
1410Z  29 APR 1977
05 MIN INTEGRATION

DIFFUSION DATA

          12 FT          54 FT          6 FT LAPSE    DIR      5       25       292
TOWER  DIR  SPD   DIR  SPD  GST  TMP     RATE        DEV      PPM     PPM      DEV
COASTAL

110    262  03    260  08   10   75   -02.8          10.1     07.8    03.4
108
106    248  12    229  10   12   77    08.2          06.3     48.3    21.3
005    234  08    224  08   11   73   -01.7          11.4     10.4    04.6
003    247  05    264  07   11   73   -02.6          05.3     09.8    04.3
001    278  06    268  07   10   74   -00.9          07.3     14.3    06.3

BANANA
313    272  05    258  07   11   73   -01.4          04.7     14.2    06.2     04.2
311    258  06    252  09   13   74   -02.5          05.7     09.9    04.4
308    268  09    271  10   13   76   -01.9          09.0     10.5    04.6
403    221  05    215  05   08   73   -02.9          06.9     08.4    03.7
303    251  02    246  06   10   77   -02.9          15.9     06.7    02.9

INDIAN
714    225  04    238  06   09   76   -03.6          05.6     07.0    03.1
509    233  05    241  06   09   77   -02.0          04.4     12.3    05.4
803    248  04    246  06   09   77   -01.9          13.7     09.4    04.1

METEOROLOGICAL DATA

ALT   TOWER 313                    TOWER 110                    TOWER 005
 FT   DIR  SPD  GST  TMP  DPT     DIR  SPD  GST  TMP  DPT     DIR  SPD  GST  TMP  DPT
495   253  07   10   72   50
393   251  07   10
292   261  07   10
204   254  08   11   73   50      267  09   12                214  08   11
162   254  08   12   72           261  08   10   71          221  10   12   70
 54   258  07   11   72   50      260  08   10   72   50     224  08   11   71   49
 12   272  05   08                262  03   07              234  08   12
  6   1021.4MBS      73   52                        75   57                    73   51

TOWERS  001/313  COMPONENT WINDS IN FPS

HEIGHT                          AZIMUTHS
FEET      200   220   240   320

 12      -002  -005  -008  -008
 54      -004  -008  -010  -007
162      -008  -011  -013  -005
204      -006  -011  -013  -005
292      -006  -009  -011  -006
393      -007  -010  -012  -004
495      -007  -010  -012  -005
```

While upper air (≥ 300 metres height) conditions are periodically updated in the computer, tower observations may be interrogated more frequently, at 5-minute intervals. The computer updates the sound velocity field description each time a new set of data is received from either a radiosonde or from Tower 001 or Tower 313. A typewriter console in the CCAFS Weather Station is used to command desired readouts. Displays are shown on either or both a video screen and a hard-copy printer. Both data tabulations and graphic displays can be produced.

One of the most useful output formats is a graph of directed sound velocity versus height along with the appropriate acceptability criteria curve for a specified direction. An example is shown in Figure 26. Provision is made, through computer storage, for showing a time history of data curves as needed for assessing trends during a countdown. The computer then allows quick determination of where and what is the "trouble." It could be an easterly wind at 150 metres, a strong southeasterly flow at 1 to 3 km, a slow surface warming caused by a cloud cover, etc. When the weather problem elements have been identified, the forecaster can select specific tools (such as satellite photos, synoptic weather charts, or sea breeze cycle diagrams) to make detailed prediction for change. Predictions can be typed into the computer to yield a forecast sound velocity field for comparison with observations. About the only negative feature of this computerized system is that it attracted a large audience in the middle of the busy weather station. To counter this as well as to disseminate analyses to decision-making participants at remote locations, a closed-circuit television (CCTV) system is used for periodic briefings. Receivers are available throughout the test range.

Briefing Schedules

Trident launches have been scheduled for various hours from 0700 EST to 1100 EST. Weather and propagation evaluations are typically begun at about H-24 before a scheduled launch. This evaluation determines whether workers are to be ordered to arrive at duty stations early in the morning and before regular work hours. That order can be changed as late as about 1600 EST (H-19 to H-15) if there is a deteriorated weather outlook or missile difficulty. Near H-8, a number of things begin to happen; some crews prepare to go to work, range surveillance ships start to their stations, and participating aircraft are given preflight checks. No system was established for halting operations at this time, however, even if weather conditions were not developing as anticipated.

In practice, the major weather and propagation evaluation was made at H-3 to hold participating aircraft on the ground if the weather was not suitable. After this time, the weather watch became essentially continuous and often intense. Early morning conditions were usually not acceptable because of low surface temperatures and the threat of inversion propagation enhancement. Therefore, operations proceeded only under the aegis of a favorable weather forecast and thus under conditions of significant uncertainty. Further critical times occur near H-1 when various road closures were activated and certain work areas were evacuated, and near H-15 minutes when critical missile functions were started. The latest hold time, to avoid irreversible internal missile function activation, was near H-6 minutes. After that time, there was one more tower weather observation before the

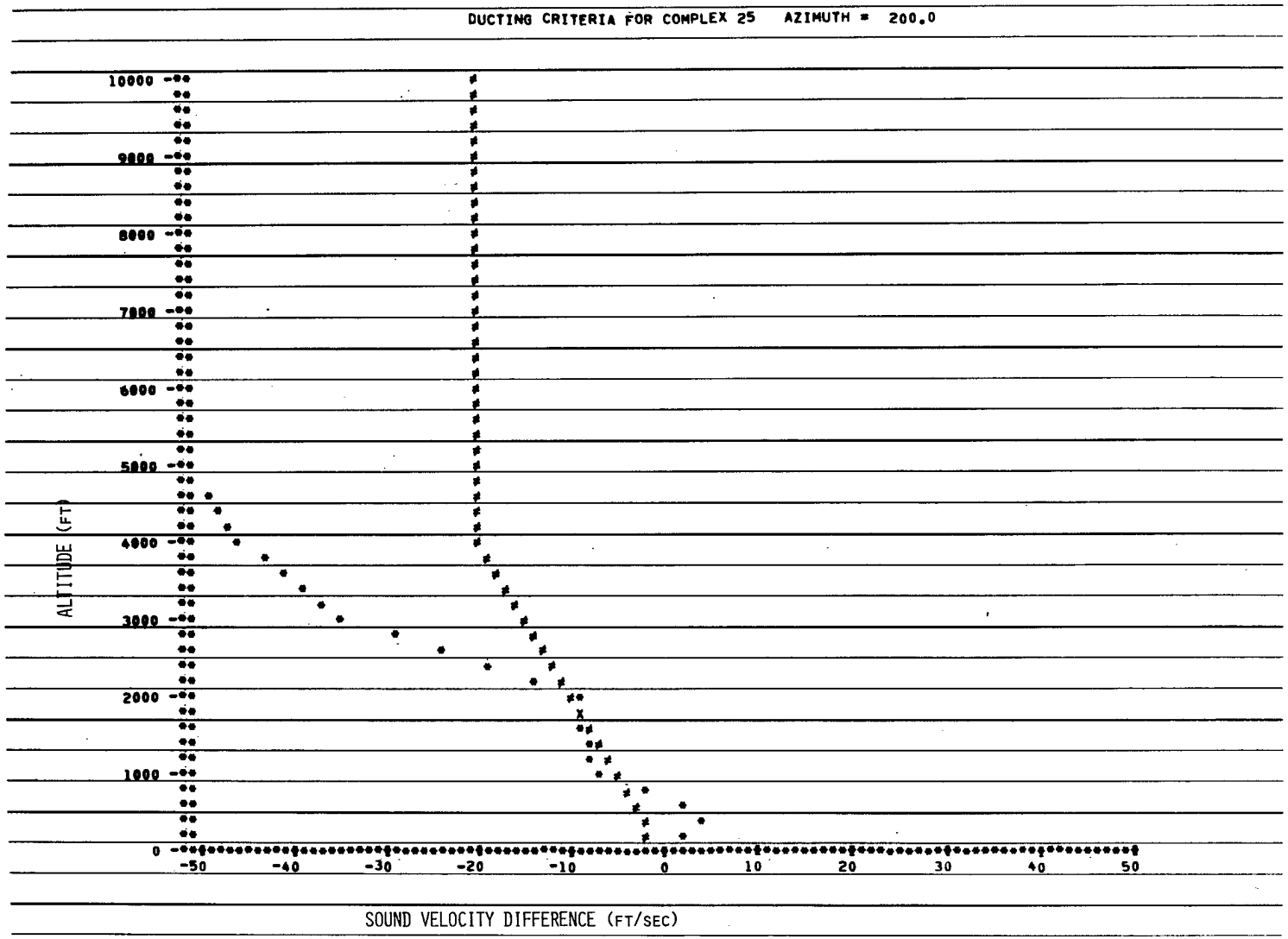

Figure 26. Example of Computer Output of Sound Velocity-Height Structure

fire signal, but it was never necessary to try to stop a countdown at that time because of a severe deterioration in observed conditions. Weather conditions exactly at launch time cannot be obtained with existing control software. Therefore, the closest observation (within ±2 minutes) is used to define the zero-hour boundary layer. A radiosonde is also released soon after each launch to document upper air conditions.

Forecast Accuracy

Weather-dependent decision making during a test countdown is greatly influenced by the confidence level that is felt for the weather prediction. There are not many objective tools available for assisting these decisions. Most forecast verification studies have been concerned with 24- or 48-hour predictions that coincide with synoptic observing and weather map production schedules. A statistical climatological estimate of predictability was developed for this project, to allow a rational probabilistic assessment of the acceptability of shot-time wind conditions. The error assessment method has been evaluated for the chance of a wind component directed toward CC (210° azimuth), but this methodology may be generally applied to wind vector prediction.

If a forecast is for a 300° wind direction, exactly bordering on the satisfactory, the likelihood of good conditions (with no wind component toward 210°) is 50%. If the forecast is for strong winds from 210°, the likelihood of abortive error becomes much smaller. The other side of this coin is, of course, if strong winds from 030° are predicted, there is still some finite chance of good conditions resulting in spite of what a forecaster might contend. The problem and solution is approached as it was for predicting fallout trajectories from atmospheric nuclear tests.[58] It is a relatively simple form of the general problem of integrating for probability inside a polygonal area in the field of a bivariate normal probability distribution.[59] The simpler case with a circular normal distribution is sketched in Figure 27. Tables are available[59] for the integrated probability, T(a,h), of falling in the shaded area A, defined by the scalar coefficients a and h.

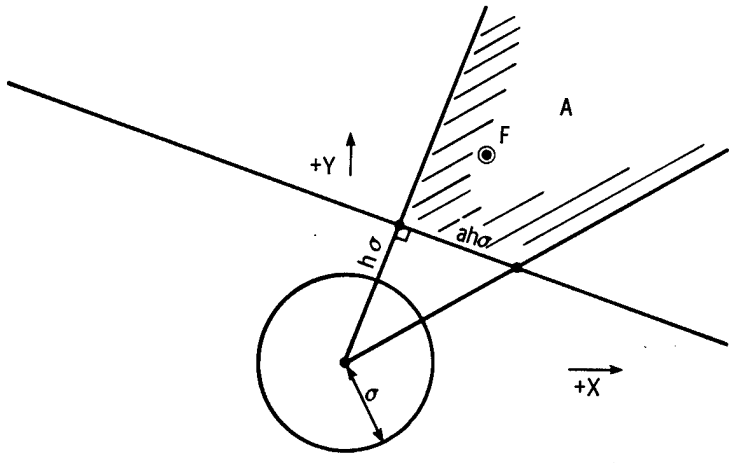

Figure 27. Diagram of Circular Normal Probability Distribution Integration

In Figure 28, the forecast wind vector is for D direction, U speed. The error distribution should be nearly a circular normal distribution with vector magnitude $|\vec{\sigma}|$. Bivariate normal tables[59] give the probability of falling outside ("unsafe") the boundary which passes h from the predicted wind vector point. The probability of hazard would be the same for vector forecasts $\vec{F}_1$ and $\vec{F}_2$. There would be a larger probability of hazard with forecast $\vec{F}_3$ than $\vec{F}_4$, because $\vec{F}_3$ is closest to the unsafe boundary.

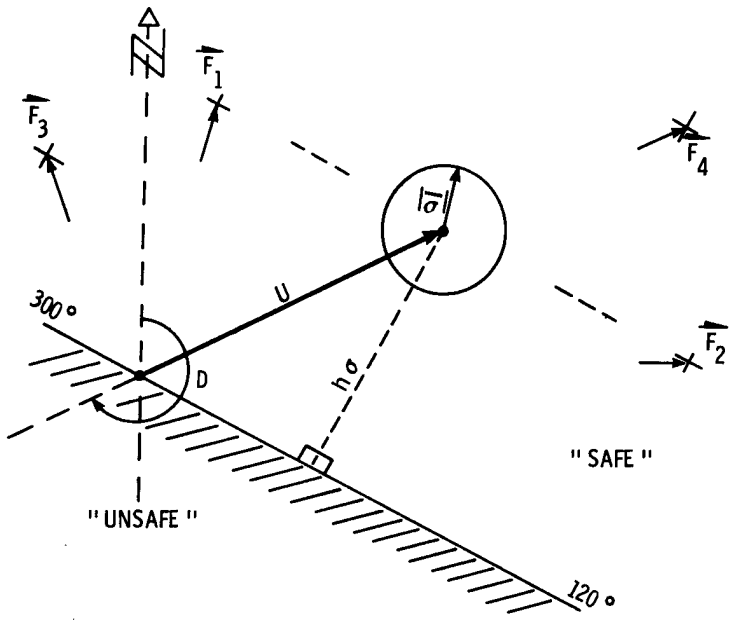

Figure 28. Diagram of the Wind Forecast Reliability Problem

Apparently there has been no adequate treatment of the errors committed in making wind vector forecasts for Cape Canaveral (or most other places). Therefore, an optimized objective statistical wind prediction system, dubbed BREEZE,[60] was used in assessing forecast ability. Where it has been tested,[61] it has been found to predict as well as any competing system.

BREEZE predictions can be produced and evaluated by interpolation between wind statistics that are available for Miami and Jacksonville.[62] At the 95-kPa pressure altitude level, about 400 metres above ground and in the free air circulation, wind variability does have a nearly circular normal distribution (ellipticity near 0.92) and component standard deviations that range from about 5.7 to 5.9 m/s (double for knots) for winter and spring seasons. The t = 24-hour time-lag correlation coefficient is about $\rho_{ut} = 0.4$ for zonal, $\rho_{vt} = 0.3$ for meridional winds. BREEZE predictions are obtained from an optimized combination of persistence of (u_o, v_o), where (u,v) are zonal and meridional wind components and seasonal averages $(\bar{u}, \bar{v})$, such that the best forecast for wind components at time t is

$$u_t = \rho_{ut} u_o + (1 - \rho_{ut})\bar{u} \qquad (21)$$

$$v_t = \rho_{vt} v_o + (1 - \rho_{vt})\bar{v} \tag{22}$$

Forecast error variances are

$$\sigma_f^2(ut) = \sigma_u^2(1 - \rho_{ut}^2) \tag{23}$$

$$\dot{\sigma}_f^2(vt) = \sigma_v^2(1 - \rho_{vt}^2) \tag{24}$$

$$\sigma_f^2(t) = f_{ut}^2 + f_{vt}^2 \tag{25}$$

Evaluation of Florida wind statistics[62] gives an error vector magnitude of 8.20 m/s for 24-hour forecasts, 8.72 m/s for 48-hour forecasts, and 5.56 m/s for 6-hour forecasts. At 1 hour, it decreases to 2.5 m/s. Figures 29 and 30 have been drawn in polar coordinates to show 24- and 48-hour, and 1- and 6-hour probabilities, respectively, of hazardous wind conditions occurring over the field of vector forecasts.

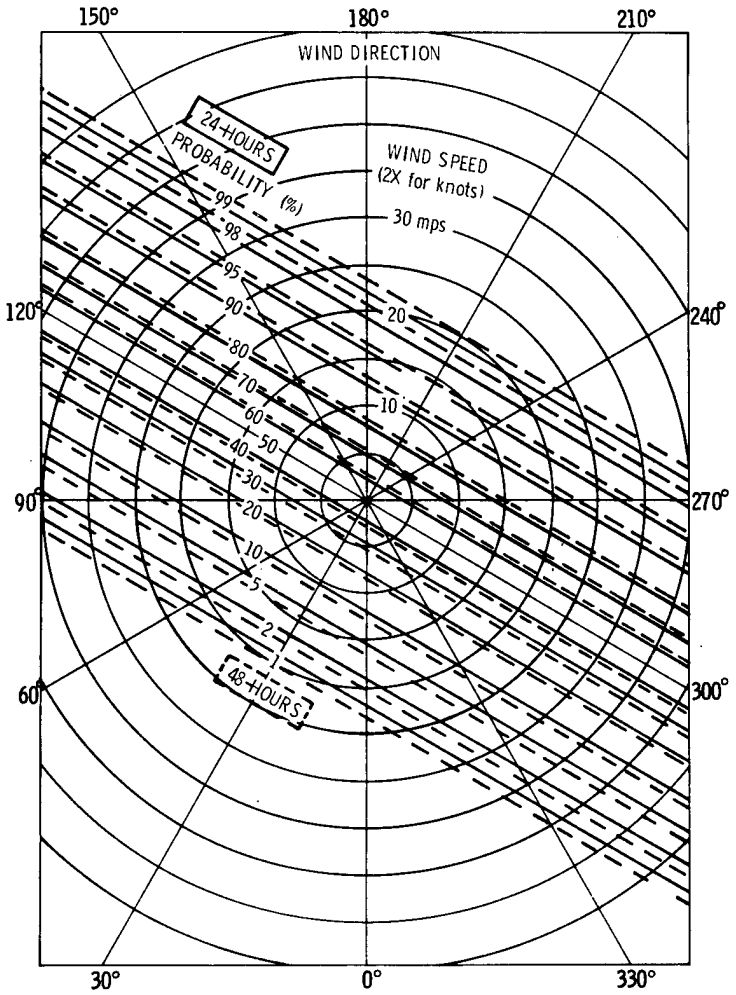

Figure 29. Probability of No Wind Component toward 210° Azimuth with Given Wind Vector Forecasts: 24- and 48-Hour Predictions

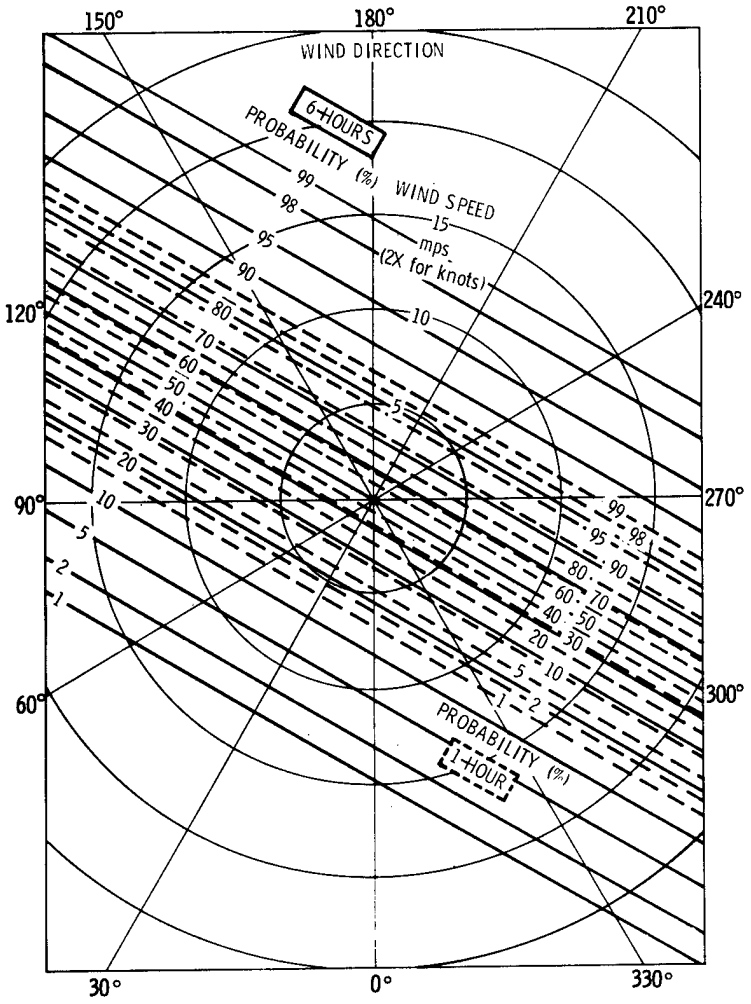

Figure 30. Probability of No Wind Component toward 210° Azimuth with Given Wind Vector Forecasts: 1- and 6-Hour Predictions

By example, Figure 29 shows that a forecast wind component toward 030° of at least 10.5 m/s (21 knots) is necessary to give a 90% chance of successful verification. Note that, by contrast, a 10.5 m/s forecast component toward Cape Canaveral (210°) still has a 10% chance of reversing to good conditions in 24 hours.

At this point, meteorology passes the buck to management to determine the success probability levels that are needed to turn a countdown ON or OFF. A decision must depend upon balancing the probable cost of counting against the probable cost of missing a shot opportunity after a count was discontinued.

As an exercise, January 1975 observations were taken as a set of forecasts, and shot safety probabilities were estimated for 64 cases. If the countdown were turned ON whenever the success expectation exceeded 50%, there should have been 70% successes versus 30% errors when the countdown was turned OFF. In 64 tries there would have been about 28 shots, 12 countdown aborts, 17 correct cutoffs, and 7 missed shot opportunities.

With 66% confidence required to turn ON a countdown, there would have been 20 counts started, 17 shots or 84% success rate, 3 aborts, 26 correct shutdowns, 18 missed opportunities, and 3.8 days of delay per shot. On the other hand, if missed opportunities were extremely expensive and only 20% confidence were needed to start the count, there would be 61 counts started, 35 shots, 26 aborted counts, 3 correct cutoffs, no missed opportunities, and 1.8 days of delay per shot. These exercises demonstrate the necessary tradeoffs, but management must determine the value system.

Only the wind condition at 1 000 feet (300 metres) was evaluated; other forecast parameter contingencies, such as temperature, sea breeze, etc., add error variance and decrease reliability.

Airblast Pressure Monitoring

Five airblast gage stations were sited as shown in Figure 1 to document the propagated pressure wave in case of a Trident explosion. Power was provided by nicad batteries. Pressure transducers were Statham Model PM-283 sensors, which are undamped and have natural frequencies above 2 kHz. They use a corrugated diaphragm about 4 cm in diameter. A command receiver with each station transmitter canister permitted remote control of power (on/off) and calibration (on/off). Transducer output was amplified, led to a voltage-controlled oscillator (VCO), and then transmitted by L-band radio telemetry. At the receiving station, telemetered L-band signals were preamplified, sent through a down-converter to a P-band receiver, thence to a magnetic tape recorder. This recorder was a transistorized version, built to Sandia specifications, of the older, well-known Consolidated System-D. Analog outputs from carrier amplifiers, along with an IRIG coded time signal, were recorded by an Ampex CP-100 magnetic tape recorder. Paper trace records were also made at the recording station, on a Consolidated recording oscillograph. Pressure transducers were calibrated against precision manometers by the Sandia Transducer Evaluation and Calibration Division.

After monitoring eight Trident launches with no explosions, Sandia's airblast recording effort was terminated for economy reasons. Also, Sandia participation in the "weather watch" was ended at the same time, the judgment being that USAF range safety and weather personnel had acquired sufficient appreciation, understanding, and experience to make this evaluation without assistance.

System Performance

As previously stated, there were no explosive failures during launch from Trident tests, that numbered 14 as of November 1978. There was thus no damaging or hazardous blast wave imposed on the communities around CCAFS. The test schedule in Table 13 shows that predictions for the average number of weather delays were satisfactorily verified.

Table 13

Trident Test Schedule and Delays

	Scheduled Test	Actual Test	Delay Cause
1	1000 EST 1/17/77	1403 EST 1/18/77	28-h delay; weather
2	1000 EST 2/14/77	1810 EST 2/15/77	32-h delay; weather
3	1000 EST 3/25/77	1017 EST 3/28/77	3-day delay; hardware
4	0900 EDT 4/28/77	1009 EDT 4/29/77	1-day delay, weather; plus 1 h fishing boats
5	0700 EDT 6/27/77	0700 EDT 6/27/77	No delay
6	1000 EDT 8/10/77	1518 EDT 8/18/77	8-day delay; 4 weather, 3 weather forecast, 1 hardware
7	0700 EDT 8/31/77	1016 EDT 9/3/77	3-day delay; 2 weather, 1 other
8	0800 EDT 10/17/77	1408 EDT 10/19/77	2-day delay; weather
9	12/?/77	12/?/77	No delay
10	1/16/78	1/17/78	1-day delay; weather
11	2/14/78	2/14/78	No delay
12	4/12/78	4/12/78	No delay
13	6/19/78	6/22/78	3-day delay; weather
14	8/10/78	8/10/78	No delay

Meteorological data acquisition and processing, as it finally evolved, was a great success. It demonstrated how much information could be made available on a well-instrumented test range with modern computer technology. Video display outputs aided briefings and helped decision makers to better understand the weather factors that were important.

Weather forecasting performance was about as expected, with only one serious failure to predict the arrival of a period of acceptable conditions. In verification of Murphy's Law, that the worst will happen, a Friday forecast for continued bad weather was incorrect. The unattractive alternative was to schedule a full weekend of overtime contrary to the forecaster's advice. With weak summertime circulation patterns, significant changes are possible in times much shorter than the 4 days involved in deciding on Friday to take the next look at the weather on Monday.

Of course, the optimum-economy action cannot be determined without extensive cost data. Most difficult to establish is the total program delay cost which probably shows some elasticity to occasional short delays. The most practical difficulty is, however, for the field manager with his proximate concerns for extra and immediate costs of overtime work. Hopefully, weather-dependent program management can be educated to assemble reasonable cost estimates that can be used with objective prediction assessments to provide optimized decision-making strategies for weather watching.

SUMMARY

Should a Trident motor have exploded on Launch Pad 25 at CC, the 45.4 Mg (50 t) TNT airblast yield equivalent would have caused some window damage in the town of Cape Canaveral. At worst, depending on atmospheric conditions, nearly 40% of the windows would have been broken at considerable hazard to residents. At best, with minimized propagation in an atmosphere that was refracting the blast wave upward and above the community, possibly two dozen panes could have been cracked. These would probably not be broken with such force as to cause any hazard except for falling glass.

Some of the time, when Cape Canaveral is protected from strong propagation, there would be strong propagation toward the northwest and Titusville. Inversion propagation, with 3X magnification of overpressures, would break about 3 dozen panes there. Good days for both towns, usually with west or southwest winds aloft, only occur on about 20% of the dates in July and August. If downwind effects on Titusville could be judged acceptable but with no calculated sound ducting, then about 50% of July and August dates would be available for testing.

If window glazing was truly practiced to meet hurricane wind standards, these damages would be considerably reduced. If doors and windows were opened during each test event, nearly all damage could be avoided with minimized atmospheric propagation conditions.

A "weather watch" was established to determine whether good or bad propagations might be expected in the event of such a missile failure and explosion. It is not reasonable to expect accurate long-range (3-day) predictions of the necessary wind details. A rawinsonde observation release at about H-1.5 allows reasonably confident data acquisition, processing, blast prediction, and recommendations to the test director. This, as well as earlier observations, is within the capability of the CC weather observing system. There could, however, be several days of delay in waiting for conditions needed to minimize airblast propagations.

Instrumentation was installed to observe blast propagation in event of a launch accident. This would have allowed estimation of effective explosion yield as well as verification of blast amplitudes in nearby communities. Measurements greatly facilitate evaluation of damage claims for validity and adjustment.

After eight successful Trident launches, Sandia participation in airblast prediction and measurement was terminated for economy reasons. ETR weather and range safety officials had acquired the necessary skills to make the "weather watch" without supervision or assistance. The likelihood of a Trident explosion was deemed too small to warrant the expense of continuing the operation of the pressure gage monitoring system.

CONCLUSIONS

- A Trident missile explosion near Pad 25, CCAFS, would cause window damage in Cape Canaveral. Under some weather conditions there would be considerable hazard to residents.
- Airblast propagation potentials could be reduced by testing only with acceptable sound velocity-height gradients and no surface wind component directed toward Cape Canaveral.
- Weather restrictions could be expected to cause an average of 2 days delay per test with minor seasonal variation.
- Weather observation and computer facilities at CCAFS were satisfactory for supporting an adequate "weather watch" against strong airblast propagation conditions.

RECOMMENDATIONS

There are several facets of blast prediction that are not well enough understood to give great confidence in explosion effects estimates. Some problem areas have been listed here that require further research in hopes of reducing restrictions caused by a safe-conservative prediction.

- Boundary layer propagation enhancement and attenuation needs to be correlated (if possible) with the vertical gradient of sound velocity. This would facilitate incremental damage prediction, rather than large-step-function prediction which must be made at present.
- The enhancement or attenuation effect of surface winds needs to be distinguished from the sound velocity-height gradient effect.
- Wave-frequency and yield-dependent mechanics of propagations need to be better understood for boundary layer conditions that may diffract, scatter, or cause constructive interference in explosion waves.
- Statistical models for window glass breakage under uniform pressure loads need to be better established and supported by theory.
- The hazard from broken, falling window glass needs to be explored.
- Management models should be developed for cost-effective countdown strategies in weather-dependent hazardous operations.

REFERENCES

[1] Airblast Characteristics for Single Point Explosions in Air, with a Guide to Evaluation of Atmospheric Propagation and Effects, (fourth draft) ANSI Standard S2.20-197X (New York: American National Standards Institute, 8 April 1978).

[2] E. F. Cox, H. J. Plagge, and J. W. Reed, "Meteorology Directs Where Blast Will Strike," Bulletin of the American Meteorological Society, 35:3, pp 95-103, March 1954.

[3] J. W. Reed et al, "Evaluation of Window Pane Damage Intensity in San Antonio Resulting from Medina Facility Explosion on November 13, 1963," Annals of the New York Academy of Sciences, 152:Art 1, pp 565-584, October 1968.

[4] E. R. Fletcher, D. R. Richmond, and R. K. Jones, Velocities, Masses and Spatial Distributions of Glass Fragments from Windows Broken by Airblast, Defense Nuclear Agency Report (Albuquerque: Lovelace Foundation), in preparation.

[5] P. D. Schomer, R. J. Goff, and L. M. Little, The Statistics of Amplitude and Spectrum of Blasts Propagated in the Atmosphere, Tech Rep N-13 (Champaign, Illinois: Construction Engineering Research Laboratory, November 1976).

[6] Letter from M. M. Swisdak, Jr., U.S. Navy Surface Weapons Center, Silver Spring, MD, subject: "Long Range Airblast Measurements on DAWS Tests," 9 August 1977.

[7] R. D. Daniels and K. Overbeck, Launch Feasibility Study for Trident II, Tech Rpt No. 1330 (Redondo Beach, California: J. H. Wiggins Co., July 1978).

[8] J. W. Reed, Test Plan for Intermediate Range Airblast Propagation Measurements, SAND78-1703 (Albuquerque: Sandia Laboratories, December 1978).

[9] Letter from B. G. Craig, Division M-3, Los Alamos Scientific Laboratory, Los Alamos, New Mexico, January 1976.

[10] S. Glasstone, ed, The Effects of Nuclear Weapons, rev ed (Washington: Government Printing Office, 1962).

[11] C. D. Broyles, IBM Problem M Curves, SC-TM-268-56(51) (Albuquerque: Sandia Laboratories, December 1956).

[12] J. W. Reed, "Airblast Overpressure Decay at Long Range," J Geophysical Research, 77(9), pp 1623-1629, March 1972.

[13] C. E. Needham, M. L. Havens, and C. S. Knauth, Nuclear Blast Standard (1kt), AFWL-TR-73-55 rev, (Kirtland Air Force Base, New Mexico: April 1975).

[14] J. W. Reed, Climatology of Airblast Propagations from Nevada Test Site Nuclear Airbursts, SC-RR-69-572 (Albuquerque: Sandia Laboratories, December 1969).

[15] J. W. Reed, Explosion Wave Amplitude Statistics for a Caustic at Ranges of 30 to 45 Miles, SC-RR-67-860 (Albuquerque: Sandia Laboratories, February 1968).

[16] J. W. Reed and H. W. Church, Blast Predictions at Christmas Island (U), Operation Dominic Hazards Evaluation Unit Report WT-2057 (Oak Ridge: USAEC-DTIE, October, 1963). (Secret).

[17] J. W. Reed, Blast Prediction and Microbarograph Measurements, Project Middle Gust Final Report, SLA-73-0484 (Albuquerque: Sandia Laboratories, August 1973).

[18] J. W. Reed, Blast Prediction and Microbarograph Measurements, Project LN-106, Project Mixed Company Final Report, POR-6603 (Albuquerque: Sandia Laboratories, October 1973).

[19] E. F. Cox, H. J. Plagge, and J. W. Reed, Damaging Air Shocks at Large Distances from Explosions, Operation Buster-Jangle Report WT-303 (Albuquerque: Sandia Laboratories, 24 April 1952).

[20] E. F. Cox, Air Shocks at Large Distances from Atomic Explosions, Operation Tumbler-Snapper Report WT-504 (Albuquerque: Sandia Laboratories, 5 January 1953).

[21]E. F. Cox and J. W. Reed, Long-Distance Blast Predictions, Microbarometric Measurements, and Upper-Atmosphere Meteorological Observations for Operations Upshot-Knothole, Castle, and Teapot, General Report on Weapons Tests WT-9003 (Oak Ridge: AEC-TIS, 20 September 1957).

[22]J. W. Reed, Distant Blast Predictions for Explosions, Minutes 15th ESB Seminar, DOD-ESB, Washington, DC, 18 September 1973.

[23]B. B. Redpath, A Review of Airblast-Induced Window Breakage, Proceedings, Society of Explosives Engineers, Louisville, Kentucky, 28 January 1976.

[24]U.S. Standard Atmosphere, 1962 (Washington: Government Printing Office, 1962).

[25]H. R. Byers, General Meteorology, (New York: McGraw Hill, 1959).

[26]American National Standard Building Code Requirements for Minimum Design Loads in Buildings and Other Structures, ANSI A58.1-1972 (New York: American National Standards Institute, 1972).

[27]Guide to Meteorological Instrument and Observing Practices, WMO-No. 8. Tp. 3 (Geneva: World Meteorological Organization, 1971).

[28]P. J. Dickinson, "Temperature Inversion Effects on Aircraft Noise Propagation," J Sound Vibr, 47:438-443, 1976.

[29]D. M. Campbell, Probe Analysis of Experimental Blast Wave Propagation Data, IDC/8115/1684 (Sunnyvale, California: Lockheed/LMSC, 17 November 1977).

[30]Letter from H. Taffett to NOTU, Hq ETR, 3 December 1976.

[31]J. W. Reed, "Cape Canaveral Sea Breezes," J Appl Meteor, 18:231-235, 1979.

[32]J. Aitchison and J. A. C. Brown, The Lognormal Distribution, (Cambridge, England: The University Press, 1969, pp 7-14).

[33]C. Wilton and B. Gabrielsen, House Damage Assessment--Summary Report, DNA-2906F (Defense Nuclear Agency) (San Mateo, California: URS Research Corporation, January 1973).

[34]R. S. Burington and D. C. May, Handbook of Probability and Statistics, rev ed (Sandusky, Ohio: Handbook Publishers, 1958).

[35]R. W. Ansevin, Correlation of the DSR with the Strength of Glass of Different Compositions and Configurations, ML TDR 64-180 (Harmar Township, Pennsylvania: Pittsburgh Plate Glass Company, August 1964).

[36]H. Marcus, Die Theorie Elasticher Gewebe (The Theory of the Elastic Grid) (Berlin, Germany: J. Springer, 1932).

[37]R. Bowles and B. Sugarman, "The Strength and Deflection Characteristics of Large Rectangular Glass Panels under Uniform Pressure," Glass Technology, 3(5), October, 1962.

[38]Glass Product Recommendations, Structural, Report 101, (Pittsburgh: Pittsburgh Plate Glass Company, undated).

[39]J. H. Iverson, Summary of Existing Structures Evaluation, Part II: Window Glass and Applications, OCD Work Unit No. 1126C Final Report (Menlo Park, California: Stanford Research Institute, December 1968).

[40]W. C. Clark, Window and Glass Hazards under Wartime Conditions and Recommended Protective Measures, AECU-3037 (Washington: U.S. Atomic Energy Commission, 1954).

[41]J. W. Reed, "Amplitude Variability of Explosion Waves at Long Ranges," J Acoust Soc of Amer, 39:5, pt 1, May 1966.

[42]J. A. Blume et al, Response of Structures to Sonic Booms Produced by XB-70, B-58, and F-104 Aircraft (San Francisco: J. A. Blume and Associates, July, 1967).

[43]R. L. Hershey and T. H. Higgins, Statistical Prediction Model for Glass Breakage from Nominal Sonic Boom Loads, FAA-RD-73-79 (Washington: U.S. Department of Transportation, January 1973).

[44]V. D. Kazakov et al, "Strength of Sheet Glass Produced by the Glass Plants," Glass and Ceramics (Trans of Steklo i. Keramika, 27, 8 August 1970).

[45]W. G. Brown, A Load Duration Theory for Glass Design, NRCC-12354 (Ottowa: National Research Council of Canada, January 1972).

[46]J. H. Wiggins, Jr., Effects of Sonic Boom, (Palos Verdes Estates, California: J. H. Wiggins Co., 1960).

[47]L. Seaman, Nonlinear Response of Windows to Sonic Booms, Interim Report No. 7 (Stanford Research Institute, National Sonic Boom Evaluation Office, USAF, June 1967).

[48]Letter from J. E. Minor, Texas Tech University, Lubbock, Texas, 11 January 1976.

[49]J. E. Minor, Appraisal of Window Pane Population and Potential Damage from Low-Level Pressure Pulses in Seven Central American Cities, Interoceanic Canal Studies Memorandum AB-10 (San Antonio: Southwest Research Institute, 11 October 1967).

[50]J. W. Reed, Second Window Pane Survey in Isthmian Areas, Interoceanic Canal Studies Memorandum AB-15, SC-M-69-313 (Albuquerque: Sandia Laboratories, June 1969).

[51]Letter from L. J. Ullian, Patrick AFB, Florida, 5 April 1978.

[52]L. H. Long, ed, The World Almanac, 1971 Edition (New York, Newspaper Enterprises Association, 1970).

[53]Letter from R. J. Bartholomew, WX-8, Los Alamos Scientific Laboratory, 17 May 1976.

[54]Associated Press, "Boom Breaks 300 Windows," Albuquerque Tribune, 1 June 1968.

[55]E. R. Fletcher, D. R. Richmond, and C. S. White, Biological Hazards, letter report on Contract AT(29-2)--2099 Mod 1 (Albuquerque: Lovelace Foundation for Medical Education and Research, October 1976).

[56]Letter from C. S. White, Oklahoma Medical Research Foundation, Oklahoma City, Oklahoma, 3 November 1976.

[57]J. W. Reed, Long Range Airblast, Operation Sailor Hat Report POR-4057 (Washington: Defense Atomic Support Agency, August 1966).

[58]J. W. Reed, Estimating Safety Probabilities from Fallout Forecasts for Nevada Test Site, SC-4073 (TR) (Albuquerque: Sandia Laboratories, 1957).

[59]D. B. Owen, The Bivariate Normal Probability Distribution, SC-3831 (TR) (Albuquerque: Sandia Laboratories, 1 August 1956).

[60]J. W. Reed, "Some Notes on Forecasting of Winds Aloft by Statistical Methods," J Appl Meteor, 6:360-372, 1967.

[61]R. L. Lavoie and C. J. Wiederanders, Objective Wind Forecasting over the Tropical Pacific, AFCRL-TN-60-832 (Honolulu: University of Hawaii, December 1960).

[62]B. N. Charles, Basic Statistics of the USWB-FCDA Upper Wind Punched Card Deck, vol 1, part B (1959) and Interlevel Wind Correlations, vol 2 (1960), U.S. Weather Bureau-Sandia Corporation Cooperative Project in Climatology.

APPENDIX A

Sea Breeze Wind Components
(Cape Canaveral, Florida
Meteorological Tower 313
U, east; V, north (m/s))

Table A-1

Sea Breeze Wind Components at 3.7, 16.5, and 49.4 Metres

CAPE CANAVERAL FT. MYERS SEA BREEZE WIND COMPONENTS (U-EAST/WEST-V-NORTH) IN METERS PER SECOND

ANEMOMETER HEIGHT 3.7 METERS.

TIME	MONTH																					
	JAN		FEB		MAR		APR		MAY		JUN		JUL		AUG		SEP		OCT		NOV		DEC	
HOURS (Z)	U	V	U	V	U	V	U	V	U	V	U	V	U	V	U	V	U	V	U	V	U	V	U	V
0	-.5	.0	-.1	.4	-.5	.2	-.5	.3	-.6	.2	-.2	.5	-.2	.5	-.1	.3	-.7	.2	-.1	.1	-.2	.1	-.3	.2
1	-.4	.1	.0	.3	-.2	.2	-.2	.3	-.1	.1	.1	.4	.0	.4	.2	.2	-.5	.2	.0	.1	-.2	.2	-.2	.3
2	-.2	.1	.1	.2	-.1	.2	-.0	.3	.1	.1	.2	.1	.2	.2	.4	.1	-.3	.2	-.1	.2	-.1	.2	-.2	.4
3	-.2	.1	-.0	.2	.1	.2	.1	.3	.3	.2	.4	.0	.3	.1	.5	.1	-.1	.4	-.0	.3	-.0	.3	-.1	.5
4	-.1	.2	-.0	.2	.1	.2	.3	.4	.4	.3	.5	.1	.4	-.0	.5	.1	.0	.4	.0	.3	.1	.3	.0	.5
5	-.0	.2	.1	.2	.2	.2	.5	.4	.5	.2	.6	.2	.4	-.1	.5	.1	.2	.4	.0	.4	.2	.3	.1	.4
6	.1	.2	.2	.2	.2	.1	.6	.3	.6	.2	.6	.2	.5	-.3	.6	.1	.5	.4	.1	.5	.3	.3	.2	.4
7	.2	.1	.2	.1	.3	.0	.7	.2	.7	.1	.7	.2	.6	-.3	.7	.0	.6	.0	.2	.5	.4	.3	.2	.4
8	.3	.1	.1	.0	.5	-.0	.8	.1	.8	.0	.7	.1	.6	-.4	.8	-.0	.6	-.1	.3	.4	.5	.2	.3	.3
9	.3	.1	.1	-.0	.6	-.1	.8	.0	.9	-.1	.8	.1	.6	-.4	.8	-.1	.7	-.2	.4	.4	.6	.1	.3	.2
10	.3	.1	.1	-.1	.6	-.2	.8	-.0	.8	-.1	.8	.0	.6	-.4	.8	-.1	.9	-.1	.5	.3	.6	-.0	.4	.1
11	.3	.1	.1	-.0	.6	-.3	.9	-.0	.7	-.2	.7	.1	.5	-.4	.8	-.2	1.1	-.3	.6	.4	.6	.0	.3	-.0
12	.3	-.0	.1	-.0	.6	-.3	.8	-.1	.6	-.2	.7	.1	.3	-.3	.6	-.2	1.0	-.1	.6	.3	.6	.0	.4	-.1
13	.4	-.1	.1	-.0	.7	-.2	.6	-.2	.5	-.2	.5	.2	.4	-.2	.5	-.1	1.0	-.1	.4	.1	.5	.0	.4	-.2
14	.4	-.2	.2	-.1	.6	-.1	.5	-.3	.3	-.2	.4	.0	.4	-.1	.2	-.0	.7	.1	.1	-.1	.2	-.1	.4	-.4
15	.4	-.1	.3	-.2	.4	.0	.2	-.4	.1	-.3	.1	-.3	.4	-.1	.0	-.0	.3	.1	-.1	-.3	-.1	-.1	.2	-.4
16	.3	-.1	.4	-.3	.2	-.0	-.1	-.5	-.2	-.4	-.2	-.6	.1	-.2	-.3	-.1	.0	-.2	-.3	-.4	-.3	-.2	.1	-.4
17	.2	-.0	.2	-.3	-.1	-.1	-.4	-.5	-.4	-.4	-.7	-.6	-.3	-.1	-.7	-.2	-.1	-.4	-.3	-.6	-.4	-.4	-.2	-.3
18	.2	-.1	.0	-.2	-.5	-.1	-.8	-.4	-.5	-.2	-1.1	-.5	-.8	.0	-1.1	-.2	-.5	-.3	-.4	-.7	-.5	-.5	-.2	-.5
19	-.2	-.1	-.3	-.1	-.7	-.2	-1.0	-.3	-.9	-.1	-1.4	-.4	-1.2	-.2	-1.4	-.2	-.9	-.3	-.5	-.7	-.6	-.5	-.3	-.5
20	-.5	-.3	-.5	-.2	-.9	.0	-1.2	-.2	-1.2	-.1	-1.4	-.3	-1.3	-.3	-1.5	-.1	-1.2	-.2	-.5	-.7	-.7	-.4	-.4	-.5
21	-.6	-.2	-.4	-.2	-.9	.0	-1.3	-.1	-1.5	-.2	-1.3	-.2	-1.1	-.4	-1.3	.0	-1.3	-.1	-.5	-.5	-.6	-.3	-.5	-.3
22	-.5	-.2	-.5	-.2	-.9	.2	-1.2	-.1	-1.2	-.3	-1.0	.2	-.9	-.6	-1.0	.2	-1.2	.2	-.3	-.3	-.5	-.1	-.5	-.1
23	-.5	-.1	-.3	.1	-.7	.2	-.8	.2	-.8	.3	-.5	.5	-.6	.7	-.6	.3	-.9	.3	-.2	-.1	-.4	.1	-.4	.1

ANEMOMETER HEIGHT 16.5 METERS.

TIME	MONTH																					
	JAN		FEB		MAR		APR		MAY		JUN		JUL		AUG		SEP		OCT		NOV		DEC	
HOURS (Z)	U	V	U	V	U	V	U	V	U	V	U	V	U	V	U	V	U	V	U	V	U	V	U	V
0	-.8	-.1	-.8	-.0	-1.0	.3	-1.1	.3	-1.0	.0	-.8	.3	-.7	.4	-.4	.7	-.8	.3	-.3	-.1	-.6	.1	-.8	.1
1	-.7	-.1	-.7	.3	-.8	.3	-.8	.4	-.6	.0	-.3	.4	-.4	.3	.4	.7	-.6	.4	-.3	.1	-.6	.2	-.7	.4
2	-.5	-.1	-.5	.6	-.6	.3	-.6	.5	-.2	.1	.1	.4	-.2	.2	.6	.6	-.4	.5	-.4	.2	-.5	.3	-.5	.5
3	-.5	.0	-.4	.7	-.4	.3	-.3	.6	.2	.3	.2	.5	-.1	.1	.5	.5	-.3	.6	-.3	.4	-.4	.4	-.3	.6
4	-.4	.1	.0	.7	-.1	.4	.0	.7	.4	.6	.3	.6	.1	-.2	.6	.5	-.1	.6	-.3	.4	-.2	.4	.0	.5
5	-.2	.2	.4	.7	.2	.4	.4	.7	.7	.8	.6	.7	.3	-.4	.8	.6	.1	.6	-.2	.5	.1	.5	.2	.5
6	.2	.2	.6	.6	.4	.3	.7	.8	1.0	.7	1.0	.7	.7	-.2	1.0	.5	.4	.5	-.2	.5	.3	.5	.3	.5
7	.4	.2	.7	.4	.7	.2	.9	.4	1.2	.5	1.3	.7	1.0	-.1	1.1	.5	.6	.4	-.0	.6	.5	.5	.3	.5
8	.5	.2	.6	.2	.3	.0	1.1	.3	1.3	.3	1.6	.6	1.1	-.1	1.5	.5	.9	.2	.2	.6	.6	.3	.5	.5
9	.6	.2	.7	.1	.8	-.1	1.3	.2	1.4	.2	1.7	.5	.9	-.5	1.5	.3	1.0	-.1	.4	.5	.8	.1	.6	.3
10	.6	.2	.7	-.0	.8	-.3	1.4	.1	1.5	.1	1.6	.3	.6	-.6	1.4	.0	1.1	-.2	.7	.4	.8	.0	.8	.1
11	.6	.2	.6	-.1	.8	-.4	1.6	.0	1.5	.0	1.4	.3	.4	-.7	1.1	-.6	1.2	-.3	.8	.5	.7	-.0	.8	-.1
12	.5	-.0	.6	-.1	.8	-.4	1.5	-.0	1.2	-.2	1.3	.3	.2	-.2	1.0	-.6	1.2	-.2	.8	.3	.7	-.0	.7	-.2
13	.6	-.1	.6	-.2	1.0	-.3	1.2	-.2	1.0	-.2	.8	.4	1.0	-.2	.8	-.6	1.0	-.3	.6	.1	.6	-.0	.6	-.3
14	.6	-.1	.5	-.3	1.0	-.2	.6	-.3	.8	-.1	.6	.1	2.4	.2	.6	-.5	.6	-.2	.4	-.0	.3	-.1	.6	-.4
15	.6	-.1	.4	-.5	.8	.0	.5	-.5	.7	-.2	.2	-.4	2.6	.3	.3	-.5	.2	-.3	.1	-.1	.0	-.2	.3	-.5
16	.5	-.1	.3	-.6	.5	.0	.2	-.6	.4	-.5	-.0	-.9	.5	.6	-.1	-.5	-.2	-.3	-.0	-.3	-.2	-.4	.2	-.4
17	.3	-.0	.2	-.7	-.1	-.2	-.4	-.8	-.4	-.7	-.9	-1.1	-1.2	.1	-.6	-.7	-.4	-.3	-.1	-.5	-.2	-.5	-.0	-.4
18	.1	-.1	-.2	-.6	-.4	-.3	-.8	-.9	-1.3	-.7	-1.6	-1.2	-2.1	.1	-1.4	-1.1	-.6	-.4	-.2	-.8	-.2	-.5	-.2	-.5
19	-.2	-.1	-.4	-.5	-.7	-.5	-1.3	-.8	-1.9	-.5	-2.1	-1.1	-1.8	.1	-2.5	-.9	-.8	-.5	-.3	-.9	-.4	-.5	-.3	-.5
20	-.5	-.1	-.9	-.3	-1.1	-.3	-1.6	-.6	-2.2	-.4	-2.2	-1.0	-1.9	.4	-2.5	-.5	-1.0	-.5	-.4	-.9	-.5	-.5	-.5	-.5
21	-.7	-.1	-1.0	-.2	-1.2	-.1	-1.7	-.3	-2.2	-.2	-2.0	-.6	-1.5	.1	-2.1	.2	-1.1	-.4	-.3	-.7	-.5	-.3	-.7	-.3
22	-.8	-.1	-1.0	-.2	-1.3	.2	-1.7	-.0	-2.0	-.1	-1.7	-.3	-1.1	.3	-1.7	.4	-1.1	-.2	-.3	-.6	-.6	-.1	-.9	-.2
23	-.9	-.1	-.9	-.2	-1.2	.3	-1.4	.2	-1.4	-.1	-1.2	.0	-.8	.3	-1.1	.6	-1.0	.0	-.3	-.3	-.6	-.0	-.9	-.1

ANEMOMETER HEIGHT 49.4 METERS.

TIME	MONTH																					
	JAN		FEB		MAR		APR		MAY		JUN		JUL		AUG		SEP		OCT		NOV		DEC	
HOURS (Z)	U	V	U	V	U	V	U	V	U	V	U	V	U	V	U	V	U	V	U	V	U	V	U	V
0	-1.0	.0	-.9	.1	-1.3	.2	-1.4	.4	-1.3	.1	-1.2	.4	-1.0	1.0	-.8	.5	-1.4	.4	-.6	-.2	-.9	.0	-1.0	.1
1	-.8	-.0	-.9	.5	-1.2	.4	-1.2	.6	-.9	.1	-.5	.6	-.5	.9	-.3	.7	-1.1	.7	-.7	-.1	-.9	.1	-.9	.3
2	-.6	.0	-.7	.7	-.9	.5	-.4	.7	-.5	.4	-.0	.5	.1	.5	.0	.8	-.8	.9	-.8	.1	-.4	.3	-.6	.5
3	-.4	.1	-.6	.9	-.6	.6	-.6	.7	-.1	.7	-.1	.5	.3	.4	.4	.8	-.6	1.0	-.7	.2	-.7	.4	-.4	.5
4	-.2	.2	-.0	.7	-.1	.6	-.2	.9	.1	1.0	.0	.7	.5	.3	.5	.8	-.3	1.1	-.6	.4	-.4	.5	-.0	.5
5	-.0	.2	.4	.7	-.0	.5	.3	.9	.7	1.1	.4	.8	.8	.4	.7	.9	.1	1.2	-.4	.5	-.1	.6	.2	.5
6	.3	.0	.5	.6	.2	.4	.7	.8	1.1	1.1	1.1	.9	1.0	.3	1.0	.8	.5	1.2	-.4	.6	.2	.6	.3	.6
7	.5	-.1	.5	.6	.5	.4	1.0	.6	1.4	.9	1.4	.9	1.3	.2	1.2	.8	.9	1.1	-.2	.7	.6	.5	.4	.5
8	.6	-.1	.6	.4	.4	.2	1.2	.4	1.4	.6	1.6	.8	1.4	.1	1.3	.5	1.3	.8	.0	.6	.9	.3	.5	.4
9	.7	-.0	.5	.2	.4	.0	1.4	.3	1.4	.5	1.7	.7	1.4	.0	1.3	.4	1.6	.3	.3	.5	1.1	-.0	.7	.2
10	.7	.1	.3	.2	.4	-.1	1.5	.1	1.5	.4	1.7	.5	1.4	-.2	1.2	.0	1.7	.0	.6	.4	1.2	-.2	.6	-.1
11	.7	.1	.7	.3	.4	-.3	1.7	.0	1.6	.2	1.6	.4	1.1	-.4	1.2	-.2	1.7	-.2	.7	.4	1.1	-.3	.8	-.4
12	.7	-.0	.7	.5	-.1	.4	1.8	-.1	1.6	.4	.9	.6	.7	-.6	1.1	-.3	1.8	-.2	.8	.3	1.0	-.3	.8	-.4
13	.7	-.1	.6	-.2	1.1	-.4	1.8	-.4	1.4	-.3	1.2	.6	.5	-.7	1.0	-.3	1.6	-.4	.8	.2	.7	-.2	.6	-.4
14	.7	-.1	.4	-.3	1.2	-.2	1.1	-.4	1.3	-.5	1.0	-.6	.6	-.7	.7	-.3	1.2	-.6	.7	.0	.9	-.1	.6	-.4
15	.5	-.0	.4	-.5	1.0	-.0	.7	-.6	.8	-.7	.6	-.4	.5	-.6	.4	-.4	.7	-.8	.5	-.1	.1	-.1	.4	-.4
16	.4	-.0	.3	-.7	.7	-.1	.4	-.7	.4	-.7	.2	-.1	.3	-.6	-.2	-.7	.1	-1.0	.5	-.2	-.1	-.2	.3	-.3
17	.3	.0	.2	-.9	.1	-.4	-.2	-1.0	-.4	-1.1	-.7	-1.1	-.3	-.5	-.4	-1.0	-.3	-1.1	.4	-.4	-.1	-.4	.0	-.3
18	.2	.1	-.2	-.9	-.2	-.6	-.7	-1.1	-1.2	-1.1	-1.5	-1.4	-1.0	-.5	-1.5	-1.1	-.7	-1.1	.2	-.7	-.2	-.5	-.1	-.4
19	-.1	.1	-.4	-.7	-.5	-.8	-1.2	-1.1	-1.4	-1.0	-2.0	-1.4	-1.9	-.3	-1.9	-1.1	-1.2	-1.1	-.0	-.4	-.4	-.5	-.1	-.4
20	-.7	-.1	-.9	-.9	-1.1	-.4	-1.6	-.9	-2.0	-1.0	-2.4	-1.4	-2.6	-.6	-2.1	-1.0	-1.5	-1.1	-.1	-.6	-.6	-.6	-.3	-.4
21	-1.0	-.1	-1.1	-.3	-1.1	-.3	-1.7	-.9	-2.3	-.9	-2.8	-1.3	-3.0	.1	-2.4	-.7	-1.8	-.9	-.2	-.7	-.7	-.6	-.7	-.2
22	-1.1	-.0	-1.1	-.3	-1.1	-.0	-1.7	-.9	-2.1	-1.1	-2.8	-1.5	-2.6	.4	-1.9	-.6	-1.4	-.9	-.3	-.6	-.7	-.1	-1.0	-.1
23	-1.1	-.0	-1.1	-.2	-1.1	.1	-1.5	-.2	-1.7	-.1	-1.5	-.0	-1.5	.8	-1.1	.2	-1.7	-.0	-.4	-.4	-.6	.0	-1.1	.0

Table A-2

Sea Breeze Wind Components at 62.2 and 150.9 Metres

[illegible] WIND COMPONENTS IN METERS PER SECOND

[illegible] ANEMOMETER HEIGHT [illegible] METERS.

TIME	MONTH																					
	JAN		FEB		MAR		APR		MAY		JUN		JUL		AUG		SEP		OCT		NOV		DE	
HOURS (Z)	U	V	U	V	U	V	U	V	U	V	U	V	U	V	U	V	U	V	U	V	U	V	U	V
0	-.6	.2	-.5	.2	-1.5	.4	-1.5	.6	-1.4	.2	-1.1	.5	-.4	1.0	-.8	.6	-1.5	.3	-.6	-.1	-.4	.1	-1.0	.4
1	-.7	.1	-.6	.4	-1.3	.5	-1.3	.6	-.9	.1	-.4	.7	-.3	.9	-.2	.7	-1.3	.7	-.7	.0	-1.0	.2	-.8	.5
2	-.6	.0	-.4	.4	-1.0	.7	-1.1	.6	-.9	.4	.0	.6	.1	.6	.2	.7	-1.0	.9	-.4	.2	-.4	.3	-.5	.6
3	-.5	-.1	-.4	1.1	-.7	.7	-.5	.6	-.3	.4	-.0	.6	.3	.6	.5	.8	-.8	1.1	-.8	.3	-.7	.5	-.2	.6
4	-.3	.1	.1	1.1	-.3	.7	-.3	1.0	.1	1.1	.1	.7	.4	.6	.6	.8	-.4	1.1	-.6	.4	-.4	.5	.2	.6
5	-.2	.1	.6	.9	.0	.7	.1	1.0	.5	1.1	.5	.8	.7	.4	.2	.9	.0	1.2	-.5	.6	-.1	.6	.3	.5
6	.2	-.1	1.0	.7	.4	.6	.7	1.0	.9	1.1	1.0	.8	1.0	.3	1.0	.9	.5	1.2	-.4	.6	.2	.6	.4	.6
7	.3	-.1	1.1	.4	.6	.5	1.0	.7	1.3	.9	1.7	1.0	1.2	.1	1.2	.9	.9	1.0	-.2	.7	.5	.5	.5	.5
8	.5	-.1	1.0	.1	.2	.3	1.3	.9	1.5	.7	2.0	.9	1.4	.1	1.4	.7	1.3	.7	.0	.6	.8	.3	.6	.4
9	.5	-.1	1.0	-.0	.9	.0	1.5	.2	1.6	.6	2.1	.7	1.5	-.0	1.5	.4	1.5	.3	.3	.5	1.0	-.0	.8	.1
10	.6	-.2	.8	-.2	.9	-.2	1.7	.0	1.7	.5	1.7	.3	1.4	-.2	1.3	-.0	1.6	-.1	.5	.3	1.1	-.2	.8	-.3
11	.5	-.2	.7	-.3	1.0	-.4	1.4	-.0	1.6	.3	1.5	.6	1.2	-.4	1.1	-.3	1.7	-.3	.7	.4	1.1	-.4	.7	-.6
12	.5	-.2	.6	-.3	1.1	-.6	1.4	-.2	1.7	-.1	1.4	.1	.8	-.7	1.0	-.5	1.7	-.3	.8	.2	1.1	-.4	.6	-.7
13	.5	-.2	.6	-.4	1.3	-.6	1.5	-.4	1.6	-.3	1.1	.1	.8	-.8	1.1	-.5	1.6	-.4	.8	.1	.8	-.3	.5	-.6
14	.6	-.2	.5	-.4	1.5	-.5	1.3	-.5	1.2	-.7	.9	-.3	.8	-.8	1.0	-.5	1.2	-.5	.7	.0	.5	-.2	.5	-.6
15	.6	-.1	.4	-.6	1.3	-.2	.9	-.7	.6	-.9	.5	-.8	.7	-.7	.6	-.5	.7	-.7	.5	.0	.2	-.3	.3	-.5
16	.5	-.0	.2	-.7	.9	-.3	.6	-.8	.5	-1.2	.0	-1.3	.2	-.7	-.0	-.7	.1	-.9	.5	-.1	.0	-.3	.3	-.5
17	.4	.1	.1	-.9	.4	-.5	-.2	-1.0	-.4	-1.2	-.8	-1.3	-.6	-.6	-.8	-.9	-.2	-.9	.3	-.4	-.1	-.4	-.0	-.4
18	.1	.2	-.3	-.8	-.2	-.7	-.7	-1.1	-1.2	-1.2	-1.6	-1.3	-1.3	-.5	-1.7	-1.0	-.6	-.9	.3	-.7	-.2	-.4	-.2	-.5
19	-.2	.3	-.4	-.7	-.7	-.8	-1.2	-1.1	-1.4	-1.0	-2.3	-1.2	-2.1	-.2	-2.2	-1.0	-1.0	-1.0	.0	-.9	-.4	-.4	-.4	
20	-.6	.3	-1.2	-.4	-1.1	-.6	-1.7	-.8	-2.2	-.8	-2.5	-1.1	-2.3	-.1	-2.3	-.9	-1.3	-1.0	-.1	-.9	-.6	-.3	-.5	-.3
21	-.7	.3	-1.3	-.2	-1.3	-.4	-1.9	-.4	-2.3	-.6	-2.3	-.6	-2.0	.1	-2.1	-.6	-1.5	-.9	-.2	-.7	-.7	-.1	-.8	-.1
22	-.7	.2	-1.2	-.2	-1.4	-.0	-1.6	-.1	-2.3	-.2	-2.0	-.2	-1.6	.4	-1.8	-.1	-1.7	-.5	-.3	-.6	-.7	-.0	-1.0	.1
23	-.7	.2	-1.1	-.0	-1.5	.2	-1.8	.2	-1.8	.1	-1.6	.2	-1.3	.8	-1.3	.2	-1.6	-.1	-.4	-.4	-.9	.0	-1.1	.3

ANEMOMETER HEIGHT 150.9 METERS.

TIME	MONTH																					
	JAN		FEB		MAR		APR		MAY		JUN		JUL		AUG		SEP		OCT		NOV		DEC	
HOURS (Z)	U	V	U	V	U	V	U	V	U	V	U	V	U	V	U	V	U	V	U	V	U	V	U	V
0	-.6	.1	-.8	.3	-1.5	.8	-1.5	.6	-1.6	.5	-.9	.7	-2.3	3.1	-.8	.8	-1.4	.1	-.7	-.2	-1.0	.3	-1.0	.4
1	-.5	.0	-.6	.6	-1.4	1.1	-1.4	.9	-1.1	.5	-.5	.9	-.9	3.1	-.3	1.0	-1.1	.5	-.9	.0	-1.1	.3	-.9	.6
2	-.4	-.1	-.5	1.0	-1.1	1.3	-1.2	1.1	-.6	.4	-.0	.7	.1	2.7	.1	1.1	-.7	.7	-1.1	.3	-.9	.4	-.7	.6
3	-.3	.0	-.3	1.3	-.6	1.2	-.9	1.2	-.2	1.1	-.0	.5	.9	2.7	.4	1.1	-.6	1.0	-1.0	.4	-.8	.5	-.4	.6
4	-.2	.2	.1	1.4	-.1	1.0	-.4	1.3	.2	1.4	.2	.7	1.4	2.7	.4	1.1	-.3	1.2	-.9	.6	-.5	.6	-.1	.5
5	-.0	.4	.6	1.3	.2	.9	.3	1.2	.7	1.4	.5	1.0	2.1	2.6	.6	1.1	-.1	1.4	-.7	.7	-.2	.7	.2	.5
6	.2	.3	1.0	1.0	.4	.8	.9	1.0	1.2	1.2	1.2	1.1	2.9	2.0	.9	1.1	.5	1.4	-.6	.8	.1	.8	.4	.6
7	.4	.3	1.1	.6	.6	.7	1.3	.6	1.6	.8	1.6	1.0	3.8	1.1	1.1	1.0	.8	1.3	-.3	.8	.5	.8	.6	.6
8	.4	.3	1.0	.4	.8	.4	1.4	.3	1.7	.5	1.7	.8	4.5	.5	1.2	.8	1.2	1.0	.0	.7	.8	.4	.7	.4
9	.5	.3	.8	.1	.9	.2	1.5	.0	1.8	.3	1.7	.6	4.6	.0	1.3	.4	1.3	.5	.3	.4	1.0	-.1	.7	.1
10	.6	.4	.6	-.1	.9	-.1	1.4	-.1	1.8	.3	1.7	.2	4.1	-.1	1.2	-.0	1.5	.1	.6	.2	1.0	-.5	.8	-.3
11	.6	.2	.5	-.4	.9	-.3	1.5	-.3	1.9	-.0	1.5	.1	3.3	-.4	1.0	-.3	1.5	-.2	.7	.3	.9	-.8	.7	-.6
12	.6	-.2	.4	-.5	.9	-.6	1.3	-.4	1.7	-.5	1.4	-.1	2.8	-.8	.9	-.7	1.6	-.4	.7	.1	.7	-.8	.6	-.7
13	.6	-.6	.4	-.6	1.1	-.7	1.3	-.6	1.4	-.8	1.0	-.1	2.7	-1.5	1.0	-.9	1.5	-.5	.6	-.1	.4	-.6	.5	-.7
14	.6	-.6	.3	-.7	1.1	-.9	1.2	-.7	1.0	-1.1	.8	-.6	2.8	-2.5	1.0	-.9	1.2	-.7	.7	-.2	.2	-.4	.4	-.7
15	.5	-.4	.2	-.9	1.0	-.8	1.0	-.9	.8	-1.3	.5	-1.1	1.9	-3.6	.7	-.9	.6	-.7	.7	-.2	.2	-.3	.3	-.6
16	.3	-.2	.2	-.9	.7	-.9	.7	-1.0	.4	-1.4	.0	-1.4	-.4	-4.4	.1	-.9	.1	-.8	.7	-.1	.1	-.3	.2	-.5
17	-.0	-.0	.1	-1.0	.3	-1.0	.0	-1.2	-.4	-1.4	-.8	-1.4	-3.2	-4.3	-.6	-1.0	-.2	-.8	.6	-.4	.2	-.3	.1	-.4
18	-.2	-.1	-.2	-.9	-.1	-1.1	-.5	-1.3	-1.2	-1.1	-1.6	-1.2	-5.3	-3.3	-1.5	-1.1	-.6	-.9	.5	-.7	.2	-.3	-.0	-.4
19	-.4	-.1	-.7	-.8	-.5	-1.1	-1.1	-1.1	-1.9	-1.0	-2.2	-1.1	-6.2	-2.1	-1.9	-1.0	-1.0	-1.0	.3	-.8	.1	-.3	-.1	-.4
20	-.5	-.2	-1.0	-.6	-.9	-.8	-1.6	-.0	-2.2	-.6	-2.4	-.9	-6.2	-1.0	-2.2	-.9	-1.4	-1.0	.2	-.8	-.2	-.3	-.4	-.3
21	-.6	-.1	-1.2	-.4	-1.1	-.5	-1.8	-.2	-2.5	-.2	-2.1	-.6	-5.5	-.1	-1.9	-.7	-1.5	-1.0	.1	-.6	-.4	-.1	-.7	-.1
22	-.7	-.0	-1.1	-.2	-1.3	-.1	-1.7	.1	-2.4	.3	-1.8	-.1	-4.5	1.2	-1.6	-.3	-1.5	-.8	-.2	-.6	-.6	.1	-.9	.2
23	-.7	.0	-.9	.0	-1.4	.4	-1.7	.3	-2.0	.4	-1.3	.3	-3.4	2.4	-1.2	.2	-1.5	-.4	-.4	-.5	-.9	.2	-1.0	.4

APPENDIX B

Proof of Symbol Definitions Necessary in Marcus Formula

Equation (17), as stated by Bowles and Sugarman[37] and attributed to Marcus,[36] used L for panel length, B for panel breadth. If it is assumed that length means the long dimension, the aspect ratio is

$$r = L/B, \tag{B-1}$$

so that area,

$$A = LB = rB^2 \tag{B-2}$$

Substitution in Eq. (16) yields

$$f = \frac{3A\Delta p}{4H^2} \left[\left(1 - \frac{5r^2}{6(r^4 + 1)}\right)\left(\frac{r^3}{r^4 + 1}\right)(1 + Rr^2)\right] \tag{B-3}$$

The bracketed terms are, however, unbounded in the limit as $r \rightarrow \infty$. Stress, f, must approach zero in this extreme where the plate becomes a line supported on both sides.

Alternatively, if length is assumed to mean the short dimension, and breadth is the long dimension, $B = Lr$ and $A = rL^2$, so that

$$f = \frac{3A\Delta p}{4H^2} \left[\left(1 - \frac{5r^2}{6(1 + r^4)}\right)\left(\frac{r}{1 + r^4}\right)\left(1 + \frac{R}{r^2}\right)\right] \tag{B-4}$$

In this case,

$$\text{Lim } (f) = 0, \; r \rightarrow \infty \tag{B-5}$$

as it should. Unfortunately, the original Marcus paper[36] could not be obtained to establish the true source of the confusion. In consequence, the symbols in Eq. (17) have been transposed so that length and breath refer to long and short dimensions, respectively. Furthermore, in the reduction to a formulation for square plates, as is most commonly considered, there is no problem.

DISTRIBUTION:

U.S. Department of Energy
Division of Military Applications
Attn: Maj. Gen. J. K. Bratton
Washington, DC 20545

U.S. Department of Energy
Albuquerque Operations Office
P.O. Box 5400
Kirtland Air Force Base, NM 87185
Attn: C. B. Quinn
Spec. Prog. Div.

Commander (10)
USN-SSPO
Crystal Mall Bldg. 3
Arlington, VA 22202

E. F. Gormel (3)
NOTU SPP-30
Patrick AFB, FL 32925

L. J. Ullian (3)
AFETR/SEM
Patrick AFB, FL 32925

Major D. Pina
AFETR/WE
Patrick AFB, FL 32925

J. S. Malik, J-DO-T
Los Alamos Scientific Laboratory
Los Alamos, NM 87544

R. J. Bartholomew, WX-8
Los Alamos Scientific Laboratory
Los Alamos, NM 87544

Warren Hendrickson
Lockheed - LMSC
P.O. Box 504
Sunnyvale, CA 94086

NSWC-HQ (2)
White Oak,
Silver Spring, MD 20910
Attn: J. Petes, WR-15
J. Pittman WR-15

P. Schomer
Corps of Engineers, CERL
P.O. Box 4005
Champaign, IL 61820

Dr. Donald R. Richmond
Lovelace Foundation for Medical
Education and Research
5200 Gibson Blvd., SE
Albuquerque, NM 87108

J. Jantz (2)
SAMTEC/SEY
Vandenberg AFB, CA 93437

Major P. T. Burnett
SAMTEC/WE
Vandenberg AFB, CA 93437

Defense Documentation Center
Cameron Station
Alexandria, VA 22314
Attn: TC

Director Defense Nuclear Agency
Washington, DC 20305
Attn: SPAS, J. F. Moulton, Jr.

Chairman
Department of Defense Explosives
Safety Board
RM-GB270, Forrestal Building
Washington, DC 20301

Commander, FC, DNA (2)
Kirtland AFB, NM 87185
Attn: FCTD-A, Technical Library
FCTD-T

Director
Defense Advanced Research Projects
Agency
1400 Wilson Blvd.
Arlington, VA 22209
Attn: Document Control

Assistant to the Secretary of Defense
Atomic Energy, DOD
The Pentagon
Room 3E 1069
Washington, DC 20301
Attn: Document Control

Director
Air University Library
Maxwell AFB, AL 36112
Attn: LDE

Air Force Office of Scientific Research
1400 Wilson Blvd
Arlington, VA 22209
Attn: Document Control

Warren Chan
GE-TEMPO-DASIAC
816 State St.
Santa Barbara, CA 93102

Capt. J. P. Kahler
Staff Meteorology/WE
Holloman AFB, NM 88330

Leo Ingram
Army Engineers Waterways
Experiment Station
P.O. Box 631
Vicksburg, MS 39180

Lt. T. C. Cloutier
USAEHA-BAD
Aberdeen Proving Ground, MD 21010

Dr. John A. Blume
John A. Blume and Associates
Sheraton-Palace Hotel
100 Jessie Street
San Francisco, CA 94105

Dr. Everett F. Cox
Haven Hotel
235 6 St. NW
Winter Haven, FL 33880

DISTRIBUTION (Continued)

Mr. Robert E. Fuss
U.S. Naval Ship Engineering Center
Prince Georges Center
Hyattsville, MD 20782

Mr. John H. Keefer, DRXBR-TE
U.S. Army Ballistic Research
Laboratories
Aberdeen Proving Ground, MD 21005

Mr. Joseph E. Minor
Civil Engineering Department
Texas Tech University
Lubbock, TX 79409

Dr. Donald L. Montan, L-200
University of California
Lawrence Livermore Laboratory
P.O. Box 808
Livermore, CA 94550

Dr. John H. Wiggins, Jr.
J. H. Wiggins Company
1650 Pacific Coast Highway
Redondo Beach, CA 90277

K. T. Smith, AMXTE-AEO
Tooele Army Depot
Tooele, UT 84074

R. E. Allen
Division of Safety Standards
& Compliance
DOE-HQ
Germantown, MD 20767

Dr. Henning E. von Gierke
6570th Aerospace Medical
Research Laboratory
Wright-Patterson AFB, OH 45433

R. Nelson
SAI
#5 San Pedro Park
2201 San Pedro NE
Albuquerque, NM 87110

NASA Langley Research Center
Hampton, VA 23665
Attn: H. H. Hubbard
H. R. Henderson MS-325

P. McCalman (2)
Code TO-NTS-2
NASA Kennedy Space Center, FL 32899

John P. Taylor
Aeronautics and Space Engineering Board
National Academy of Engineering
2101 Constitution Avenue, NW
Room JH-738
Washington, DC 20418

M. A. Whitcomb
NRC-CHABA
2101 Constitution Ave
Washington, DC 20418

K. C. Spengler
American Meteorological Society
45 Beacon St.
Boston, MA 02108

1100 C. D. Broyles
1111 J. R. Banister
1111 L. J. Vortman
1120 T. L. Pace
1123 B. C. Benjamin
1123 B. C. Holt
1132 A. B. Church
1132 J. L. Montoya
4500 E. H. Beckner
4514 M. L. Merritt
4530 R. W. Lynch
4533 B. D. Zak
4533 H. W. Church
4533 J. W. Reed (20)
8000 T. B. Cook, Jr.
8266 E. A. Aas
3141 T. L. Werner (5)
3151 W. L. Garner (3)
for DOE/TIC (Unlimited Release)
DOE/TIC (25)
(R. P. Campbell, 3154-3)